9-1-2000

Chemistry of group(IV) phosphinimide complexes.

Nancy L. S. Yue
University of Windsor

Chemistry of Group(IV) Phosphinimide Complexes

by

Nancy L. S. Yue

A Thesis
Submitted to the Faculty of Graduate Studies and Research
through the School of Physical Sciences,
Department of Chemistry and Biochemistry
in Partial Fulfillment of the Requirements for
the Degree of Master of Science in Chemistry at the
University of Windsor

Windsor, Ontario, Canada
September, 2000

Your file Votre référence
ISBN: 0-494-04962-6
Our file Notre référence
ISBN: 0-494-04962-6

Abstract

Complexes of zirconium and titanium using phosphinimine as the ligand system were prepared. Some of these complexes were tested for activity in ethylene polymerization.

Complexes of the form $Cp^*Zr(NPR_3)Cl_2$ where R = *i*-Pr **41**, *t*-Bu **53** were readily prepared. A series of the corresponding dialkyl derivatives $Cp^*Zr(NPR_3)R'_2$ where R = *i*-Pr, R' = Me **42**, η^3-allyl **43**, Ph **45**, Cp **47** and R = *t*-Bu, R' = Me **54**[70], η^3-allyl **44**, Ph **46**, Cp **48** were also generated. Complexes **41**, **44**, **46**, **47**, **49**, **50** and **54**[70] were characterized crystallographically. Catalysts derived from complexes **41** and **53** gave minimal activities while complexes **42** and **54** gave no activity in ethylene polymerization. In the presence of $[Ph_3C][B(C_6F_5)_4]$, complex **49** $Cp^*Zr(NP$*i*-$Pr_3)$(*s-cis*-η^4-2,3-dimethyl-1,3-butadiene) achieved higher activity while the tri-*t*-butyl analogue **50** achieved no activity in ethylene polymerization. Further GPC studies of the generated polyethylene suggest degradation occurred and the formation of more than one active species under the employed polymerization conditions.

A new class of ancillary ligands, phosphine-phosphinimide R_3PNPPh_2 where R = *i*-Pr **58**, *t*-Bu **59** were developed. Compounds of the form R_3PNPPh_2R' where R = *i*-Pr, R' = TMA **60**, $B(C_6F_5)_3$ **62**, NTMS **63** and R = *t*-Bu, R' = TMA **61**, NTMS **64** were generated. The corresponding titanium dichloride complexes $CpTi(NPPh_2(NPR_3))Cl_2$ where R = *i*-Pr **65**, *t*-Bu **66** and dimethyl analogues $CpTi(NPPh_2(NPR_3))Me_2$ where R = *i*-Pr **67**, *t*-Bu **68** were subsequently prepared. Complexes **58, 60, 62** and **65** were characterized crystallographically. Catalysts derived from complexes **65** and **66** achieved high activity, while those from **67** and **68** showed no activity in ethylene polymerization.

This is presumably due to steric congestion. Complexes **65** and **66** are in fact promising new homogeneous "single site" catalyst precursors.

Dedication

This work is dedicated to the memory of my father, Sik Ying Yue.

Acknowledgments

I would like to acknowledge a number of people who have been important to me during the past two highly stressful years of my life. I am deeply thankful to Dr. Douglas W. Stephan for his guidance, encouragement and his belief in my capabilities. I am also grateful to my mother, Susanna Ching Yu Hui; my brother, Andrew Kwok Chung Yue; and my beloved husband, Wing Yean Chang for being so supportive, patient and understanding.

I would also like to thank all the past and present members in our group for their friendships, support and helpful advice over the past two years. I will treasure every moment that we have shared. Special thanks to Dr. Eva Witt, Dr. Jeff Stewart, Dr. Fred Guérin, Dr. Charles Carraz, Dr. Luc LePichon, Dr. Jim Kickham, Dr. Pingrong Wei, Aaron Hoskin, Chris Ong, Silke Courtenay, Chad Beddie, Emily Hollink and Sarah Smith.

I am grateful to Dr. B. Zielinski, Dr. S. J. Loeb and Dr. K. E. Taylor for their advice. I am also thankful to Mike Fuerth, Sharon Horne, Kimberly Lefebvre, Pat Aroca, Vivi Lazarescu, Samantha Murray, Sandra Horton, Jerry Vriesacker, Terry Edwards, Mike Siwek, Jim Olsen and Al Ditchburn for their expertise. I would also like to thank the faculty, fellow graduate students, undergraduate students and staff from the School of Physical Sciences, Chemistry and Biochemistry for their friendships.

Lastly, I am also thankful for the friendships and support from all the graduate students and undergraduate students in the Department of Biological Sciences. Special thanks to Dr. M. J. Crawford and Dr. B. Dixon for their support and advice.

Table of Contents

List of Figures

List of Schemes

List of Tables

Abbreviations

Å	Angstrom
Ar	aryl
br	broad
Cp	cyclopentadienyl anion (η^5-C_5H_5)
Cp*	pentamethylcyclopentadienyl anion (η^5-C_5Me_5)
°C	degree Celsius
d	doublet
δ	chemical shift
equiv	equivalent
Et	ethyl (C_2H_5)
Fc	calculated structure factor
Fo	observed structure factor
g	grams
GPC	gel permeation chromatography
h	hour
Hz	Hertz
I	nuclear spin
i-Pr	isopropyl ($CH(CH_3)_2$)
J	coupling constant
^2J	two-bond coupling constant
^3J	three-bond coupling constant
m	multiplet

m	meta
mol	mole
M	molar
MAO	methylaluminoxane
Me	methyl (CH_3)
MHz	Megahertz
min	minutes
mg	milligrams
mL	milliliter
mmol	millimoles
M_n	number-average molar mass
M_w	weight-average molar mass
M_w/M_n	polydispersity index
NMR	nuclear magnetic resonance
ORTEP	Oak Ridge Thermal Ellipsoid Program
o	ortho
p	para
PDI	polydispersity index
Ph	phenyl (C_6H_5)
psi	pounds per square inch
ppm	parts per million
quart	quartet
quin	quintet

R	agreement factor
R_w	weighted agreement factor
RPM	number of rotations per minute
s	singlet
t-Bu	tertiary butyl ($C(CH_3)_3$)
THF	tetrahydrofuran
TMA	trimethylaluminum
t	triplet
trityl	tetrakis(pentafluorophenyl)borate ($[Ph_3C][B(C_6F_5)_4]$)
v br	very broad

Chapter One
Introduction

Synthesis, modifications and applications of catalyst precursors for olefin polymerization have became one of the most active research areas in organometallic chemistry. Bent metallocene complexes with group(IV) metals are by far the most promising catalyst precursors and were the most extensively studied in the past. This is due to the fact that these catalyst precursors are homogeneous in nature and thus act as "single site" catalysts to polymerize olefins. In addition, some of these catalyst precursors achieve very high activity and provide control over the stereochemistry of the generated polymers. This thesis describes the synthesis, reactivity and applications in ethylene polymerization of zirconium phosphinimide and titanium phosphinimine-phosphinimide complexes. Studies have shown that phosphinimide type ligands are both electronically and sterically analogous to cyclopentadienyl (Cp) ligands. Thus, the resulting phosphinimide complexes provide similar metal atom environments to those in bent metallocene complexes. This introductory chapter describes the background, nature and generation of group(IV) homogeneous catalysts, followed by a brief discussion of group (IV) phosphinimides complexes.

1.1 Historical Background of Group IV Homogeneous Catalysts

Application of organometallic compounds as catalyst precursors in olefin polymerization was first discovered by K. Ziegler in 1955.[1] The Ziegler catalyst is a two-component system consisting of titanium(IV) chloride ($TiCl_4$) and triethylaluminum ($AlEt_3$). In this system, $TiCl_4$ is the catalyst precursor while $AlEt_3$ is the cocatalyst or

initiator. In general, ethylene is inactive under the conditions of atmospheric pressure and room temperature. On the other hand, ethylene was polymerized into linear polyethylene (PE) in the presence of the Ziegler catalytic system, (Eq 1.1).

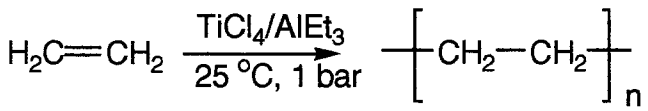

(1.1)

Simultaneous with Ziegler's work, G. Natta[2] discovered that under the same conditions, the Ziegler's catalyst not only induced ethylene polymerization but also induced propene polymerization stereoselectively (Eq. 1.2). The resulting crystalline

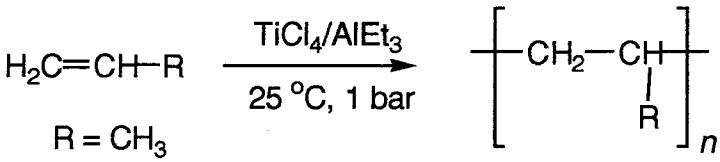

(1.2)

polypropylene (PP) was found to be isotactic in nature. In other words, all the asymmetric carbon atoms have the same stereochemical configuration. Subsequently, isotactic PP proved to be an excellent and useful material with properties such as high density, hardness and tensile strength.

The classical unmodified Ziegler-Natta catalyst system ($TiCl_4/AlEt_3$) is heterogeneous. In other words, polymerization takes place on the surface of the catalyst. The resulting polymer generally has broad molecular weight distribution,[3] this is an indicative of multiple active sites. Since many properties of polymers depend upon the size of the polymer chain, therefore modifications of Ziegler catalysts are essential to overcome the drawback of the traditional Ziegler-Natta catalysts.

A few years after the synthesis of the first group(IV) bent metallocenes (Cp_2TiBr_2 and Cp_2ZrBr_2) by Wilkinson *et al*[4] in 1953 and the discovery of activation of ethylene

and propylene by Ziegler, Natta and co-workers[5] tested a combination of Cp_2TiCl_2 and $AlEt_3$ for olefin polymerization. The results showed low activity and only low molecular weight oily polymer was obtained. The active species was believed to be a titanium-aluminum heterodimetallic complex. Breslow[6] later reported titanocene dichloride (Cp_2TiCl_2) with Et_2AlCl resulted in an active catalyst for olefin polymerization, particularly when ethylene containing a small amount of oxygen was used. However, the resulting activity was not comparable to the Ziegler-Natta catalysts due to the initial formation of an inactive reduced titanium(III) species. Meyer[7] and Breslow[8] also observed independently that addition of trace amounts of water promoted the rate of polymerization while other additives such as alcohols or oxygen did not show the same results.

In 1976, Kaminsky and co-workers[9] observed that addition of water activated the polymerization-inactive $Cp_2ZrMe_2/AlMe_3$ system to polymerize ethylene with extremely high activity. Maximum activity was achieved when $Al:H_2O$ ratio was between 2:1 and 5:1, while no activity was observed when $Al:H_2O$ ratio dropped below 1:3. This result indicated that partial hydrolysis of the alkyl aluminum species took place and formed aluminoxanes with the formula of $(RAlO)_n$.

Aluminoxane is a more efficient activator presumably because it is a stronger Lewis acid than the tri-alkyl aluminum. The serendipitous discovery gave what is nowadays the most commonly used, highly efficient activator, namely, methyl aluminoxane (MAO).[10, 11] Kinetic studies showed that a relatively large excess of MAO was required because the rate of reaction depended linearly on the catalyst concentration but quadratically on the MAO concentration.

The exact composition and structure of MAO still remains ambiguous. The only reported structurally characterized alkylaluminoxane was derived from hydrolysis of tri-*tert*-butyl aluminum as described by Barron and co-workers.[12] The generally accepted structure of MAO is a highly symmetrical cluster compound in which the central aluminum is four coordinated, while each oxygen atom is bridged by three peripheral aluminum atoms.

Unlike the classical heterogeneous Ziegler-Natta catalyst, metallocene catalyst precursors are homogeneous. This provides better contact between the catalyst precursor and the monomer during polymerization. As a result, homogeneous catalysts are more active than the heterogeneous Ziegler-Natta catalysts. This also provides control over the stereochemistry and the architecture of the polymer produced. Consequently, an enormous variety of homogeneous catalysts have been explored by a number of research groups.[13-17]

1.2 Nature of Homogeneous Catalysts

Ever since the discovery of homogeneous catalysts and cocatalysts, a large number of studies on the mechanistic pathway of olefin polymerization have been carried out. The mechanistic pathway for olefin polymerization has been generalized, even though the structure of MAO is still not fully understood (Scheme 1.1).[18] It is now commonly believed that MAO first alkylates the metallocene dichloride or metallocene monoalkyl complex (**1**) through ligand exchange reaction. This is followed by the abstraction of either Cl^- or CH_3^- anion from the metallocene complex. This results in the generation of a "cation-like" metallocene (**2**), which is the actual active species with a

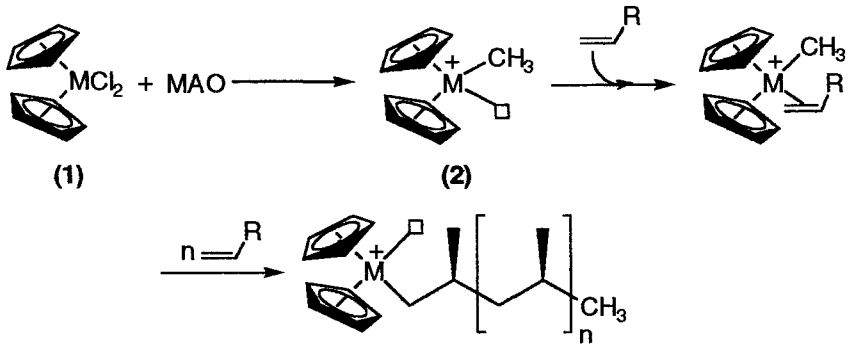

Scheme 1.1 General mechanism of olefin polymerization by bent metallocene **1**.

single active center, and an anionic MAO counterpart.[19, 20] A monomer of olefin is now able to coordinate to the unsaturated active site of the cationic metal center. This further undergoes insertion of the olefin into the metal-alkyl bond and creation of a new free co-ordination site simultaneously. Repeated insertion of incoming olefin monomers will thus generate a polymer chain. Growth of individual polymer chain is then terminated either by unimolecular rearrangement of the ion pair or through chain transfer to aluminum.

When metallocene dialkyl complexes are used as catalysts precursors, the need for the alkylation step by the cocatalyst is eliminated. In order to generate cationic d^0 group(IV) metal complexes from the neutral catalyst precursors, oxidizing agents such as $AgBPh_4$ or $[Cp_2Fe][BPh_4]$, and protonating agents such as $[HNR_3]^+[B(C_6X_5)_4]^-$ can be used in place of MAO. Alkyl abstracting agents such as $[Ph_3C]^+[B(C_6F_5)_4]^-$ or strong organo-Lewis acid like $B(C_6F_5)_3$ (**3**) are also commonly used to stoichiometrically remove the alkyl anionic ligand to form the "cation-like" active species (**4**) (Eq 1.3).[21-24]

$$\underset{\textbf{3}}{L_2Zr(CH_3)_2} + B(C_6F_5)_3 \longrightarrow \underset{\textbf{4}}{L_2ZrCH_3^+CH_3B(C_6F_5)_3^-} \qquad (1.3)$$

As an alternative, a new generation of active species known as zwitterionic metallocenes has evolved. A zwitterionic metallocene consists of a counterion covalently bonded to an ancillary ligand, but maintains a separation from the metal center. This reduces ionic interaction between the metal and the counteranion. This presumably contributes to their highly active nature. Another advantage of zwitterionic metallocene compounds is that they exhibit higher solubility in hydrocarbon solvent than the more ionic cationic-like species. Solubility is important because commercial olefin polymerization is usually carried out in hydrocarbon solvent.

In principle, zwitterionic metallocene compounds fall into three families. These are categorized according to the position of the counterion within the molecule. Namely, "girdle zwitterions" (**5**), "ring zwitterions" (**6**) and "bridge zwitterions" (**7**).[25]

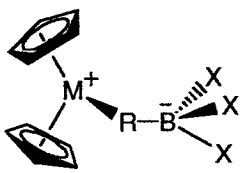

5

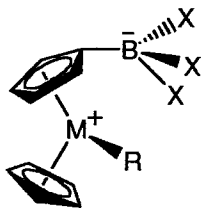

6

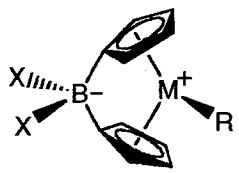

7

"Girdle zwitterion" refers to the location of the counterion at the alkyl ligand. The first "girdle zwitterion" (**10**) was discovered by Hlatky and Turner in 1989.[26] The reactions between $[Bu_3NH][B(C_6H_4R)_4]$ and $Cp^*_2ZrMe_2$ (**8**) generated species **9** via methyl abstraction. Elimination of methane then gave species **10** (Scheme 1.2).

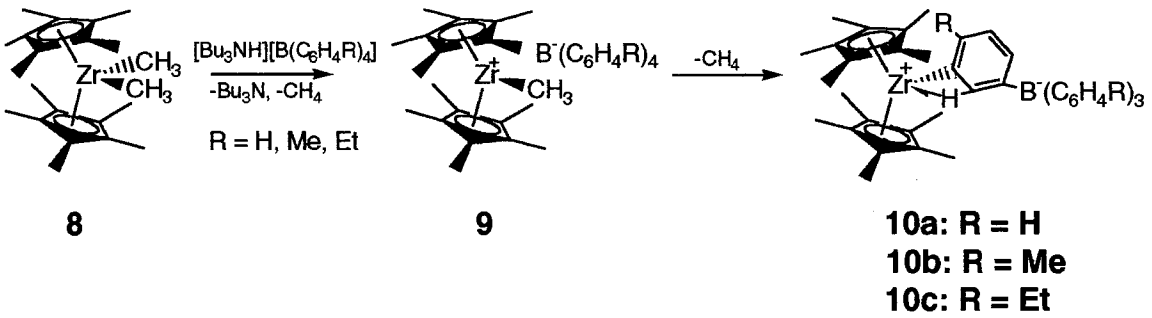

8 **9** **10a: R = H**
10b: R = Me
10c: R = Et

Scheme 1.2 First girdle metallocene-based zwitterions **10**.

Compound **10b** was found to function as a catalyst for olefin polymerization with an activity of 375 g PE $mmol^{-1}$ h^{-1} atm^{-1} under mild conditions. The common structural motif found in "girdle zwitterionic" metallocenes involves an "agostic interaction". This weak interaction arises when the proton or fluorine atom *ortho* to the boron atom as in **10** and $B(C_6F_5)_3$ respectively, weakly coordinated to the central metal. The resulting metal-hydrogen or metal-fluoride bond also functions as a weak donor ligand and therefore provides additional stability for these types of complexes. This phenomenon is also observed for a wide variety of metallocene-based complexes, such as those metallacyclic zirconium complexes (**11**),[27] "constrained-geometry" titanium complexes (**12**),[28] and hydrocarbyl titanium complexes (**13**).[29, 30]

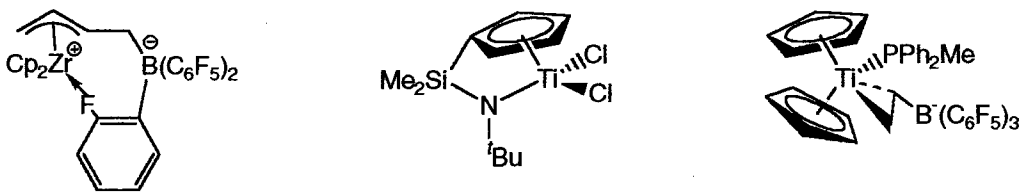

11 **12** **13**

A second type of zwitterionic metallocenes is the "ring zwitterions". "Ring zwitterions" indicated the counterion is attached to the cyclopentadienyl ring. One

interesting feature of ring zwitterions is that the stability of the compound is dependent on the length of the tether between the ring and the borate anion. As illustrated in Scheme 1.3, the three-carbon allyl group of species **14** is too long to sustain ring-type zwitterionic structures. Thus, it undergoes rearrangement involving alkyl exchange and benzyl abstraction to give compounds **15** and **16** respectively.[31, 32]

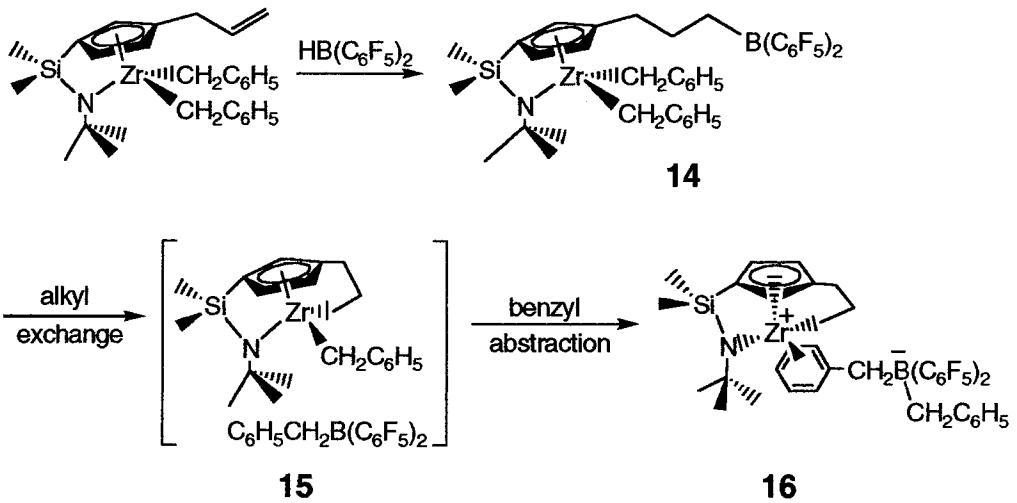

Scheme 1.3 Synthesis of unstable ring zwitterion **16**.

On the other hand, more stable "ring zwitterions" **18** was achieved by electrophilic attack of the Cp ring.[25, 29, 33] In this situation, the Zr-C bond is sterically protected as in species **17**, thus preventing the borane attack (Scheme 1.4).[25]

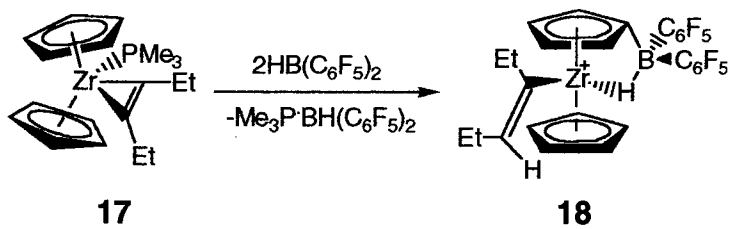

Scheme 1.4 Synthesis of stable ring zwitterion **18** by electrophilic attack on Cp.

Unlike "girdle" and "ring zwitterions", preparation of "bridge zwitterions" is challenging. In fact, there is no documented case of direct synthesis of "bridge zwitterions". Attempts to synthesize "bridge zwitterions" tend to generate products of the form **19**[34] and **20**[35]. This is presumably attributable to the fact that the boron linker is small in size.

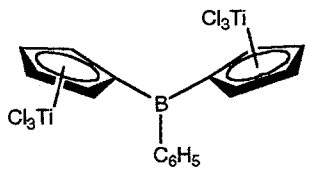

19

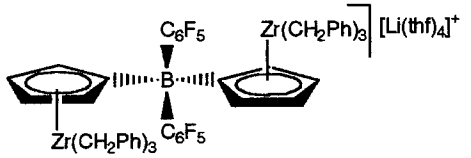

20

Rufanov and co-workers[36a] later demonstrated that boron-bridged *ansa*-zirconocene such as species **21** can be synthesized (Scheme 1.5)[36]. This was achieved from the reaction between trimethylstannyl substituted cyclopentadiene and $ZrCl_4$. In

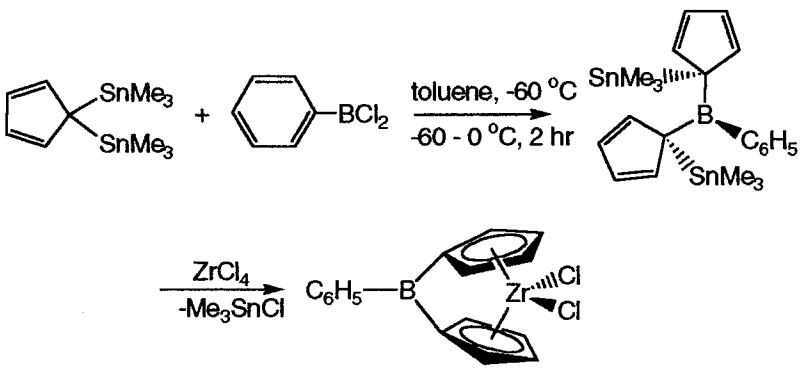

21

Scheme 1.5 Synthesis of boryl-bridged *ansa*-metallocene **21**.

addition, the anionic analogue of **21** with Cl^- on the bridged boron instead was found to be active in polymerize olefin in the presence of MAO with high activity.[37]

1.3 New Generation of Group IV Homogeneous Catalysts for Olefin Polymerization

The most commonly used strategy in designing new catalysts for olefin polymerization is by replacing one or both (6-e⁻ donor) cyclopentadienyl ligands of the metallocene with other (2-e⁻ donor) anionic ancillary ligands. These ligands should provide some degree of control over the coordination number, coordination geometry and the formal oxidation state of the metal. More importantly, these ligands should be bulky and rigid enough to sterically protect the active site and to provide stereoselective control for α-olefins respectively.

For group(IV) catalysts, alternative ancillary ligands can be categorized into carbon-, oxygen- and nitrogen-based. Carbon-based ancillary ligands such as alkyl (**22**), allyl (**23**) and modified cyclopentadienyl (**24**) are commonly used. Systems like **22**[38-42]

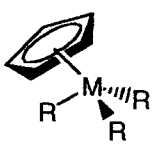

R = Me, CH_2Ph

22

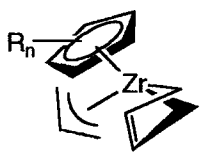

R_n = 1,3-$(SiMe_3)_2$

23

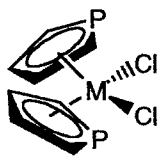

24

and **23**[27a] when activated with the appropriate Lewis acid demonstrated moderate activity (10 - 100 g $mmol^{-1}$ h^{-1} bar^{-1}) while complex **24**[43] afforded high activity (10 - 1000 g $mmol^{-1}$ h^{-1} bar^{-1}) during ethylene polymerization.

The use of bulky chelating oxygen donor ligands for olefin polymerization was first introduced in 1995 by Schaverien.[44] The advantage of using alkoxide ligands is their sterically hindered nature. This provides protection of the active site. In addition, these

systems are stereochemically rigid. This rigid framework for the metal center is a necessity for stereospecific transformation.

Chelating alkoxide complexes such as species **25** can be easily prepared by protonolysis of MX_4 or MR_2X_2 or MR_4 (M = Ti or Zr, R = CH_2Ph, X = Cl) with the corresponding chelating ligands such as biphenols and binaphthols (Scheme 1.6).

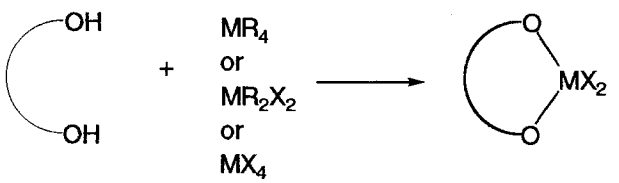

25

Scheme 1.6 General synthetic pathway for chelating alkoxide group(IV) species **25**.

Examples of a variety of chelating oxygen-based complexes are shown below. Catalyst precursor **26** showed moderate activity (130 g $mmol^{-1}$ h^{-1} bar^{-1}) in ethylene

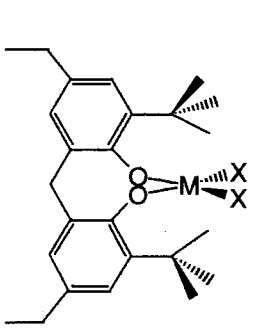

26

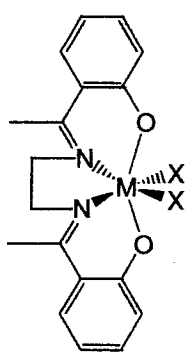

27

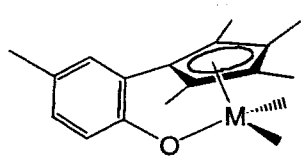

28

polymerization, while a significant increase in activity was obtained by incorporating an additional donor(s) in the alkoxide ligand backbone as in **27**.[45] Incorporation of an aryloxide ligand to the Cp ligand also achieved a highly active polymerization catalyst precursor **28** for ethylene with an activity of 2100 g $mmol^{-1}$ h^{-1} bar^{-1}.[46]

Ligand systems containing nitrogen have received tremendous attention during the past decade. This is due to the fact that a formal 10-electron species $[(R_2N)_2ZrR]^+$, which is more electrophilic and thus a more active species than a 14-electron species $[Cp_2ZrR^+]$, is generated during polymerization. Monodentate amide ligands as in **29** afforded moderate activity of 13 g $mmol^{-1}$ h^{-1} bar^{-1}.[15] On the other hand, bis(amido)

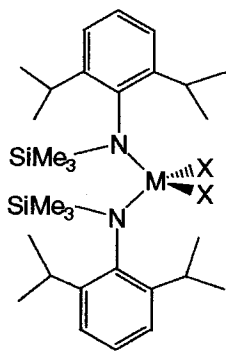

29

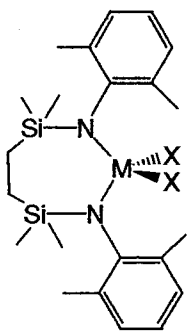

30

complex with silicon incorporated in the backbone such as species **30** were highly active ethylene polymerization catalyst precursors with an activity of 990 g $mmol^{-1}$ h^{-1} bar^{-1}.[15] These complexes are generally prepared by salt-elimination reactions using either the adduct of THF coordinated or the noncoordinating metal tetrachloride and the lithiated silylamides. Dramatic increase in activity is mostly due to the so-called "silicon effect". The silicon atom on the silylamido ligand functions as an electron withdrawing group that withdraws electron from the metal center through the nitrogen-metal bond. This in turn increases the Lewis acidity of the central metal, thus stabilizing the whole system.[47] In addition, the bulky aryl substituents on the nitrogen donor provide steric protection against attack by the cocatalyst. Lack of steric protection of the ligand may result in complete loss of the ligand[48] or intramolecular C-H activation.[49]

A more remarkable nitrogen-based catalytic system is the "constrained-geometry catalysts" (CGC) as in species **12** and **31**[50, 51]. Such systems can be described as a

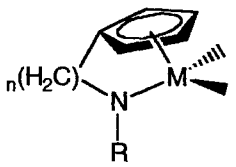

31

combination of Cp ligands with an amide functionality to form a hybrid "half-metallocene" system. In fact, species **12** is now being applied in industry. The general synthetic method in preparing species **31** involves the reaction of the dianionic ligand and the metal halides MX_n. Bases such as Et_3N are used to trap HX generated during reaction. The open nature of the catalyst active site allows incorporation of other olefins such as styrene,[52] hexene, octene and norbornene into polyethylene. Two other interesting features are the increased stability towards MAO and generation of higher molecular weight polymers when compared with bis-cyclopentadienyl metallocenes.

Amido ligands can be further extended into bis(amido) ligands with an additional donor group placed between the two amido functionalities as in **32**, which also afforded

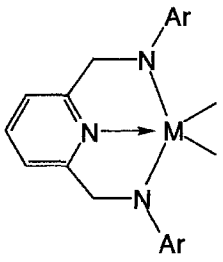

32

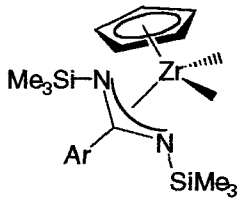

33

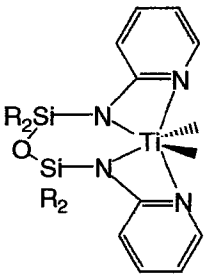

34

very high activity of 1500 g $mmol^{-1}$ h^{-1} bar^{-1} for zirconium[53] and very low activity for titanium.[54] Advantages of the pyridine-diamide ligand are the restricted rotation about the N-C_{ipso} bond and the availability of a variety of substituted anilines. This provides

different degrees of steric protection with minimum change in the electronic environment around the metal. Other bis(amido) ligands such as **33**[55] and **34**[56] were also explored but only moderate to low activities were achieved.

1.4 Group IV Phosphinimide Complexes

Another nitrogen-based catalytic system that has not received much attention in ethylene polymerization is the phosphorane iminato or phosphinimide complex (**35**).

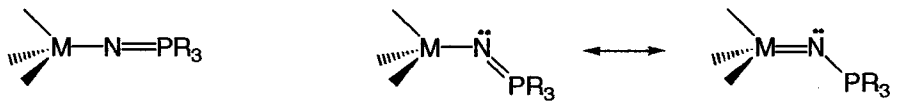

35A **35B**

In general, phosphinimide complexes exist in either linear a M-N-P arrangement (**35A**) with bond angles between 161 and 177°, or a bent M-N-P arrangement (**35B**) with bond angles between 130 and 140°.

The bonding moiety of transition metal phosphinimide complexes can be generalized as in Figure 1.1.[57] The sp^3 hybrid orbitals of the phosphorus atom give rise

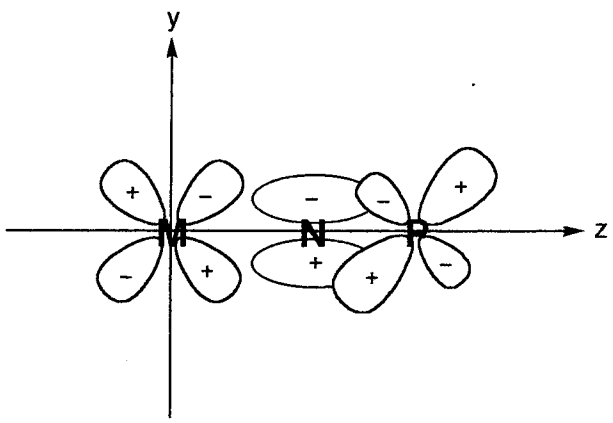

Figure 1.1 Bonding moiety of transition metal phosphinimide complexes.

to four σ bonds. Three of them are bonded to the alkyl groups and the fourth to the nitrogen. This leaves an electron in a *d* orbital. The nitrogen atom then utilizes its linear *sp* hybrid orbitals for two σ-bonds. One of them is bonded to the phosphorus and the other to the central metal. This leaves three electrons in the $2p_x^2 2p_y^1$ orbitals. The resulting $2p_y^1$ orbital from the nitrogen then overlap with the $3d_{z2}^1$ orbital from the phosphorus to form a d_π-p_π bonding.

The phosphinimide ligand group $[NPR_3]^-$ is isoelectronic with a variety of ligands, such as silyl imido $[NSiR_3]^-$ and silyloxy $[OSiMe_3]^-$ as well as phosphorane oxide.[58] Dehnicke and co-workers[59, 60] later noted the electronic properties of the phosphinimide ligands are in fact analogous to cyclopentadienyl ligands.

In addition, Wolczanski *et al*[61] was the first to report the steric similarity between tri-*tert*-butylmethoxide (tritox) ($(CH_3)_3C)_3CO$) and the cyclopentadienyl ligand. This conclusion was drawn based on the observation on their cone angles, which are 125° and 136° respectively. As a result, both steric and electronic properties of cyclopentadienyl and phosphinimide ligands were found to be similar.

A number of synthetic strategies can be used to achieve phosphinimide complexes. Reactions between either terminal (M≡N) or bridging (M≡N-M) nitrido complexes with phosphines (R_3P) in boiling dichloromethane were first used to prepare molybdenum or tungsten phosphinimide complexes (**36** in Eq. 1.4).[62]

$$N{\equiv}MCl_3 + PPh_3 \longrightarrow M(NPPh_3)Cl_3 \qquad (1.4)$$

M = Mo, W

36

The mechanism involves nucleophilic attack of the phosphorus atom of the phosphine on the nitrido nitrogen atom. Phosphinimide complexes can also be obtained from reduction of nitrosyl complexes (**37**) with phosphines stoichiometrically (Eq. 1.5).

$$\underset{\textbf{37}}{M{=}N{=}O} + 2\,PR_3 \longrightarrow M{=}N{=}PR_3 + OPR_3 \qquad (1.5)$$

A more common synthetic approach is to use transition metal azido complexes (MX_nN_3) as the starting material. This was first discovered by Strähle *et al*[63] for niobium phosphinimide complexes. In a similar manner, phosphinimide complexes can be prepared from metal halides (MX_n) and iminophosphoranes ($R_3P{=}NR'$). The mechanistic pathways for both syntheses are based on the well investigated two-step classical Staudinger reaction.[64] Utilizing ^{15}N labelling techniques, the γ-N from the azide was found to initially add electrophilically to a P(III) center. Intramolecular elimination of dinitrogen (β-N and γ-N) unit from the intermediate phosphazide (**38**) in the 4-membered ring transition state generates the resulting compound (Scheme 1.7).

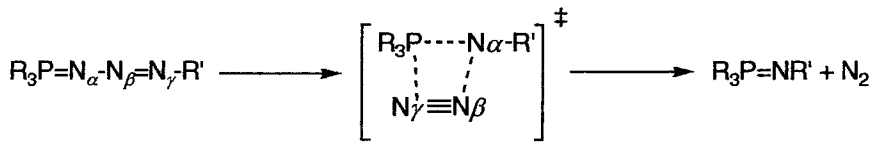

38

Scheme 1.7 Mechanism of Staudinger Reaction.

A large number of structural studies of phosphinimide transition metal complexes were carried out by Dehnicke *et al*[57], but only a few were reported as monomeric species. Of particular interest is the titanium phosphinimide complex [($TiCl_3(NPPh_3)$)]. The Ti-N-P vector in this complex is linear with a Ti-N-P bond angle of 180 °.

It was not until recently that Stephan and co-workers[13, 14, 65, 66] reported a series of systematic studies on the chemistry and applications of the analogous monomeric titanium phosphinimide complexes **39** and **40**. It was found that titanium phosphinimide complexes such as **39**[13] and **40**[14], presumably, due to their Lewis acidic nature,

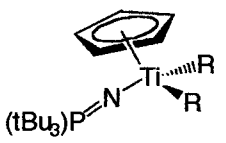

R = Cl or Me

39

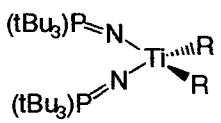

R = Cl or Me

40

polymerized olefins with extremely high activity. In particular, the methyl analogue of species **40** in the presence of cocatalyst gives rise to a highly active catalytic system.[14]

1.5 Summary and Scope of Thesis

Group(IV) metallocene complexes are known to be catalyst precursors in olefin polymerization. These catalyst precursors generally achieve high activity. These species act as homogeneous, "single site" catalysts. By manipulating both the steric and electronic properties of ancillary ligands, a new generation of homogeneous catalyst has evolved. In fact, the resulting monomeric titanium phosphinimide complexes have been proven to be more active than bis(cyclopentadienyl) systems.

The primary goal of this thesis is to synthesize new group(IV) homogeneous "single site" catalysts based on phosphinimide ligands. Conventionally, zirconium complexes are more active catalyst precursors than titanium complexes employing the same ligand system. As a result, the following chapter will focus on the syntheses and applications of zirconium phosphinimide complexes and the corresponding derivatives.

In a subsequent effort, a new class of ancillary ligands, namely phosphinimine-phosphinimides has been developed. This was employed to synthesize the corresponding titanium complexes, which were further tested for activity in ethylene polymerization.

Chapter Two
Synthesis, Reactivity and Applications of Zirconium Phosphinimide Complexes

2.1 Introduction

Based on the electronic and the steric similarities between the phosphinimide and cyclopentadienyl ligands, our laboratory successfully demonstrated that phosphinimide ligands could be employed to mimic the chemical environment of metallocenes in designing well-defined homogeneous olefin polymerization catalyst precursors. In fact, monomeric titanium phosphinimide complexes and their dimethyl derivatives were found to be extremely active in olefin polymerization.[13, 14] While a large number of structural studies of transition metal phosphinimide complexes are known,[58] we have been recently involved in a thorough and systematic study of the chemistry of such compounds.[66] In addition, zirconium complexes are normally found to be more active catalysts than the corresponding titanium complexes with the same ligand system. Consequently, synthetic routes, reactivity and application in olefin polymerization of zirconium phosphinimide analogues were investigated.

2.2 Experimental

General Data All preparations were performed under an atmosphere of dry, anaerobic N_2 employing either Schlenk line techniques or a Vacuum Atmospheres inert atmosphere glove box. Solvents were reagent grade, either distilled from the appropriate drying agents under N_2 or obtained directly from an Innovative Technologies solvent purification system, and degassed by the freeze-thaw method at least three times prior to

use. Tri-*iso*-propyl phosphine, tri-*tert*-butyl phosphine and pentamethylcyclopentadienyl-zirconium trichloride were used as received from Strem Chemical Co. All Grignard reagents, NaCp and magnesium powder were used as received from Aldrich Chemical Co. 2,3-dimethyly-1,3-butadiene received from Aldrich Chemical Co. was distilled prior to used. The ligand precursors $R_3PNSiMe_3$ and R_3PNLi were prepared as described in the literature.[67] MAO and $[Ph_3C][B(C_6F_5)_4]$ were used as received from NOVA Chemicals. ^1H, $^{13}C\{^1H\}$ and $^{31}P\{^1H\}$ spectra were recorded on a Bruker Avance 300 spectrometer operating at 300, 75 and 121 MHz respectively. ^1H and $^{13}C\{^1H\}$ spectra were internally referenced to trace amounts of protonated solvents and chemical shifts are reported relative to $SiMe_4$, while $^{31}P\{^1H\}$ spectra were referenced externally to 85% H_3PO_4. Combustion analyses were performed by Guelph Chemical Labs Inc., Guelph, Ontario.

Ethylene Polymerization (i) A solution of 6 to 10 μmol of catalyst precursor in 2.0 mL of dry toluene was added to a flask containing 2.0 mL of dry toluene. 500 equivalents of a 10% by weight toluene solution of MAO was added to the flask. Alternatively, the catalyst precursors were combined with $[Ph_3C][B(C_6F_5)_4]$ under an ethylene atmosphere at 25 °C. The flask was attached to a Schlenk line with cold trap, a stopwatch was started and the flask was evacuated three times for five seconds and refilled with pre-dried 99.9% ethylene gas. The solution was rapidly stirred under 1 atmosphere of ethylene at room temperature. The polymerization was stopped by the injection of a 1.0 N HCl/methanol solution. The total reaction time was noted and the polymer was isolated.

(ii) A 1L autoclave was dried under vacuum (10^{-2} mmHg) for several hours. Dried toluene (500 mL) was transferred into the vessel under a positive pressure of N_2, and was heated to 30 °C. The temperature was controlled (to *ca.* ± 2 °C) with an external heating/cooling bath and was monitored by a thermocouple that extended into the polymerization vessel. A solution of MAO (500 equiv.) in toluene was injected, and the mixture was stirred for 3 min at a rate of 150 RPM. The catalyst precursor in a solution of toluene was then injected while the reaction mixture was stirred for 3 minutes at the same rate. The rate of stirring was further increased to 1000 RPM, and the vessel was vented of N_2 and was pressurized with ethylene (33 psi). Any recorded exotherm was within the allowed temperature differential of the heating/cooling system. The solution was stirred for 1 hour, after which time the reaction was quenched with 1 M HCl in MeOH. The precipitated polymer was subsequently washed with MeOH, and dried at 100 °C for at least 24 hours prior to weighing.

Synthesis of Cp*ZrCl$_2$(NP-*i*-Pr$_3$), 41

To a slightly turbid yellow toluene solution (80 mL) of Cp*ZrCl$_3$ (1.00 g; 3.00 mmol) was added a toluene solution (10 mL) of *i*-Pr$_3$P=NLi$^+$ (0.54 g; 3.00 mmol). The solution was stirred at room temperature overnight. The resulting solution was filtered. Removal of toluene under vacuum gave a yellow solid. **41:** Yield: 1.11 g (74%). $^{31}P\{^1H\}$ NMR (25 °C, C_6D_6): δ 27.37. ^1H NMR (25 °C, C_6D_6): δ 2.16 (s, 15H, CH_3), 1.61 (m, 3H, CH, $|J_{H-H}|$ = 7 Hz), 0.92 (quart, 18H, CH_3, $|J_{H-H}|$ = 7 Hz). $^{13}C\{^1H\}$ NMR (25 °C, C_6D_6): δ 122.1 (s, Cp*), 26.3 (d, CH, $|J_{P-C}|$ = 59 Hz), 17.1 (s, CH_3), 12.3 (s, CH_3). Anal. Calcd for $C_{19}H_{36}Cl_2NPZr$: C: 48.39; H: 7.69; N: 2.97%. Found: C: 48.25; H: 8.83; N: 3.04%.

Synthesis of $Cp^*Zr(CH_3)_2(NP\text{-}i\text{-}Pr_3)$, 42

To a yellow benzene solution (5 mL) of $Cp^*ZrCl_2(NP\text{-}i\text{-}Pr_3)$ (100 mg; 0.21 mmol) was added a (0.14 mL, 0.42 mmol) 3.0 M diethyl ether solution of CH_3MgBr. The solution was stirred at room temperature overnight. Removal of benzene under vacuum gave a yellow solid. The solid was extracted with (4 x 5 mL) hexane. Filtration was followed by evaporation of hexane to achieve a yellow product. **42:** Yield: 73 mg (80%). $^{31}P\{^1H\}$ NMR (25 °C, C_6D_6): δ 22.5. ^1H NMR (25 °C, C_6D_6): δ 2.10 (s, 15H, CH_3), 1.64 (m, 3H, CH, $|J_{H\text{-}H}|$ = 7 Hz), 0.98 (quart, 18H, CH_3, $|J_{H\text{-}H}|$ = 7 Hz), 0.08 (s, 6H, CH_3). $^{13}C\{^1H\}$ NMR (25 °C, C_6D_6): δ 117.1 (s, Cp*), 31.3 (s, CH_3), 26.8 (d, CH, $|J_{P\text{-}C}|$ = 58 Hz), 17.5 (s, CH_3), 12.0 (s, CH_3).

Synthesis of $Cp^*Zr(\eta^3\text{-allyl})_2(NP\text{-}i\text{-}Pr_3)$, 43, $Cp^*Zr(\eta^3\text{-allyl})_2(NP\text{-}t\text{-}Bu_3)$, 44

Compounds **43** and **44** were prepared through similar routes, thus only one representative procedure is described. To a clear yellow benzene solution (5 mL) of $Cp^*ZrCl_2(NP\text{-}i\text{-}Pr_3)$ (100 mg; 0.21 mmol) was added a (0.14 mL. 0.42 mmol) 1.0 M diethyl ether solution of allylMgBr. After stirring for 30 minutes, the mixture became brownish orange in colour. The solution was allowed to stir overnight. Removal of benzene under vacuum gave a brownish orange viscous oil. The oil was extracted with (2 x 5 mL) hexane, followed by filtration and evaporation under vacuum. A brownish orange oil was obtained. **43:** Yield: 71%. $^1P\{^1H\}$ NMR (25 °C, C_6D_6): δ 21.3. ^1H NMR (25 °C, C_6D_6): δ 6.00 (quint, 2H, CH, $|J_{H\text{-}H}|$ = 12 Hz), 3.23 (d, 4H, CH_2, $|J_{H\text{-}H}|$ = 12 Hz), 1.88 (s, 15H, Cp*). 1.54 (m, 3H, CH, $|J_{H\text{-}H}|$ = 7 Hz), 0.84 (quart, 18H, $|J_{H\text{-}H}|$ = 7 Hz). $^{13}C\{^1H\}$ NMR

(25 °C, C_6D_6): δ 143.4 (s, CH), 115.1 (s, Cp*), 73.4 (s, CH_2), 26.4 (d, CH, $|J_{P-C}|$ = 57 Hz), 17.6 (s, CH_3), 12.2 (s, CH_3).

44: Yield: 73 % white solid. $^{31}P\{^1H\}$ NMR (25 °C, C_6D_6): δ 29.1. ^1H NMR (25 °C, C_6D_6): δ 6.04 (quint, 2H, CH, $|J_{H-H}|$ = 12 Hz), 3.27 (d, 4H, CH_2, $|J_{H-H}|$ = 12 Hz), 1.89 (s, 15H, Cp*). 1.12 (d, 27H, CH_3, $|J_{H-H}|$ = 18 Hz). $^{13}C\{^1H\}$ NMR (25 °C, C_6D_6): δ 143.6 (s, CH), 115.1 (s, Cp*), 73.3 (s, CH_2), 41.1 (d, C, $|J_{P-C}|$ = 46 Hz), 30.1 (s, CH_3), 12.2 (s, CH_3).

Synthesis of Cp*ZrPh$_2$(NP-*i*-Pr$_3$), 45; Cp*ZrPh$_2$(NP-*t*-Bu$_3$), 46

Both compounds **45** and **46** were synthesized in similar routes, thus only one representative procedure is described. To a yellow benzene solution (5 mL) of Cp*ZrCl$_2$(NP-*i*-Pr$_3$) (100 mg; 0.21 mmol) was added a (0.14 mL) diethyl ether solution of C_6H_5MgBr (3.0 M; 0.42 mmol). The solution was stirred at room temperature overnight. Removal of benzene under vacuum gave yellow oil. The solid was extracted with (4 x 5 mL) hexane. Evaporation of hexane gave a yellow product. **45:** Yield: 82%. $^{31}P\{^1H\}$ NMR (25 °C, C_6D_6): δ 24.7. ^1H NMR (25 °C, C_6D_6): δ 7.94 (m, 4H, *o*-C_6H_5, $|J_{H-H}|$ = 7 Hz), 7.35 (m, 4H, *m*-Ar, $|J_{H-H}|$ = 7 Hz), 7.23 (m, 2H, *p*-Ar, $|J_{H-H}|$ = 7 Hz), 2.03 (s, 15H, Cp*), 1.60 (m, 3H, CH, $|J_{H-H}|$ = 7 Hz), 0.85 (quart, 18H, CH_3, $|J_{H-H}|$ = 7 Hz). $^{13}C\{^1H\}$ NMR (25 °C, C_6D_6): δ 189.1 (s, *ipso*-Ar), 137.0 (s, *o*-Ar), 126.9 (s, *m*-Ar), 126.8 (*p*-Ar), 119.5 (s, Cp*), 26.4 (d, CH, $|J_{P-C}|$ = 57 Hz), 17.5 (s, CH_3), 12.6 (s, CH_3).

46: Yield: 79 % white solid. $^{31}P\{^1H\}$ NMR (25 °C, C_6D_6): δ 35.8. ^1H NMR (25 °C, C_6D_6): δ 7.95 (m, 4H, *o*-Ar, $|J_{H-H}|$ = 7 Hz), 7.34 (m, 4H, *m*-Ar, $|J_{H-H}|$ = 7 Hz), 7.21 (m, 2H, *p*-Ar, $|J_{H-H}|$ = 7 Hz), 1.98 (s, 15H, Cp*), 1.10 (d, 27H, CH_3, $|J_{H-H}|$ = 12 Hz). $^{13}C\{^1H\}$

NMR (25 °C, C_6D_6): δ 189.5 (s, *ipso*-Ar), 136.8 (s, *o*-Ar), 126.9 (s, *m*-Ar), 126.7 (s, *p*-Ar), 119.5 (s, Cp*), 40.7 (d, C, $|J_{P-C}|$ = 47 Hz), 30.0 (s, CH_3), 12.7 (s, CH_3). Anal. Calcd for $C_{34}H_{52}NPZr$: C: 68.40; H: 8.78; N: 2.35%. Found: C: 61.50; H: 8.72; N: 2.39%.

Synthesis of (Cp*)CpZrCl(NP-*i*-Pr$_3$), 47; (Cp*)CpZrCl(NP-*t*-Bu$_3$), 48

Both compounds **47** and **48** were prepared in similar routes, thus only one representative procedure is described. To a yellow THF solution (5 mL) of Cp*(^{i}Pr$_3$P=N)ZrCl$_2$ (100 mg; 0.21 mmol) was added a THF solution of (3 mL) NaCp·(THF)$_2$ (123mg; 0.53 mmol). The solution was stirred at room temperature overnight. Removal of benzene under vacuum gave a yellow solid. The solid was extracted with (4 x 5 mL) hexane, followed by filtration and evaporation under vacuum. **47:** Yield: 57% light yellow solid. $^{31}P\{^1H\}$ NMR (25 °C, C_6D_6): δ 24.0. ^1H NMR (25 °C, C_6D_6): δ 6.13 (s, 5H, Cp), 1.99 (s, 15H, Cp*), 1.75 (m, 3H, CH, $|J_{H-H}|$ = 7 Hz), 0.98 (quart, 18H, CH_3, $|J_{H-H}|$ = 7 Hz). $^{13}C\{^1H\}$ NMR (25 °C, C_6D_6): δ 119.0 (s, Cp*), 111.7 (s, Cp), 27.9 (d, CH, $|J_{P-C}|$ = 57 Hz), 17.4 (s, CH_3), 12.5 (s, CH_3). Anal. Calcd for $C_{24}H_{41}ClNPZr$: C: 57.51; H: 8.24; N: 2.79%. Found: C: 57.76; H: 9.11; N: 2.91%.

48: Yield: 68 % light yellow solid. $^{31}P\{^1H\}$ NMR (25 °C, C_6D_6): δ 37.8. ^1H NMR (25 °C, C_6D_6): δ 6.27 (s, 5H, Cp), 2.02 (s, 15H, Cp*), 1.28 (d, 27H, CH_3, $|J_{H-H}|$ = 12 Hz). $^{13}C\{^1H\}$ NMR (25 °C, C_6D_6): δ 119.9 (s, Cp*), 112.3 (s, Cp), 41.2 (d, C, $|J_{P-C}|$ = 46 Hz), 30.5 (s, CH_3), 12.9 (s, CH_3).

Synthesis of Cp*(*i*-Pr_3P=N)Zr(*s-cis*-η^4-2,3-dimethyl-1,3-butadiene), 49; Cp*(*t*-Bu_3P=N)Zr(*s-cis*-η^4-2,3-dimethyl-1,3-butadiene), 50

Both compounds **49** and **50** were prepared in similar routes, thus only one representative procedure is described. To a clear yellow THF solution (5 mL) of Cp*$ZrCl_2$(NP-*i*-Pr_3) (200 mg; 0.42 mmol), an excess of Mg powder (30 mg; 1.26 mmol) was added. Addition of 2,3-dimethyl-1,3-butadiene (34.5 mg; 0.42 mmol) was followed after 30 minutes of stirring. The solution mixture was allowed to stir for two days at room temperature. Removal of THF under vacuum gave a dark green solid. The solid was extracted with hexane (4 x 5 mL), followed by filtration and evaporation. **49:** Yield: 76 % orange crystalline solid. $^{31}P\{^1H\}$ NMR (25 °C, C_6D_6): δ 19.1. ^1H NMR (25 °C, C_6D_6): δ 2.73 (d, 2H, CH_2, $|J_{H-H}|$ = 9 Hz), 2.14 (s, 15H, Cp*), 2.10 (s, 6H, CH_3), 1.55 (m, 3H, CH, $|J_{H-H}|$ = 7 Hz), 0.87 (quart, 18H, CH_3, $|J_{H-H}|$ = 7 Hz), -0.06 (d, 2H, CH_2, $|J_{H-H}|$ = 9 Hz). $^{13}C\{^1H\}$ NMR (25 °C, C_6D_6): δ 122.2 (s, C), 115.6 (s, Cp*), 57.2 (s, CH_2), 28.0 (d, CH, $|J_{P-C}|$ = 57 Hz), 25.0 (s, CH_3), 17.9 (s, CH_3), 12.7 (s, CH_3). Anal. Calcd for $C_{25}H_{46}NPZr$: C: 62.19; H: 9.60; N: 2.90%. Found: C: 53.82; H: 9.80; N: 2.95%.

50: Yield: 75 % orange crystalline solid. $^{31}P\{^1H\}$ NMR (25 °C, C_6D_6): δ 33.2. ^1H NMR (25 °C, C_6D_6): δ 2.20 (s, 6H, CH_3), 2.17 (d, 2H, CH_2, $|J_{H-H}|$ = 11 Hz), 2.12 (s, 15H, Cp*), 1.12 (d, 27H, CH_3, $|J_{P-H}|$ = 12 Hz), 0.38 (d, 2H, CH_2, $|J_{H-H}|$ = 11 Hz). $^{13}C\{^1H\}$ NMR (25 °C, C_6D_6): δ 121.6 (s, C), 115.8 (s, Cp*), 55.3 (s, CH_2), 40.0 (d, C, $|J_{P-C}|$ = 48 Hz), 30.5 (s, CH_3), 25.6 (s, CH_3), 12.7 (s, CH_3). Anal. Calcd for $C_{28}H_{52}NPZr$: C: 64.07; H: 9.98; N: 2.67%. Found: C: 56.88; H: 10.55; N: 2.55%.

General Information on X-Ray Data Collection and Reduction

All X-ray data collection, data reduction, structure solution and refinement obtained in this thesis were performed by using the same method; thus only one general description is given.

X-ray quality crystals were manipulated and mounted in either 0.5 mm or 0.7 mm capillaries in a glove box, thus a dry, O_2-free environment for each crystal was maintained. Diffraction experiments were performed on a Siemens Smart systems CCD diffractometer employing graphite-monochromatized Mo Kα radiation (λ = 0.71073 Å) and collecting a hemisphere of data with 30-second exposure times. Data were further processed using the SHELX crystallographic software operating on a SGI Indy workstation. An empirical absorption correction was applied to the data using SADABS. The reflections with $F_o^2 > 3\sigma F_o^2$ were used in the refinements.

General Information of Structure Solution and Refinement

Non-hydrogen atomic scattering factors were taken from literature tabulations.[68] Atom positions were determined either by SHELXTL-93 direct methods or a Patterson routine with successive difference Fourier map calculations. Refinements were carried out by full-matrix least-squares techniques on *F* minimizing the function $\omega(|F_o| - |F_c|)^2$ where the weight ω is defined as $4F_o^2/2\sigma(F_o^2)$ and F_o and F_c are the observed and calculated structure factor amplitudes, respectively. In the final cycles of refinements, all non-hydrogen atoms were assigned anisotropic temperature factors. Hydrogen atom positions were calculated to ride on the carbon atoms to which they were bound assuming a C-H bond length of 0.95 Å and hydrogen atom temperature factors were fixed at 110%

of the temperature factors of the carbon atoms to which they were bound. All hydrogen atom contributions were calculated but not refined. After final cycles of refinement no chemically significant residual electron density was observed.

X-Ray Structure Determinations of 41, 54[69], 44, 46, 47, 49 and 50

Data were collected at room temperature. No crystal decay was observed for any of the compounds. The resulting crystallographic values are given in Table 2.1. ORTEP drawings of **41**, **54**[69], **44**, **46**, **47**, **49** and **50** are shown in Figures 2.1, 2.2, 2.3, 2.4, 2.5 and 2.7 respectively, with 30% thermal ellipsoids. Selected bond distances and angles are listed in the captions for Figures 2.1, 2.2, 2.3, 2.4, 2.5 and 2.7 respectively. Other structural parameters are given in Table A1.1 – A1.6 in Appendix One.

Table 2.1: Crystallographic Parameters for 41, 44 and 46

	41	44	46
Formula	$C_{19}H_{36}Cl_2NPZr$	$C_{28}H_{52}NPZr$	$C_{34}H_{52}NPZr$
Formula weight	471.58	524.90	596.96
a(Å)	8.275(2)	8.75600(10)	16.8506(2)
b(Å)	15.282(5)	11.6427(2)	11.446
c(Å)	19.690(5)	15.8052(1)	33.7035(5)
α(°)	90	101.015(1)	90
β(°)	90	90.495(1)	102.803(1)
γ(°)	90	110.786(1)	90
Crystal system	Orthorhombic	Triclinic	Monoclinic
Space group	$P2_12_12_1$	P-1	$P2_1/n$
Volume ($Å^3$)	2490.0(12)	1473.47(3)	6339.01(12)
D_{calc} (gcm^{-1})	1.258	1.183	1.251
Z	4	2	8
Abs coeff, μ, cm^{-1}	0.722	0.442	0.419
Temp (°C)	293(2)	293(2)	293(2)
F(000)	984	564	2544
2θ range (°)	1.69 – 25.00	1.91 – 25.00	1.26 – 25.00
h	-9 – +9	-10 – +10	-20 – +18
k	-17 – +18	-13 – +9	-13 – +13
l	-21 – +23	-18 – +18	-40 – +38
Refl collected	12905	7696	31839
R_{int}	0.0488	0.0119	0.043
Data $F_o^2>3\sigma(F_o^2)$	4350	5032	11015
Parameters	217	280	667
R(%)a	0.0658	0.0433	0.0514
R_w(%)a	0.1590	0.1191	0.1400
Peak, hole ($e^-Å^{-3}$)	0.840, -0.288	0.900, -0.652	0.757, -0.756
Goodness of fit	1.066	1.046	0.750

$^aR = \Sigma ||F_o| - |F_c|| / \Sigma |F_o|$, $Rw = [\Sigma(|F_o| - |F_c|)^2| / \Sigma |F_o|^2]^{0.5}$

Table 2.2: Crystallographic Parameters for 47, 49 and 50

	47	49	50
Formula	$C_{24}H_{41}ClNPZr$	$C_{25}H_{46}NPZr$	$C_{28}H_{52}NPZr$
Formula weight	501.22	482.82	524.90
a(Å)	8.2990(1)	9.3541(2)	10.4976(3)
b(Å)	15.2858(3)	17.8965(4)	15.9192(4)
c(Å)	20.3234(1)	16.5357(3)	17.7561(4)
α(°)	90	90	90
β(°)	98.36	102.319(1)	96.213(1)
γ(°)	90	90	90
Crystal system	Monoclinic	Monoclinic	Monoclinic
Space group	$P2_1/n$	$P2_1/c$	$P2_1/n$
Volume ($Å^3$)	2550.78(6)	2704.4(1)	2949.85(13)
D_{calc} (gcm^{-1})	1.305	1.186	1.182
Z	4	4	4
Abs coeff, μ, cm^{-1}	0.608	0.476	0.441
Temp (°C)	293(2)	293(2)	293(2)
F(000)	1056	1032	1128
2θ range (°)	1.67 – 24.99	2.23 – 25.00	1.72 – 25.00
h	-11 – +11	-11 – +11	-12 – +12
k	-20 – +16	-21 – +14	-18 – +18
l	-19 – +27	-19 – +19	-21 – +13
Refl collected	11967	13553	13957
R_{int}	0.2171	0.0272	0.0662
Data $F_o^2>3\sigma(F_o^2)$	4466	4690	5056
Parameters	253	253	280
R(%)a	0.0636	0.0386	0.0612
R_w(%)a	0.1079	0.1171	0.1199
Peak, hole ($e^-Å^{-3}$)	0.525, -1.611	0.374, -0.396	0.580, -0.478
Goodness of fit	0.467	0.954	1.026

$$^aR = \Sigma \, ||F_o| - |F_c|| \, / \, \Sigma \, |F_o|, \; Rw = [\Sigma(|F_o| - |F_c|)^2| \, / \, \Sigma \, |F_o|^2]^{0.5}$$

2.3 Results and Discussion

Synthesis and Structural Features of 41 and 53[69]

Initial attempts to synthesize zirconium phosphinimide complexes of the form $(Cp^*)ZrCl_2(NPR_3)$ via the reaction of Cp^*ZrCl_3 with the appropriate trimethylsilylphosphinimine ($R_3PNSiMe_3$) were unsuccessful. ^{31}P-NMR spectra revealed no reactions took place under either room temperature or high temperature conditions. In contrast, such complexes can be readily prepared through the reaction of Cp^*ZrCl_3 with the appropriate trialkylphosphinimide lithium salt ($R_3PN^-Li^+$) (**51** and **52**) under mild conditions (Scheme 2.1).

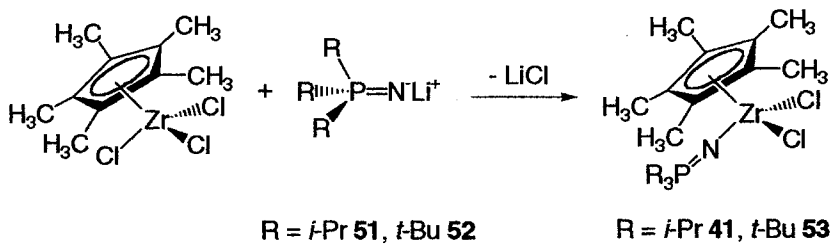

Scheme 2.1 Synthesis of monomeric zirconium phosphinimide complexes **41** and **53**.

Unlike the insoluble oligomeric (pentamethylcyclopentadienyl)zirconium trichloride $(Cp^*ZrCl_3)_n$[70], complexes **41** and **53** are monomeric. In particular, complex **41** can be crystallized from hydrocarbon solvents in high yield. The formulation of complex **41** was consistent with spectroscopic data. The pseudo tetrahedral geometry of the Zr coordination sphere was confirmed by crystallographic data (Figure 2.1). It was found that the P-N-Zr angle in the monomeric species **41** was 175.2(4)°. This is much closer to linear than that reported for the related dimeric ($[Zr_2Cl_4(NPMe_3)_4(\mu\text{-}HNPMe_3)]$) [71] and trimeric ($[Zr_3Cl_6(NPMe_3)_5]^+$)[72] species, which have angles of 159.3(2) – 155.6(2)° and 132.9(7) – 126.1(6)° respectively. The P-N bond distance of 1.569(7) Å was found

to be very close to that of the P=N double bonds in phosphinimide complexes of Ti(IV) and Zr (IV) which ranges between 1.560(1) – 1.653(4) Å.[58b] Moreover, the M-N bond distance of 1.926(7) Å was significantly shorter than the M=N double bond distances found in the dimeric and trimeric species ranging from 1.95(2) – 2.27(9) Å.[58b, 71, 72] This indicates partial M=N double bond character.

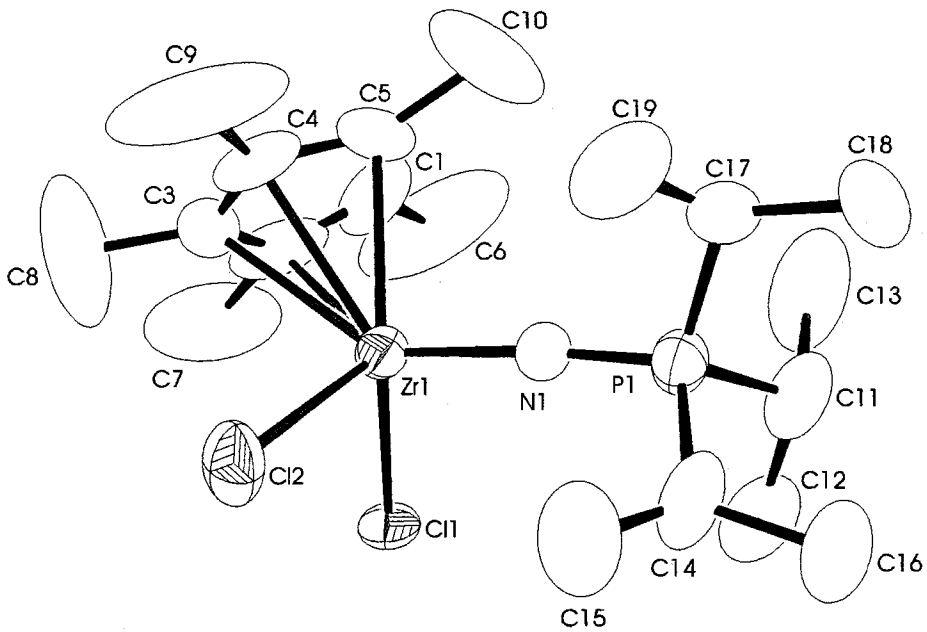

Figure 2.1 ORTEP drawing of **41**, 30% thermal ellipsoids are shown, all hydrogen atoms have been omitted for clarity. Selected bond distances and angles: Zr(1)-N(1) 1.926(7) Å, Zr(1)-Cl(1) 2.581(2) Å, Zr(1)-Cl(2) 2.559(3) Å, P(1)-N(1) 1.569(7) Å, P(1)-N(1)-Zr(1) 175.2(4)°, Cl(2)-Zr(1)-Cl(1) 94.70(10)°, N(1)-Zr(1)-Cl(1) 104.7(2)°, N(1)-Zr(1)-Cl(2) 104.0(2)°.

Salt Metathesis Reactions of 41 and 53

Although a large number of structural data for phosphinimide complexes has been reported,[58] the reactivity of such complexes has received little attention. As a consequence, pentamethylcyclopentadienyl zirconium phosphinimide dichloride complexes **41** and **53** were converted to the corresponding bis(alkyl), bis(aryl) and bis(allyl) compounds by a series of salt metathesis reactions using Grignard reagents

(RMgBr). In addition, $Cp^*ZrCl_2(NPR_3)$ was found to be a convenient starting material for the synthesis of the "mixed-ring" complexes of zirconium **47** and **48** (Scheme 2.2).

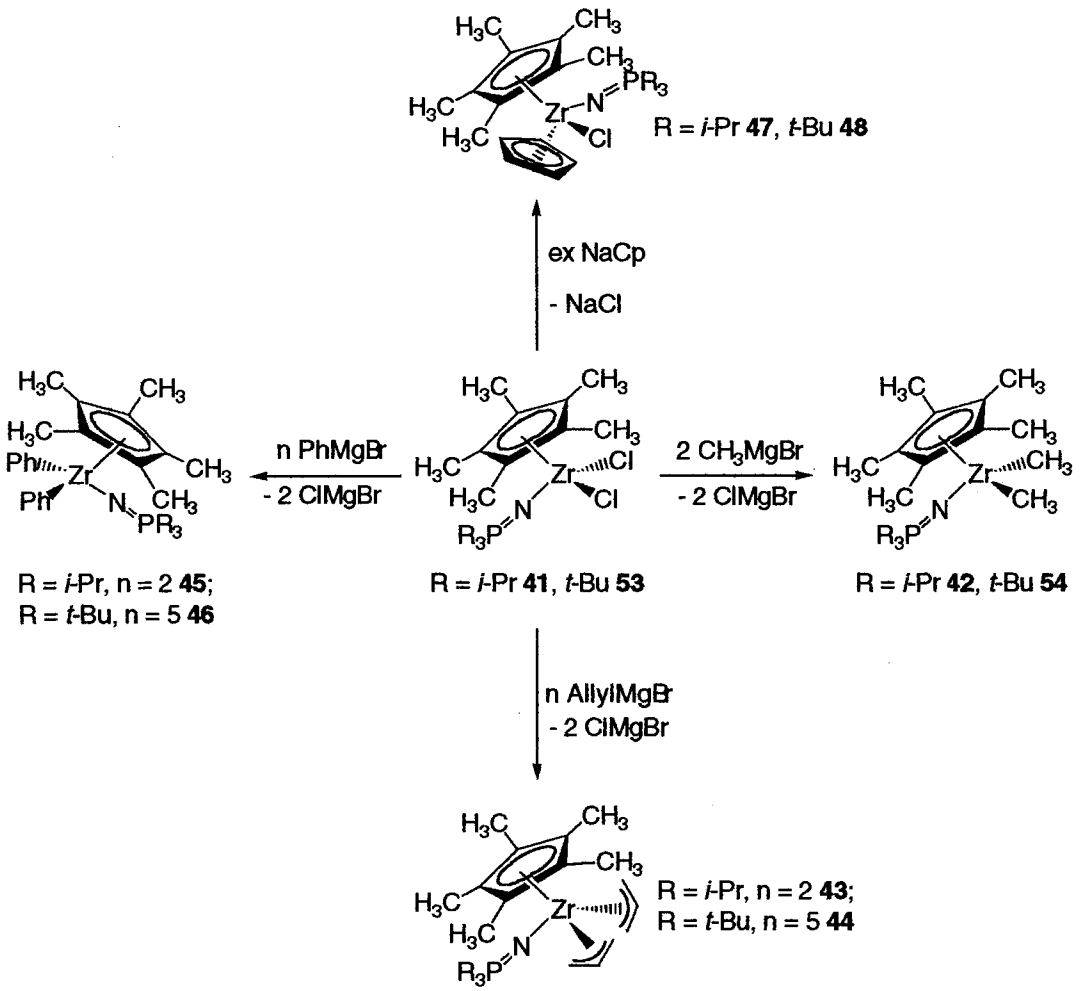

Scheme 2.2 Salt metathesis reactions of complexes **41** and **53**.

The analogous dimethyl derivatives $(Cp^*)ZrMe_2(NPR_3)$ were readily isolated in high yields as depicted in Scheme 2.2, where R = *i*-Pr **42**, *t*-Bu **54**[69]. The structures of the resulting complexes **42** and **54** were first proposed based on spectroscopic data and were later confirmed crystallographically (Figure 2.2).[69] The P-N-Zr angle in complex **54** was found to be 168.5(2)°, which is slightly less linear than that found in complex **53**. This

may be due to the steric repulsion between the bulky methyl groups and the phosphinimide ligand. The P-N bond distance of 1.574(2) Å suggests P=N double bond character and the slightly larger Zr-N bond distance of 1.955(2) Å corresponds to M-N single bond.

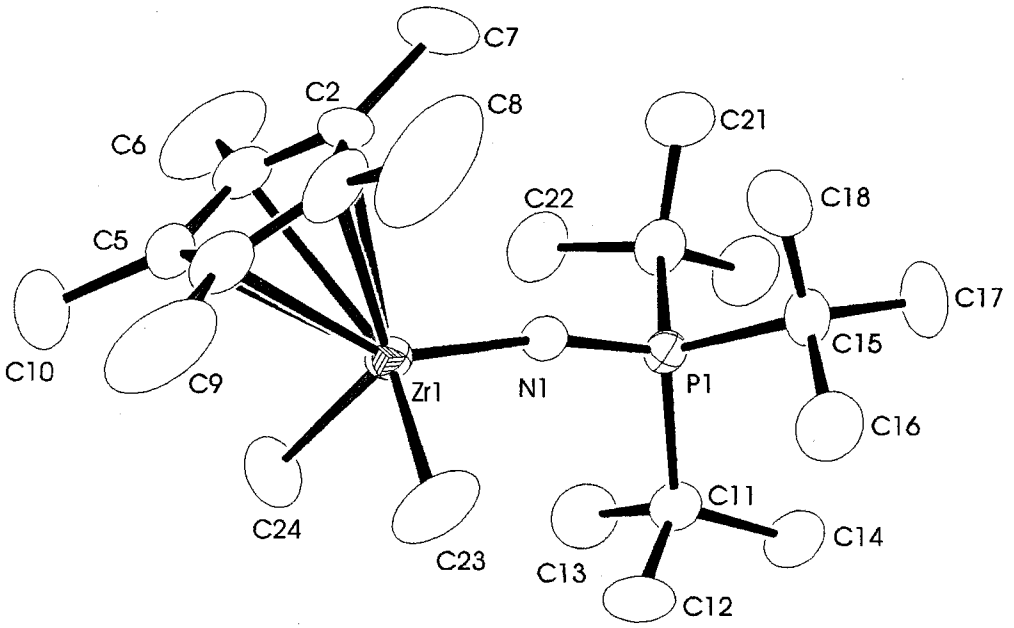

Figure 2.2 ORTEP drawing of **54**, 30% thermal ellipsoids are shown, hydrogen atoms have been omitted for clarity. Selected bond distances and angles: P(1)-N(1) 1.574(2) Å, Zr(1)-N(1) 1.955(2) Å, Zr(1)-C(23) 2.258(4) Å, Zr(1)-C(24) 2.265(4) Å, N(1)-Zr(1)-C(23) 104.4(2)°, N(1)-Zr(1)-C(24) 103.8(2)°, P(1)-N(1)-Zr(1) 168.5(2)°.[69]

Similarly, treatment of either **41** or **53** with the appropriate molar ratios of allyl-Grignard in hydrocarbon solvent affords complexes **43** and **44** in 71 and 73% yield respectively. The ^{1}H-NMR spectra obtained at 25 °C for complexes **43** and **44** clearly showed only one quintet for the CH protons of the allyl groups and one doublet for the corresponding CH_2 protons. In addition, variable-temperature ^{1}H-NMR spectra were recorded. It was observed that the resonances corresponding to the CH_2 and the CH

protons simply broadened upon cooling. This indicated the allyl groups underwent rapid η^1-η^3 interconversion in solution state even at –80 °C. Colourless single crystals of **44** were isolated from hexane solutions at room temperature. This complex was thermally stable in contrast to $CpZr(allyl)_3$, which crystallizes at –80 °C and slowly decomposes at temperatures above –10 °C even in the solid state.[73] An ORTEP drawing of complex **44** is shown in Figure 2.3.

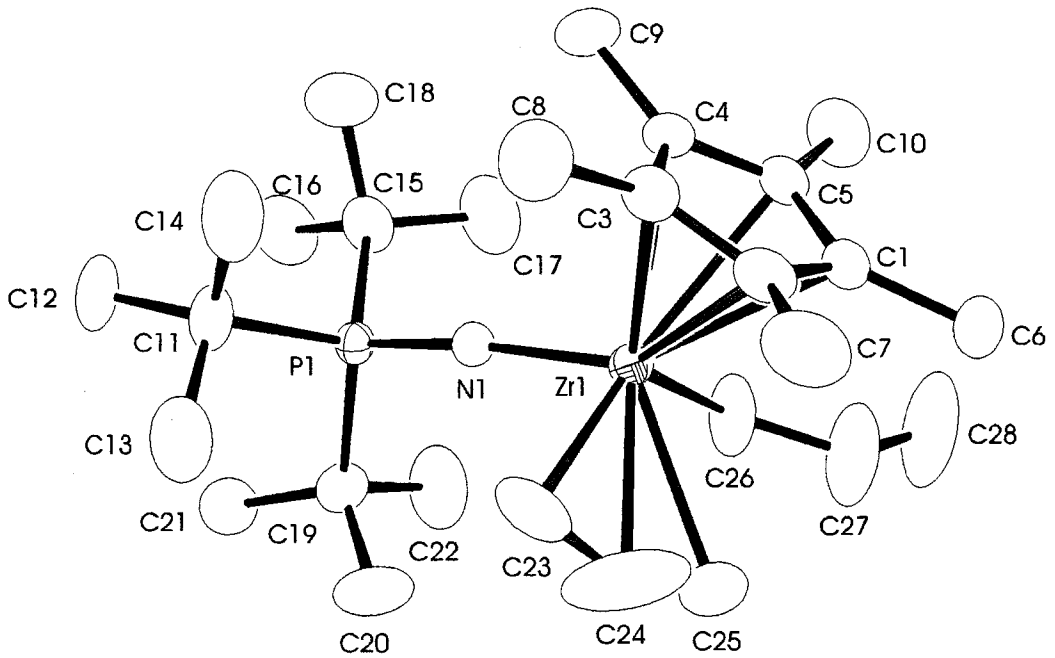

Figure 2.3 ORTEP drawing of **44**, 30% thermal ellipsoids are shown, hydrogen atoms have been omitted for clarity. Selected bond distances and angles: Zr(1)-N(1) 1.976(2) Å, Zr(1)-C(23) 2.490(5) Å, Zr(1)-C(24) 2.488(6) Å, Zr(1)-C(25) 2.543(6) Å, Zr(1)-C(26) 2.378(4) Å, P(1)-N(1) 1.588(2) Å, C(23)-C(24) 1.358(13) Å, C(24)-C(25) 1.165(13) Å, C(26)-C(27) 1.440(7) Å, C(27)-C(28) 1.163 (9) Å; P(1)-N(1)-Zr(1) 173.56(16) °, N(1)-Zr(1)-C(23) 94.20(13) °, N(1)-Zr(1)-C(24) 107.7(4) °, N(1)-Zr(1)-C(25) 118.8(2) °, N(1)-Zr(1)-C(26) 92.27(12) °.

The X-ray structure of complex **44** revealed a racemic molecule. The zirconium atom was coordinated to a η^5-pentamethylcyclopentadienyl ligand, the phosphinimide

ligand and the two differently bonded allyl groups in a pseudo tetrahedral geometry. One allyl group (C(26), C(27), C(28)) was found to be η^1-coordinated. The bond distance for Zr-C(26) was 2.378(4) Å. This was found to be significantly shorter than the distances of Zr-C(23), Zr-C(24) and Zr-C(25). The bond distance for C(26)-C(27) was 1.440(7) Å, while the bond length for C(27)-C(28) was found to be 1.163(9) Å. The second allyl group (C(23), C(24), C(25)) was found to be η^3-coordinated. The bond distances between the zirconium and the three carbon atoms of the allyl group were found to be similar. The C(24)-C(25) bond length was found to be significantly shorter than the C(23)-C(24) bond length. Pronounced allyl ligand distortions observed in the solid state structure of complex **44** suggests that the solid state structure can be regarded as a model for the intermediate stage in the dynamic η^3-η^1 intramolecular rearrangement of the allyl ligands observed in solution.[73, 74]

As shown in Scheme 2.2, pentamethylcyclopentadienyl bis(aryl) zirconium phosphinimide complexes **45** and **46** were also prepared in a similar manner via the reactions of phenyl Grignard reagents with complex **41** and **53** in 82 and 79% yield respectively. Complex **45** was formulated based on spectroscopic data, while complex **46** was fully characterized by both spectroscopic and crystallographic data. Single-crystals of **46** were isolated from hexane at room temperature. The corresponding ORTEP drawing is shown in Figure 2.4.

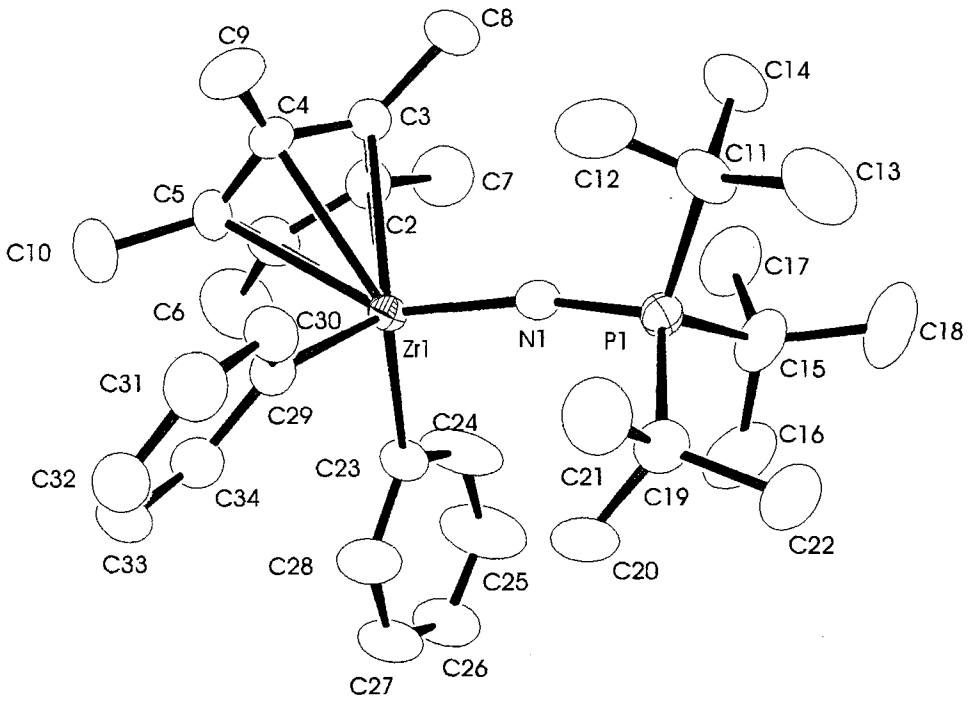

Figure 2.4 ORTEP drawing of **46**, 30% thermal ellipsoids are shown, hydrogen atoms have been omitted for clarity. Selected bond distances and angles: Zr(1)-N(1) 1.922(4) Å; P(1)-N(1) 1.551(4) Å; P(1)-N(1)-Zr(1) 168.2(2) °.

Reactions of diphenylzirconocene with alkynes have been studied extensively by Buchwald[75] and Erker[76] individually. In an analogous manner, attempts to use $Cp^*ZrPh_2(NPi\text{-}Pr_3)$ as the synthon were undertaken. Addition of excess donor ligand (PMe_3)[75] to trap the mononuclear η^2-benzyne type complexes of zirconium (**55**) via thermolysis was unsuccessful. Several unidentified resonances were observed from $^{31}P\{^1H\}$-NMR spectrum. Furthermore, attempts to generate metallacycles (**56**, **57**) via coupling reactions between complex **45** and symmetrical alkynes[75, 76] also failed (Scheme 2.3).

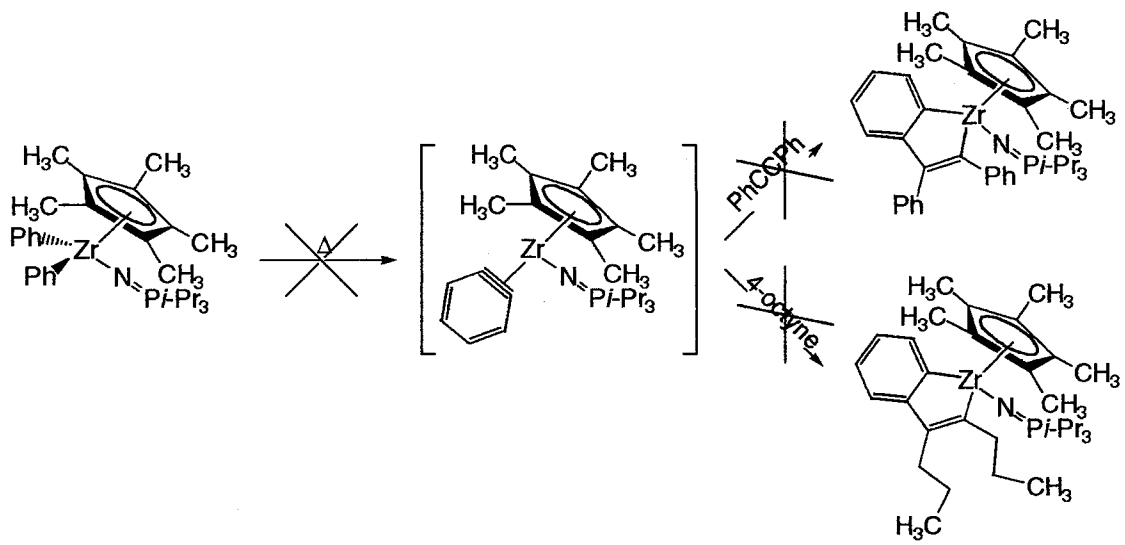

Scheme 2.3 Coupling reactions of $Cp^*ZrPh_2(NP\text{-}i\text{-}Pr_3)$ **45** with symmetrical alkynes.

$Cp^*CpZrCl(NPR_3)$ "mixed-ring" complexes of **47** and **48** were prepared cleanly from large excess of sodium cyclopentadienide (NaCp) and **41** or **53** respectively in THF at room temperature. The resulting complexes **47** and **48** were isolated in 57 and 68% yield respectively. The proposed η^5-coordination of Cp* and Cp were supported by the spectroscopic data. The resonances for both ligands were found to be singlet in both ^{1}H- and ^{13}C-NMR spectra for complexes **46** and **47**. This bonding mode was later confirmed with a crystallographic study (Figure 2.5). This result was found to be contrary to the analogous mixed-ring phosphinimide titanium complexes, which consists of an η^5-coordinated Cp* and an η^1-coordinated Cp ligands.[77] This was attributed to the fact that the coordination sphere of zirconium is larger than that of the titanium, thus it could accommodated both the Cp and Cp* ligands in η^5-coordination modes.

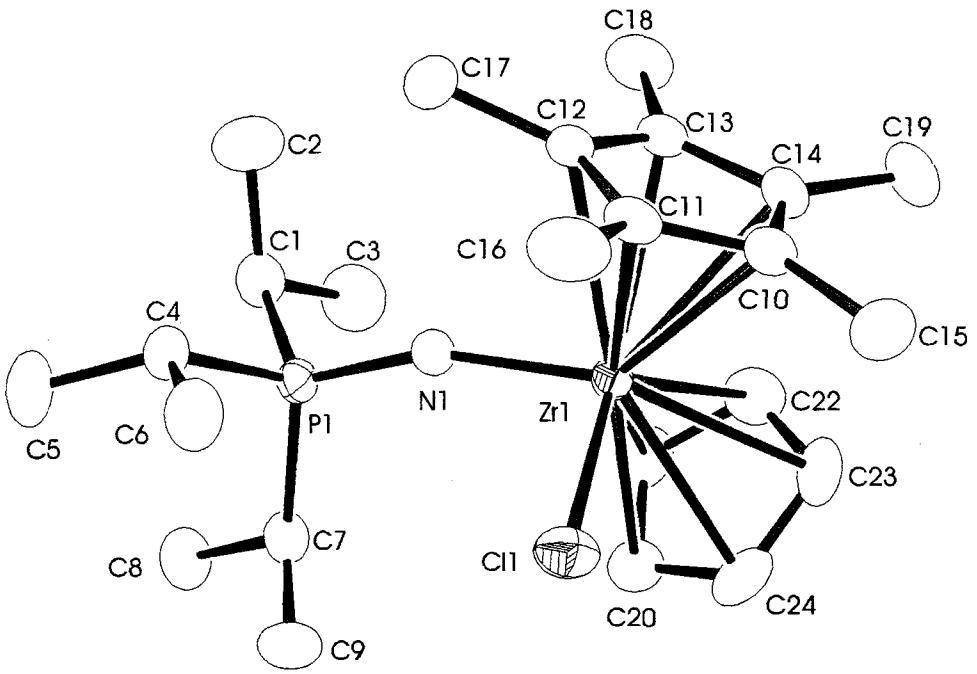

Figure 2.5 ORTEP drawing of **47**, 30% thermal ellipsoids are shown, hydrogen atoms have been omitted for clarity. Selected bond distances and angles: Zr(1)-N(1) 1.976(2) Å, Zr(1)-Cl(1) 2.5070(8) Å, Zr(1)-C(10) 2.589(3) Å, Zr(1)-C(11) 2.592(3) Å, Zr(1)-C(12) 2.581(3) Å, Zr(1)-C(13) 2.563(3) Å, Zr(1)-C(14) 2.591(3) Å, Zr(1)-C(20) 2.567(3) Å, Zr(1)-C(21) 2.536(3) Å, Zr(1)-C(22) 2.526(3) Å, Zr(1)-C(23) 2.570(3) Å, Zr(1)-C(24) 2.585(3) Å, P(1)-N(1) 1.565(2) Å; N(1)-Zr(1)-Cl(1) 98.60(7) °, P(1)-N(1)-Zr(1) 161.2(2) °.

Reactions of 41 and 53 with 2,3-dimethyl-1,3-butadiene

Reactivity studies of pentamethylcyclopentadienyl phosphinimide zirconium complexes with symmetrically substituted butadienes were also investigated. Preparation of transition metal butadiene complexes via photolysis of diphenylzirconocene in the presence of a slight excess of suitable conjugated dienes has been previously reported.[78] The most commonly reported synthetic strategy for preparing transition metal butadiene complexes was by reacting the appropriate transition metal starting materials with the magnesium butadiene complex ([Mg(butadiene)·2THF]$_n$).[79-83] The magnesium butadiene

complex is oligomeric. It functions as a source of butadiene dianion.[84] The generation of the oligomeric magnesium butadiene is a time consuming process, taking between 15 hours to 5 days. Additionally, maintenance of the temperature at –78 to 40 °C over this period of time is also required. As a result, modifications of the synthetic strategy were necessary.

Reactions of $Cp^*ZrCl_2(NPR_3)$ (R = *i*-Pr$_3$ **41** and *t*-Bu$_3$ **53**) with a large excess of magnesium powder in THF, followed by the addition of exactly one equivalent of distilled 2,3-dimethyl-1,3-butadiene. A dark green solution resulted after 24 hours of stirring at room temperature. Extraction with hexane generated the desired orange *s-cis*-η^4-2,3-substituted butadiene phosphinimide zirconium complexes **49** and **50** respectively. Crystallization occurred upon concentration of the hexane solution. This reaction scheme is illustrated in Scheme 2.4.

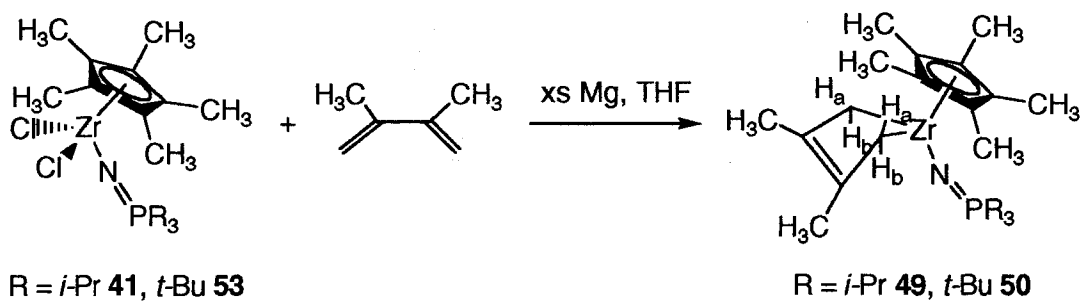

R = *i*-Pr **41**, *t*-Bu **53** R = *i*-Pr **49**, *t*-Bu **50**

Scheme 2.4 One-pot synthesis of complexes **49** and **50**.

The structural features of transition metal diene complexes had been studied extensively.[82, 85, 86, 87] A large collection of X-ray and NMR data proved that group(IV) diene complexes adopt either the bent (σ^2, π-bonded)η^4-metallacyclo-3-pentene structure (**A**), the planar (σ^2-bonded)η^2-metallacyclo-3-pentene structure (**B**) or the novel (η^4-*s-trans*-diene)metal structure (**C**). In addition, Group(IV) diene complexes of structure **A**

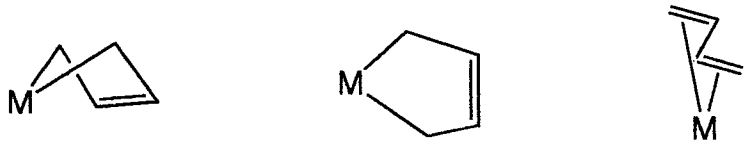

A **B** **C**

generally exhibit fluxional behaviour. This results in rapid ring inversion (flipping) via a transitory planar structure **B** and is commonly observed by variable temperature ^{1}H-NMR spectroscopy. As a consequence, variable temperature $^1H\{^{31}P\}$-NMR spectra over a temperature range of 30 to -85 °C for complexes **49** and **50** was recorded. At ambient temperature, two doublets of equal intensity corresponded to the terminal CH_2 of the diene were readily identified from the ^{1}H-NMR (500 MHz) spectrum. For complex **49**, the two doublets for the terminal CH_2 signals of the diene appeared at 2.73 ppm (J_{H-H} = 9 Hz) and –0.06 ppm (J_{H-H} = 9 Hz). In the case for complex **50**, the doublets for the terminal CH_2 signals of the diene appeared at 2.17 ppm (J_{H-H} = 11 Hz) and 1.12 ppm (J_{H-H} = 12 Hz). The proton coupling constants was found to be consistent with Cp_2Zr(2,3- dimethyl-1,3- butadiene)[80] and Cp_2Zr(1,3-butadiene).[80] This supports the suggestion of a *s-cis*-η^4-1,3-diene structure. The resonances corresponding to the terminal CH_2 protons of the diene were broadened upon cooling but no new signals were observed (Figure 2.6). This indicated a rigid structural motif, presumably due to the strong π-interations between the inner carbons and the central zirconium metal.[80]

In addition, the terminal CH_2 signals of the diene ligand of complexes **49** and **50** were assigned to the corresponding *anti* and *syn* protons. The resonance at the lower magnetic field was assigned to the *syn* protons (H_b) while the resonance at the higher magnetic field was assigned to the *anti* protons (H_a). This is attributed to the location of

the *anti* protons in the diamagnetic shielding zone generated by the Cp*-Zr bond. In other words, the *anti* protons reside in a highly shielded environment. As a result, the *anti* protons appeared at a remarkably high field region.

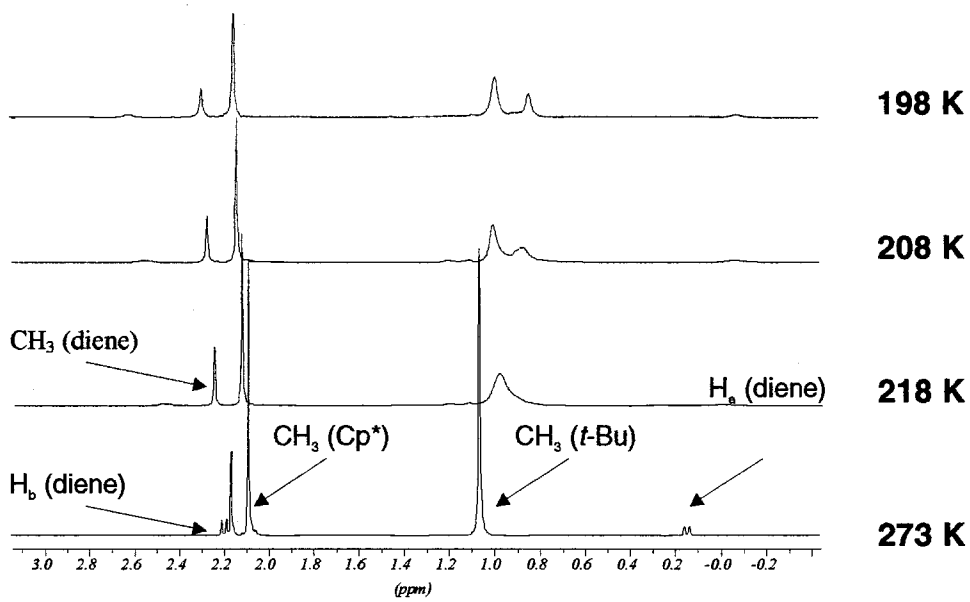

Figure 2.6 Temperature dependent $^{1}H\{^{31}P\}$-NMR of complex **50**.

Simultaneously, the resonance at 1.15 ppm attributed to the methyl protons of the *t*-butyl groups, showed marked temperature dependence. The $^{1}H\{^{31}P\}$-NMR spectrum recorded at room temperature exhibited only one sharp resonance for the *t*-butyl methyl protons. This signal began to broaden upon cooling. As the temperature reached –60 °C, the *t*-Bu methyl resonance continue to broaden and slowly split into two resonances. At –75 °C, the resonance was completely split into two resonances in a ratio of 2:1 (Figure 2.6). This phenomenon indicated rotation of the *t*-Bu_3 ligand was slow and two of the *t*-butyl groups were equivalent. This data is consistent with the temperature

dependence phenomenon arising from sterically inhibited rotation about the P-C bond. Analogous phenomena have been seen in systems with bulky substituents.[88]

Additionally, the bent (σ^2, π-bonded)η^4-metallocyclo-3-pentene structure was later confirmed by the X-ray data for both complexes **49** and **50**. The ORTEP drawings for both complexes **49** and **50** are displayed in Figure 2.7. This specific structural motif may be a result of strong steric congestion between the Cp* ligand and the methyl substituents on the diene ligand.

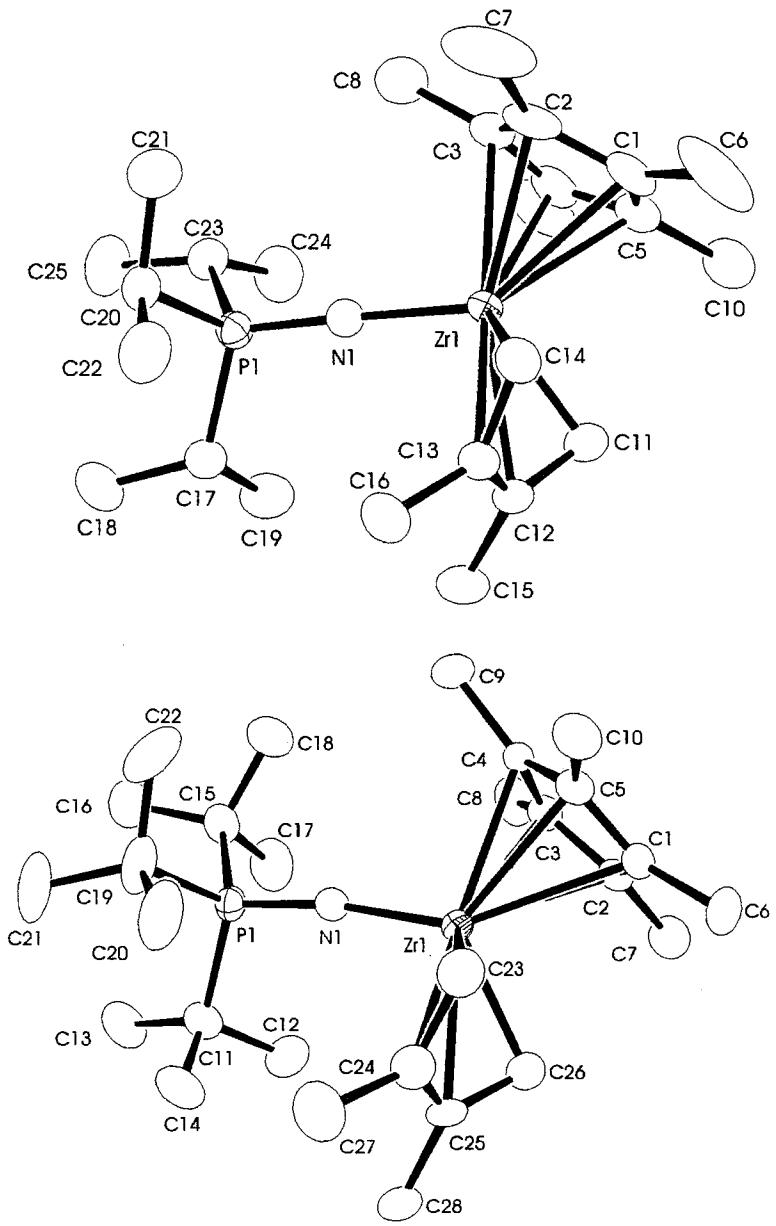

Figure 2.7 ORTEP drawings of **49** (top) and **50** (bottom); 30% ellipsoids are shown, hydrogen atoms have been omitted for clarity. Selected bond distances and angles: **49**: Zr(1)-N(1) 1.982(3) Å; P(1)-N(1) 1.564(3) Å; Zr(1)-C(11) 2.282(3) Å; Zr(1)-C(12) 2.533(3) Å; Zr(1)-C(13) 2.538(3) Å; Zr(1)-C(14) 2.288(3) Å; C(11)-C(12) 1.454(5) Å; C(12)-C(13) 1.383(5) Å; C(13)-C(14) 1.455(5) Å; C(11)-Zr(1)-C(14) 80.05(14) °; P(1)-N(1)-Zr(1) 173.52(17) °. **50**: Zr(1)-N(1) 1.996(4) Å; P(1)-N(1) 1.576(4) Å; Zr(1)-C(23) 2.258(6) Å; Zr(1)-C(24) 2.638(6) Å; Zr(1)-C(25) 2.642(5) Å; Zr(1)-C(26) 2.269(5) Å; C(23)-C(24) 1.462(9) Å; C(24)-C(25) 1.390(9) Å; C(25)-C(26) 1.476(8) Å; C(23)-Zr(1)-C(26) 80.5(2) °; P(1)-N(1)-Zr(1) 169.3(3) °.

Another structural feature revealed by crystallographic studies was the orientation of the 2,3-dimethyl-1,3-butadiene ligand. In general, two orientations are possible: *supine* (*exo*) (**A**) and *prone* (*endo*) (**B**). Complexes **49** and **50** were found to prefer the

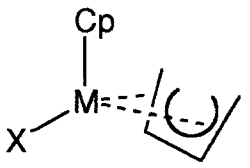

A

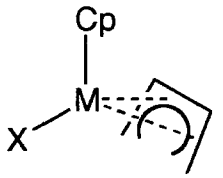

B

supine orientation to the *prone* orientation. This was also attributed to the steric crowding.

On the basis of the crystallographic data, some typical structural features for *s-cis*-diene complexes were observed. For complex **49**, the bond distances of Zr-C(14) and Zr-C(11) were found to be shorter than those of Zr-C(13) and Zr-C(12) respectively. The inner bond C(12)-C(13) was found to be shorter than C(13)-C(14) and C(11)-C(12) but was still longer than the normal C-C double bond. Exactly the same patterns were also observed for complex **50**. When comparing complex **49** to **50**, a significant different in the inner carbons and the zirconium bond distances was observed. The bond distances Zr-C(13) and Zr-C(12) were 2.538(3) and 2.533(3) Å respectively for complex **49**. This was found to be significantly shorter than the bond distances Zr-(24) and Zr-(24) of 2.638(6) and 2.642(5) Å respectively for complex **50**.

Ethylene Polymerization of Pentamethylcyclopentadienyl Zirconium Phosphinimide Complexes

Pentamethylcyclopentadienyl zirconium phosphinimide dichloride complexes (**41**, **53**) and its analogous dimethyl derivatives (**42**, **54**[69]) as well as the *s-cis*-diene complexes (**49**, **50**) were screened for ethylene polymerizations. A large excess of MAO was used as the co-catalyst for complexes **41** and **53**, while exactly one equivalent of trityl tetrakis(pentafluorophenyl)borate were employed for complexes **42**, **49**, **50** and **54**[69]. The results are tabulated in Table 2.3.

Table 2.3 Ethylene Polymerization Data for 41, 42, 49, 50, 53 and 54[69]

Catalyst Presursor	mmole of catalyst precursor	Cocatalyst[a]	Time (min)	Productivity (g mmol^{-1} h^{-1})	M_w[d]	M_w/M_n
41[b]	0.0212	MAO	60.0	1.4	506 400	41.51
41[c]	0.0212	MAO	3.00	0	0	0
53[b]	0.0195	MAO	60.0	48.2	9 220	3.34
53[c]	0.0195	MAO	3.00	0	0	0
42[c]	0.0163	TB	3.00	0	0	0
54[c]	0.0423	TB	3.00	0	0	0
49[c]	0.0414	TB	3.00	181	132 300	4.44
50[c]	0.0381	TB	3.00	0	0	0
Cp_2ZrCl_2[b]	0.0246	MAO	2.00	895	11 6353	2.8

[a]MAO: methylaluminoxane (500 equiv); TB: trityl tetrakis(pentafluorophenyl)borate (1 equiv). [b]Polymerizations were run at 33 psi pressure of ethylene and 60 - 65 °C. [c]Polymerizations were run at 1 atm pressure of ethylene and 25 °C. Molecular weight data were recorded against polyethylene standards.

It was noticed that zirconium phosphinimide complexes behave differently than the titanium analogues. Catalysts derived from **41**, **42**, **53** and **54** showed no activity under mild conditions. On the other hand, minimal activities were obtained for catalyst precursors **41** and **53** when polymerizations were carried out under forcing conditions. This result is consistent with the higher ethylene to catalyst ratio at high temperature. It

was surprising to find that the activity for the catalysts derived from the zirconium phosphinimide complexes were not comparable to those from the titanium analogues, which was found to have an activity of 500 g $mmol^{-1}$ h^{-1}.[13] This was probably due to the fact that Cp* ligand is more electron donating and sterically hindered than Cp ligand. A similar trend in the activity of the catalysts derived from the titanium analogues was also observed. It was found that the activity for catalyst precursor **53** was higher than that of **41**. Similarly, the activity for $CpTi(NPt\text{-}Bu_3)Cl_2$ was higher than $CpTi(NPi\text{-}Pr_3)Cl_2$. This was attributed to the fact that tri-*tert*-butyl phosphinimide ligand is approximately sterically equivalent to cyclopentadienyl ligand.[13] In addition, GPC data revealed that these catalyst precursors gave rise to polyethylene with bimodal molecular weight distributions. This may arise from the partial degradation of the catalysts, leading to more than one active species. Preliminary studies on the deactivation pathway for these zirconium catalysts indicated the formation of cluster in the form of $[Cp^*_4Zr_4Cl_6C]$.[89]

It had been proven that both (butadiene)zirconocene and (η^4-butadiene)bis(pentamethylcyclopentadienyl)zirconium polymerize ethylene in the presence of tris(pentafluorophenyl)borate at 20 and 121 °C respectively.[27a, 90] The activities were found to be 135[27a] and 50[91] g $mmol^{-1}$ h^{-1} respectively. As a consequence, complexes **49** and **50** were tested for activity in ethylene polymerization. It was found that in the presence of trityl, complex **49** polymerized ethylene with an activity of 181 g $mmol^{-1}$ h^{-1}, while complex **50** showed no activity. This may be attributed to the fact that the tri-*tert*-butyl phosphinimide ligand is larger in size than the tri-*iso*-propyl phosphinimide ligand. As a result, the accessibility of the zirconium center (coordination gap aperture) by ethylene is too small in the catalyst derived from complex **50**. In

addition, butadiene is a better donor ligand, thus stabilized the zirconium metal center. Similar to the polyethylene generated by complexes **41** and **53**, GPC data revealed that complex **49** gave rise to polyethylene that has bimodal molecular weight distributions. This again, suggested the presence of more than one active species resulting from the decomposition of the catalyst.

2.4 Summary

In summary, the first monomeric pentamethylcyclopentadienyl phosphinimide zirconium complexes of **41** and **53** were prepared. The reactivity of such complexes was also investigated systematically. A series of complexes (**42-48**) were readily prepared at mild conditions by salt metathesis reactions. In addition, the analogous butadiene derivatives **49** and **50** were successfully prepared via a modified one-pot synthesis. Variable-temperature $^{1}H\{^{31}P\}$-NMR studies revealed no fluxional behaviour for complexes **49** and **50**, although inhibited rotation about the P-C bond for tri-*tert*-butyl phosphinimide ligand was observed at low temperature. Complexes **41**, **44**, **46**, **47**, **49**, **50** and **54**[69] were fully characterized by both spectroscopic and crystallographic studies. Lastly, complexes **41**, **42**, **49**, **50**, **53** and **54**[69] were tested for activity in ethylene polymerization. These catalyst precursors achieved very low to high activity. The result was attributed to the presence of the more sterically hindered and electronically donating Cp* ligand. Furthermore, a higher activity was achieved for the catalyst derived from complex **49**. The resulting polyethylene was found to have bimodal molecular weight distributions. This implied the decomposition of catalyst and the presence of more than one active species under the employed polymerization conditions.

Chapter 3
Synthesis and Applications of Titanium Phosphinimine-phosphinimide Complexes

3.1 Introduction

As illustrated in the previous chapter, applications of phosphinimide zirconium complexes in the form of $Cp^*X_2Zr(NPR_3)$ as catalyst precursors achieved only minimal activity. Although the catalyst derived from phosphinimide zirconium butadiene derivative (**49**) showed higher activity, it was found not to be comparable to those derived from the phosphinimide titanium analogs of the form $CpX_2Ti(NPR_3)$. That outcome was probably due to the more sterically hindered and electronically saturated pentamethylcyclopentadienyl ligand (Cp*). In addition, the combination of the Cp* and tri-*t*-butyl phosphinimide ligands results in diminished access to the metal center. As a consequence, it is necessary to search for a new ancillary ligand system by adjusting both the steric and electronic properties based on phosphinimide ligands. In this chapter, we describe one such possibility, namely the phosphinimine-phosphinimides.

3.2 Experimental

General Data All preparations were performed under an atmosphere of dry, O_2-free N_2 employing either Schlenk line techniques or a vacuum atmospheres inert atmosphere glove box. Solvents were reagent grade, either distilled from the appropriate drying agents under N_2 or obtained directly from an Innovative Technologies solvent purification system, and degassed by the freeze-thaw method at least three times prior to use. Tri-*iso*-propyl phosphine, tri-*tert*-butyl phosphine and pentamethylcyclopentadienyl-

zirconium trichloride were used as received from Strem Chemical Co. Methyl Grignard reagents were used as received from Aldrich Chemical Co. The ligand precursor R_3PNLi were prepared as described in the literature.[67] MAO and $[Ph_3C][B(C_6F_5)_4]$ were used as received from NOVA Chemicals. ^1H, $^{13}C\{^1H\}$, $^{31}P\{^1H\}$, $^{19}F\{^1H\}$ and $^{11}B\{^1H\}$ NMR spectra were recorded on a Bruker Avance 300 spectrometer operating at 300, 75, 121, 282 and 95 MHz respectively. ^1H and $^{13}C\{^1H\}$ spectra were internally referenced to trace amounts of protonated solvents and chemical shifts are reported relative to $SiMe_4$. $^{31}P\{^1H\}$, $^{19}F\{^1H\}$ and $^{11}B\{^1H\}$ spectra were referenced externally to 85% H_3PO_4, CF_3COOH and $NaBH_4$ respectively. Combustion analyses were performed by Guelph Chemical Labs Inc., Guelph, Ontario.

Ethylene Polymerization (i) A solution of 6 to 10 μmol of catalyst precursor in 2.0 mL of dry toluene was added to a flask containing 2.0 mL of dry toluene. 500 equivalents of a 10% by weight toluene solution of methylaluminoxane (MAO) was added to the flask. Alternatively, the catalyst precursors were combined with $[Ph_3C][B(C_6F_5)_4]$ under an ethylene atmosphere at 25°C. The flask was attached to a Schlenk line with cold trap, a stopwatch was started and the flask was three times evacuated for five seconds and refilled with pre-dried 99.9% ethylene gas. The solution was rapidly stirred under 1 atmosphere of ethylene at room temperature. The polymerization was stopped by the injection of a 1.0 N HCl/methanol solution. Total reaction time was noted and the polymer was isolated.

(ii) A 1L autoclave was dried under vacuum (10^{-2} mmHg) for several hours. Dried toluene (500 mL) was transferred into the vessel under a positive pressure of N_2, and was heated to 30 °C. The temperature was controlled (to *ca.* ± 2 °C) with an external heating/cooling bath and was monitored by a thermocouple that extended into the polymerization vessel. A solution of MAO (500 equiv.) in toluene was injected, and the mixture was stirred for 3 min at a rate of 150 RPM. The catalyst precursor in a solution of toluene was then injected while the reaction mixture stirred for 3 minutes at the same rate. The rate of stirring was increased to 1000 RPM, and the vessel was vented of N_2 and pressurized with ethylene (33 psi). Any recorded exotherm was within the allowed temperature differential of the heating/cooling system. The solution was stirred for 1 hour, after which time the reaction was quenched with 1 M HCl in MeOH. The precipitated polymer was subsequently washed with MeOH, and dried at 100 °C for at least 24 hours prior to weighing.

Synthesis of *i*-Pr_3P=N-PPh_2 58; *t*-Bu_3P=N-PPh_3, 59

Compounds **58** and **59** were prepared through similar routes, thus only one representative procedure is described. (2.44 g; 0.01 mol) Ph_2PCl was added dropwise to a clear orange benzene solution (100 ml) of $^{i}Pr_3P{=}N^{-}Li^{+}$ (2.00 g; 0.01 mol). White precipitate was observed upon the addition of Ph_2PCl. The colour of the solution mixture was changed to yellow after 4 hours of stirring. Evaporation of benzene under vacuum gave a pale yellow solid. The solid was extracted with 100 ml of hexane, followed by filtration and evaporation of solvent under vacuum. **58:** Yield: 80% white crystalline solid. $^{31}P\{^{1}H\}$ NMR (25 °C, C_6D_6): δ 42.37 (d, *i*-Pr_3P, $|^{2}J_{P\text{-}P}|$ = 80 Hz), 38.90 (d, PPh_2, $|^{2}J_{P\text{-}P}|$ = 80 Hz).

^{1}H NMR (25 °C, C_6D_6): δ 8.02 (m, 4H, *o*-Ar, $|J_{H-H}|$ = 7 Hz), 7.26 (m, 4H, *m*-Ar, $|J_{H-H}|$ = 7 Hz), 7.08 (m, 2H, *p*-Ar, $|J_{H-H}|$ = 7 Hz), 1.94 (m, 3H, CH, $|J_{H-H}|$ = 4 Hz), 0.95 (quart, 18H, CH_3, $|J_{H-H}|$ = 7 Hz). $^{13}C\{^1H\}$ NMR (25 °C, C_6D_6): δ 151.2 (d, *ipso*-Ar, $|J_{P-C}|$ = 27 Hz), 130.4 (d, *o*-Ar, $|^2J_{P-C}|$ = 22 Hz), 128.1 (d, *m*-Ar, $|^3J_{P-C}|$ = 6 Hz), 127.5 (s, *p*-Ar), 25.5 (d, CH, $|J_{P-C}|$ = 59 Hz), 17.2 (s, CH_3).

59: Yield: 87% pale yellow crystalline solid. $^{31}P\{^1H\}$ NMR (25 °C, C_6D_6): δ 47.92 (d, *t*-Bu_3P, $|^2J_{P-P}|$ = 62 Hz), 40.77 (d, PPh_2, $|^2J_{P-P}|$ = 62 Hz). ^{1}H NMR (25 °C, C_6D_6): δ 8.01 (m, 4H, *m*-Ar, $|J_{H-H}|$ = 7 Hz), 7.23 (m, 4H, *o*-Ar, $|J_{H-H}|$ = 8 Hz), 7.05 (m, 2H, *p*-Ar, $|J_{H-H}|$ = 7 Hz). 1.24 (d, 27H, CH_3, $|J_{P-H}|$ = 13 Hz). $^{13}C\{^1H\}$ NMR (25 °C, C_6D_6): δ 151.7 (d, *ipso*-Ar, $|J_{P-C}|$ = 20 Hz), 130.4 (d, *o*-Ar, $|^2J_{P-C}|$ = 22 Hz), 128.4 (d, *m*-Ar, $|^3J_{P-C}|$ = 7 Hz), 127.7 (s, *p*-Ar), 41.6 (d, C, $|J_{P-C}|$ = 49 Hz), 30.3 (s, CH_3). Anal. Calcd for $C_{24}H_{37}NP_2$: C: 71.79; H: 9.29; N: 3.49%. Found: C: 71.87; H: 9.37; N: 3.34%.

Synthesis of *i*-Pr_3P=N-$P(Ph_2)$-TMA, 60; *t*-Bu_3P=N-$P(Ph_2)$-TMA, 61

Compounds **60** and **61** were prepared through similar routes, thus only on representative procedure is described. A 2.5 M hexane solution of TMA (0.42 mL; 0.84 mmol) was added to a clear benzene solution (6 mL) of *i*-Pr_3P=N-$P(Ph_2)$ (100 mg; 0.28 mmol). The solution mixture was allowed to stir at room temperature overnight. Evaporation of the resulting pale yellow benzene solution gave a white solid. The solid was then washed with (2 x 2 mL) of hexane, followed by drying under vacuum. **60:** Yield: 90 % white crystalline solid. $^{31}P\{^1H\}$ NMR (25 °C, C_6D_6): δ 39.72, 26.28. ^{1}H NMR (25 °C, C_6D_6): δ 7.77 (m, 4H, *o*-Ar, $|J_{H-H}|$ = 8 Hz), 7.16 (m, 4H, *m*-Ar, $|J_{H-H}|$ = 7 Hz), 7.09 (m, 2H, *p*-Ar, $|J_{H-H}|$ = 7 Hz), 1.80 (m, 3H, CH, $|J_{H-H}|$ = 7 Hz), 0.86 (quart, 18H, CH_3, $|J_{H-H}|$ = 7 Hz).

$^{13}C\{^1H\}$ NMR (25 °C, C_6D_6): δ 142.0 (d, *ipso*-Ar, $|J_{P-C}|$ = 30 Hz), 132.5 (d, *o*-Ar, $|^2J_{P-C}|$ = 14 Hz), 130.0 (s, *p*-Ar), 128.5 (d, *m*-Ar, $|^3J_{P-C}|$ = 9 Hz), 26.3 (d, CH, $|J_{P-C}|$ = 61 Hz), 17.4 (s, CH_3), -6.4 (s, CH_3).

61: Yield: 98 % white crystalline solid. $^{31}P\{^1H\}$ NMR (25 °C, C_6D_6): δ 44.95 (d, *t*-Bu_3P, $|^2J_{P-P}|$ = 26 Hz), 28.10 (d, PPh_2, $|^2J_{P-P}|$ = 26 Hz). ^1H NMR (25 °C, C_6D_6): δ 7.84 (m, 4H, *o*-Ar, $|J_{H-H}|$ = 8 Hz), 7.16 (m, 4H, *m*-Ar, $|J_{H-H}|$ = 6 Hz), 7.08 (m, 2H, *p*-Ar, $|J_{H-H}|$ = 7 Hz), 1.06 (m, 27H, CH, $|J_{H-H}|$ = 14 Hz), -0.15 (s, 9H, CH_3). $^{13}C\{^1H\}$ NMR (25 °C, C_6D_6): δ 141.9 (d, *ipso*-Ar, $|J_{P-C}|$ = 29 Hz), 133.4 (d, *o*-Ar, $|^2J_{P-C}|$ = 14 Hz), 130.0 (s, *p*-Ar), 128.4(d, *m*-Ar, $|^3J_{P-C}|$ = 8 Hz), 41.0 (d, C, $|J_{P-C}|$ = 51 Hz), 29.9 (s, CH_3), -5.9 (s, CH_3). Anal. Calcd for $C_{27}H_{46}AlNP_2$: C: 68.47; H: 9.79; N: 2.96%. Found: C: 68.80; H: 10.28; N: 2.99%.

Synthesis of $(B(C_6F_5)_3)Ph_2PN{=}P$-*i*-Pr_3, 62

A benzene solution of $B(C_6F_5)_3$ (140 mg; 0.28 mmol) was added to a clear benzene solution (5 mL) of *i*-$Pr_3P{=}N$-$P(Ph_2)$ (100 mg; 0.28 mmol). The solution mixture was allowed to stir at room temperature two hours. Evaporation of the resulting colourless benzene solution gave a white solid. The solid was then washed with (2 x 2 mL) of hexane, followed by drying under vacuum. **62:** Yield: 87 % white solid. $^{31}P\{^1H\}$ NMR (25 °C, C_6D_6): δ 39.83 (d, *i*-Pr_3P, $^2|J_{P-P}|$ = 59 Hz), 33.20 (v. br, PPh_2). ^1H NMR (25 °C, C_6D_6): δ 7.56 (m, 4H, *o*-Ar, $|J_{H-H}|$ = 8 Hz), 6.97 (m, 2H, *p*-Ar, $|J_{H-H}|$ = 8 Hz), 6.87 (m, 4H, *m*-Ar, $|J_{H-H}|$ = 8 Hz), 1.59 (m, 3H, CH, $|J_{H-H}|$ = 7 Hz), 0.52 (quart, 18H, CH_3, $|J_{H-H}|$ = 7 Hz). ^{11}B NMR (25 °C, C_6D_6): δ 34.83. ^{19}F NMR (25 °C, C_6D_6): δ -47.91 (d, 6F, *o*-C_6F_5, $|J_{F-F}|$ = 22 Hz), -81.00 (t, 6F, *m*-C_6F_5, $|J_{F-F}|$ = 21 Hz), -87.49 (m, 3F, *p*-C_6F_5, $|J_{F-F}|$ = 23

Hz). $^{13}C\{^1H\}$ NMR (25 °C, C_6D_6): δ 151.9, 142.0, 136.2, 135.5, 133.0, 131.2, 128.7 (d, $|J_{P-C}|$ = 15 Hz), 127.8 (d, $|J_{P-C}|$ = 15 Hz), 27.0 (d, $|J_{P-C}|$ = 61 Hz), 16.7.

Synthesis of *i*-Pr_3P=N-$P(Ph_2)$=N-TMS, 63; *t*-Bu_3P=N-$P(Ph_2)$=N-TMS, 64

Both compounds **63** and **64** were prepared in a similar manner, thus only one representative procedure is described. (129 mg; 1.12 mmol) TMS-N_3 was added dropwise to (335 mg; 0.93 mmol) of white crystalline $^iPr_3P$=N-PPh_2. Gas evolution was observed as the addition of TMS-N_3. The mixture became an orange oil after refluxed overnight. The orange oil was extracted with (2 x 5 mL) of hexane, followed by filtration and evaporation of solvent. **63:** Yield: 94% white solid. $^{31}P\{^1H\}$ NMR (25 °C, C_6D_6): δ 41.39 (d, *i*-Pr_3P, $|^2J_{P-P}|$ = 8 Hz), -6.08 (d, PPh_2, $|^2J_{P-P}|$ = 9 Hz). ^1H NMR (25 °C, C_6D_6): δ 8.10 (m, 4H, *o*-Ar, $|J_{H-H}|$ = 8 Hz), 7.20 (m, 4H, *m*-Ar, $|J_{H-H}|$ = 8 Hz), 7.08 (m, 2H, *p*-Ar, $|J_{H-H}|$ = 7 Hz), 2.06 (m, 3H, CH, $|J_{H-H}|$ = 7 Hz), 0.94 (m, 18H, CH_3, $|J_{H-H}|$ = 8 Hz), 0.41 (s, 9H, CH_3). $^{13}C\{^1H\}$ NMR (25 °C, C_6D_6): δ 144.3 (d, *ipso*-Ar, $|J_{P-C}|$ = 128 Hz), 132.0 (d, *o*-Ar, $|^2J_{P-C}|$= 10 Hz), 129.4 (*p*-Ar), 128.0 (d, *m*-Ar, $|^3J_{P-C}|$ = 12 Hz), 25.5 (d, CH, $|J_{P-C}|$ = 60 Hz), 27.5 (s, CH_3), 5.2 (s, CH_3).

64: Yield: 90% white solid. $^{31}P\{^1H\}$ NMR (C_6D_6, 25 °C, δ): 46.52 (d, *t*-Bu_3P, $|^2J_{P-P}|$ = 11 Hz), -8.36 (d, PPh_2, $|^2J_{P-P}|$ = 11 Hz). ^1H NMR (25 °C, C_6D_6): δ 8.07 (m, 4H, *o*-Ar, $|J_{H-H}|$ = 8 Hz), 7.20 (m, 4H, *m*-Ar, $|J_{H-H}|$ = 8 Hz), 7.08 (m, 2H, *p*-Ar, $|J_{H-H}|$ = 7 Hz), 1.21 (d, 27H, CH_3, $|J_{H-H}|$ = 13 Hz), 0.41 (s, 9H, CH_3). $^{13}C\{^1H\}$ NMR (25 °C, C_6D_6): δ 144.6 (d, *ipso*-Ar, $|J_{P-C}|$ = 130 Hz), 132.0 (d, *o*-Ar, $|J_{P-C}|$= 10 Hz), 129.3 (s, *p*-Ar), 128.0 (d, *m*-Ar, $|J_{P-C}|$ = 12 Hz), 41.1 (d, C, $|J_{P-C}|$ = 51 Hz), 30.1 (s, CH_3), 5.1 (s, CH_3).

Synthesis of (i-Pr_3PNPPh_2N)$TiCpCl_2$, 65; (t-Bu_3PNPPh_2N)$TiCpCl_2$, 66

Both compounds **65** and **66** were prepared in a similar manner, thus only one representative procedure is described. (i) To a clear orange toluene solution (80 mL) of $CpTiCl_3$ (420 mg; 2.00 mmol) was added a toluene solution (10 mL) of i-Pr_3P=N-$P(Ph_2)$=N-TMS (940 mg; 2.10 mmol). The solution mixture was stirred at room temperature overnight. Evaporation of toluene under vacuum gave an orange oil. The solid was extracted with 2 x 50 mL of benzene, followed by filtration and evaporation of solvent. The final orange oil was washed with (3 x 5 mL) of diethyl ether and dried under vacuum. **65:** Yield: 70% yellow solid. **66:** Yield: 91 % orange solid. (ii) To a clear orange benzene solution (50 mL) of $CpTiCl_3$ (307 mg; 1.39 mmol) was added TMS-N_3 (256 mg; 2.23 mmol). The solution mixture was stirred at room temperature for overnight, followed by the addition of benzene solution (30 mL) of $^{i}Pr_3P$=N-$P(Ph_2)$ (500 mg; 1.39 mmol). The colour of the solution mixture was changed to deep red upon addition. Gas evolution was observed after 30 seconds of stirring and the solution was changed to clear deep orange colour. The resulting solution was stirred at room temperature overnight. Evaporation of benzene gave yellow solid, which was then washed with (3 x 10 mL) hexane. **65:** Yield: 84% yellow solid. $^{31}P\{^{1}H\}$ NMR (25 °C, C_6D_6): δ 48.7 (d, i-Pr_3P, $|^{2}J_{P\text{-}P}|$ = 8 Hz), -4.87 (s, PPh_2). ^{1}H NMR (25 °C, C_6D_6): δ 8.07 (m, 4H, o-Ar, $|J_{H\text{-}H}|$ = 7 Hz), 7.15 (m, 4H, m-Ar, $|J_{H\text{-}H}|$ = 8 Hz), 7.07 (m, 2H, p-Ar, $|J_{H\text{-}H}|$ = 8 Hz), 6.24, 2.24 (d, 3H, CH, $|J_{P\text{-}H}|$ = 7 Hz), 1.03 (quart, 18H, CH_3, $|J_{H\text{-}H}|$ = 7 Hz). $^{13}C\{^{1}H\}$ NMR (25 °C, C_6D_6): δ 138.2 (d, *ipso*-Ar, $|J_{P\text{-}C}|$ = 129 Hz), 132.3 (d, o-Ar, $|^{3}J_{P\text{-}C}|$ = 11 Hz), 131.4 (s, p-Ar), 128.7 (d, m-Ar, $|^{2}J_{P\text{-}C}|$ = 13 Hz), 114.9 (s, Cp), 25.4 (d, CH,

$|J_{P-C}|$ = 59 Hz), 17.2. Anal. Calcd for $C_{26}H_{36}Cl_2N_2P_2Ti$: C: 56.03; H: 6.51; N: 5.03%. Found: C: 56.99; H: 6.71; N: 5.04%.

66: Yield: 96%. $^{31}P\{^1H\}$ NMR (25 °C, C_6D_6): δ 52.27 (d, *t*-Bu_3P, $|^2J_{P-P}|$ = 12 Hz), -11.45 (d, PPh_2, $|^2J_{P-P}|$ = 10 Hz). ^1H NMR (25 °C, C_6D_6): δ 8.11 (m, 4H, *m*-Ar, $|J_{H-H}|$ = 8 Hz), 7.14 (m, 4H, *o*-Ar, $|J_{H-H}|$ = 8 Hz), 7.06 (m, 2H, *p*-Ar, $|J_{H-H}|$ = 7 Hz), 6.29 (s, 5H, Cp), 1.13 (d, 27H, CH_3, $|J_{P-H}|$ = 14 Hz). $^{13}C\{^1H\}$ NMR (25 °C, C_6D_6): δ 138.5 (d, *ipso*-Ar, $|J_{P-C}|$ = 132 Hz), 132.5 (d, *o*-Ar, $|^3J_{P-C}|$ = 11 Hz), 131.2 (s, *p*-Ar), 128.7 (d, *m*-Ar, $|^2J_{P-C}|$ = 13 Hz), 115.0 (s, Cp), 40.9 (d, C, $|J_{P-C}|$ = 50 Hz), 29.8 (CH_3). Anal. Calcd for $C_{30}H_{45}Cl_2N_2P_2Ti$: C: 58.64; H: 7.38; N: 4.56. Found: C: 58.31; H: 7.43; N: 4.88%.

Synthesis of (*i*-Pr_3PNPPh_2N)$TiCp(CH_3)_2$, 67; (*t*-Bu_3PNPPh_2N)$TiCp(CH_3)_2$, 68

Both complexes **67** and **68** were prepared in a similar manner, thus only one representative procedure is described. To a clear orange toluene solution (10 mL) of Cp(*i*-Pr_3P=N-P(Ph_2)=N)$TiCl_2$ (150 mg; 0.27 mmol) was added a 3.0 M of diethyl ether solution of CH_3MgBr (0.20 mL; 0.59 mmol). The solution mixture was changed to orange brown in colour after 30 minutes of stirring. The solution was allowed to stir at room temperature overnight. Evaporation of toluene gave an orange brown solid. The solid was extracted with (2 x 5 mL) benzene: hexane (3:1), followed by filtration and evaporation of solvent under vacuum. **67:** Yield: 91 % yellow solid. $^{31}P\{^1H\}$ NMR (25 °C, C_6D_6): δ 44.86 (d, *i*-Pr_3P, $|J^2_{P-P}|$ = 7 Hz), -12.13 (s, PPh_2). ^1H NMR (25 °C, C_6D_6): δ 8.11 (m, 4H, *m*-Ar, $|J_{H-H}|$ = 7 Hz), 7.19 (m, 4H, *o*-Ar, $|J_{H-H}|$ = 7 Hz), 7.08, (m, 2H, *p*-Ar, $|J_{H-H}|$ = 7 Hz), 6.09 (s, 5H, Cp), 2.20 (m, 3H, CH, $|J_{H-H}|$ = 7 Hz), 0.97 (q, 18H, CH_3, $|J_{H-H}|$ = 7 Hz), 0.76 (s, 6H, CH_3). $^{13}C\{^1H\}$ NMR (C_6D_6, 25 °C, δ): 141.7 (d, *ipso*-Ar, $|J_{P-C}|$ =

126 Hz), 132.0 (d, *o*-Ar, $|^3J_{P\text{-}C}|$ = 10 Hz), 130.2 (s, *p*-Ar), 128.3 (d, *m*-Ar, $|^2J_{P\text{-}C}|$ = 12 Hz), 111.0 (s, Cp), 39.7 (s, CH_3), 25.5 (d, CH, $|J_{P\text{-}C}|$ = 60 Hz), 17.3 (s, CH_3). **68:** Yield: 88% yellow solid. $^{31}P\{^1H\}$ NMR (25 °C, C_6D_6): δ 49.03 (d, *t*-Bu_3P, $|^2J_{P\text{-}P}|$ = 11 Hz), -17.08 (d, PPh_2, $|^2J_{P\text{-}P}|$ = 10 Hz). ^1H NMR (25 °C, C_6D_6): δ 8.15 (m, 4H, *m*-Ar, $|J_{H\text{-}H}|$ = 8 Hz), 7.18 (m, 4H, *o*-Ar, $|J_{H\text{-}H}|$ = 7 Hz), 7.07 (m, 2H, *p*-Ar, $|J_{H\text{-}H}|$ = 7 Hz), 6.11 (s, 5H, Cp), 1.20 (d, 27H, CH_3, $|J_{P\text{-}H}|$ = 14 Hz), 0.82 (s, 6H, CH_3). $^{13}C\{^1H\}$ NMR (25 °C, C_6D_6): δ 142.1 (d, *ipso*-Ar, $|J_{P\text{-}C}|$ = 129 Hz), 132.2 (d, *o*-Ar, $|^3J_{P\text{-}C}|$ = 10 Hz), 130.1 (s, *p*-Ar), 128.2 (d, *m*-Ar,$|^2J_{P\text{-}C}|$ = 12 Hz), 111.1 (s, Cp), 41.0 (d, C, $|J_{P\text{-}C}|$ = 50 Hz), 40.5 (s, CH_3), 29.9 (s, CH_3).

X-Ray Structure Determinations of 58, 60, 62 and 65

All crystals were mounted in either 0.5 or 0.7 mm glass capillary tubes. Data were collected at room temperature. No crystal decay was observed for any of the compounds. The resulting crystallographic values are given in Table 3.1. ORTEP drawings of **58**, **60**, **62** and **65** are shown in Figures 3.2, 3.3, 3.5 and 3.6 respectively, with 30% thermal ellipsoids. Selected bond distances and angles are listed in the captions for Figures 3.2, 3.3, 3.5 and 3.6 respectively. Other structural parameters are given in Table A2.1 – A2.4 in Appendix Two.

Table 3.1: Crystallographic Parameters for 58, 60, 62 and 65

	58	60	62	65
Formula	$C_{21}H_{31}NP_2$	$C_{48}H_{80}Al_2N_2P_4$	$C_{39}H_{32}BF_{15}NP_2$	$C_{26}H_{36}Cl_2N_2P_2Ti$
Formula weight	359.41	862.98	879.41	557.31
a(Å)	9.27450 (10)	17.6217 (2)	14.654 (4)	10.57510 (10)
b(Å)	14.67250 (10)	15.2123 (2)	13.954 (8)	25.2061 (3)
c(Å)	15.6324 (2)	21.5862 (3)	19.314 (16)	10.9780 (2)
α(°)	90	90	90	90
β(°)	99.890 (1)	113.6220 (10)	104.11 (5)	94.7180 (10)
γ(°)	90	90	90	90
Crystal system	Monoclinic	Monoclinic	Monoclinic	Monoclinic
Space group	$P2_1/c$	$P2_1/c$	$P2_1/n$	$P2_1/n$
Volume ($Å^3$)	2095.65 (4)	5301.68 (12)	3830 (4)	2916.35 (7)
D_{calc} (Mg/m^3)	1.139	1.081	1.513	1.269
Z	4	8	4	4
Abs coeff, μ, mm^{-1}	0.210	0.207	0.218	0.603
Temp (°C)	293 (2)	293 (2)	293 (2)	293 (3)
F(000)	776	1872	1772	1168
2θ range (°)	1.92 – 24.99	1.69 – 25.00	1.82 – 25.00	1.62 – 25.00
h	-10 – +10	-20 – +20	-10 – +17	-12 – +11
k	-15 – +17	-12 – +18	-16 – +15	-29 – +24
l	-18 – +18	-25 – +25	-22 – +16	-12 – +13
Refl collected	8907	25603	18407	14695
R_{int}	0.2808	0.0406	0.1092	0.0321
Data $F_o^2>3\sigma(F_o^2)$	3647	9190	6628	5091
Parameters	217	505	523	298
R(%)a	6.91	5.14	7.32	7.15
Rw(%)a	15.71	12.47	14.96	15.04
Peak, hole ($e^-Å^{-3}$)	0.524, -1.086	0.300, -0.309	0.297, -0.464	0.541, -0.485
Goodness of fit	0.685	1.044	1.032	1.303

[a] $R = \Sigma \, ||F_o| - |F_c|| \, / \, \Sigma \, |F_o|$, $Rw = [\Sigma(|F_o| - |F_c|)^2| \, / \, \Sigma \, |F_o|^2]^{0.5}$

3.3 Results and Discussion

Synthesis and reactivity 58 and 59

In order to adjust both the electronic and steric properties of the phosphinimide ligands, a novel phosphinimine-phosphine ligand was developed. The phosphinimine-phosphines in the form of $R_3P{=}NPR'_2$ were readily prepared by stiochiometric reaction of R_3PNLi and chlorodiphenylphosphine (Ph_2PCl) under mild conditions. Elimination of lithium chloride generated the desired mixed P(V)-P(III) compounds **58** and **59** in quantitative yields (Scheme 3.1).

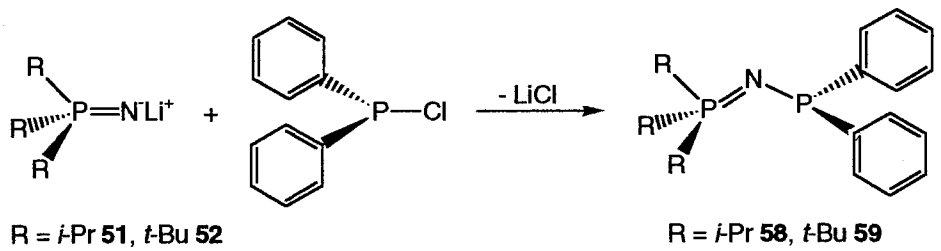

Scheme 3.1 Synthesis of phosphinimine-phosphine ligands **58** and **59**.

The presence of two non-equivalent phosphorus atoms were easily confirmed by the presence of the two doublets in the $^{31}P\{^1H\}$-NMR spectra. For compound **59**, the resonance corresponding to the P(V) atom as found slightly downfield at 47.92 ppm whereas that for the P(III) center was found at 40.77 ppm. The P(V)-P(III) coupling constants were found to be 62 Hz. In the ^{31}P-NMR spectrum, the signal assigned to P(V) was split into a multiplet centered at 47.4 ppm with coupling constant of 12 Hz. This was due to the coupling to all the methyl protons of the three *t*-butyl groups. On the other hand, only broadening of the doublet assigned to the P(III) in the proton decoupled ^{31}P-NMR spectrum was observed (Figure 3.1).

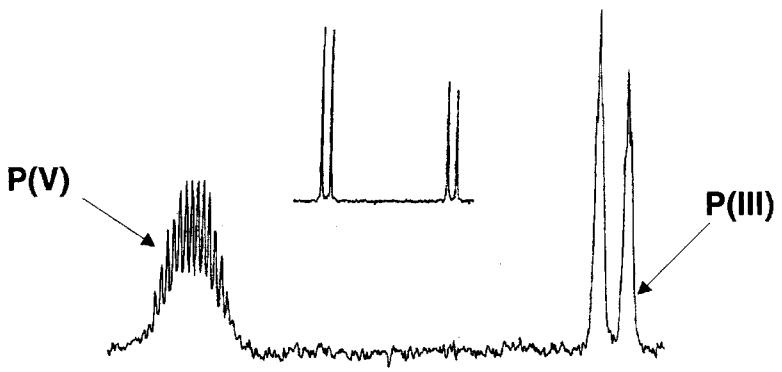

Figure 3.1 ^{31}P-NMR and ^{31}P{^{1}H}-NMR (insight) of **59**.

The proposed structure of compound **58** was further confirmed by X-ray crystallographic data as shown in Figure 3.2. It was found that the P(1)-N(1) bond

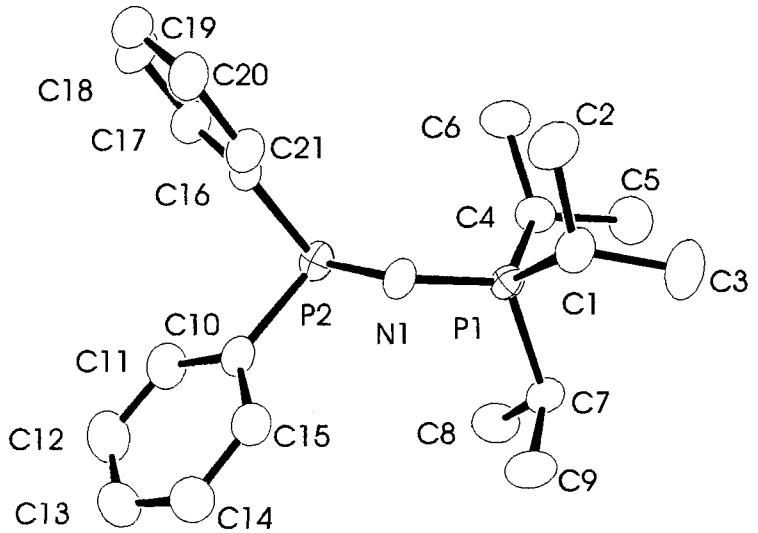

Figure 3.2 ORTEP drawing of **58**; 30% ellipsoids are shown, hydrogen atoms have been omitted for clarity. Selected bond distances and angles: P(1)-N(1) 1.584(3) Å; P(2)-N(1) 1.659(3)Å; P(1)-N(1)-P(2) 126.55(19)°.

distance 1.584(3) Å corresponds to that expected for a P-N double bond, while the P(2)-N(1) distance 1.659(3) Å corresponds to that of single bond.[91] Furthermore, the P(1)-

N(1)-P(2) bond angle was found to have a significant deviations from linearity being 126.55(19)°.

The strong Lewis basicity of compounds **58** and **59** was confirmed via independent reactions with trimethylaluminum (TMA) and tris(pentafluorophenyl)borane ($B(C_6F_5)_3$). These reactions are shown in Scheme 3.2. Coordination of aluminum to the

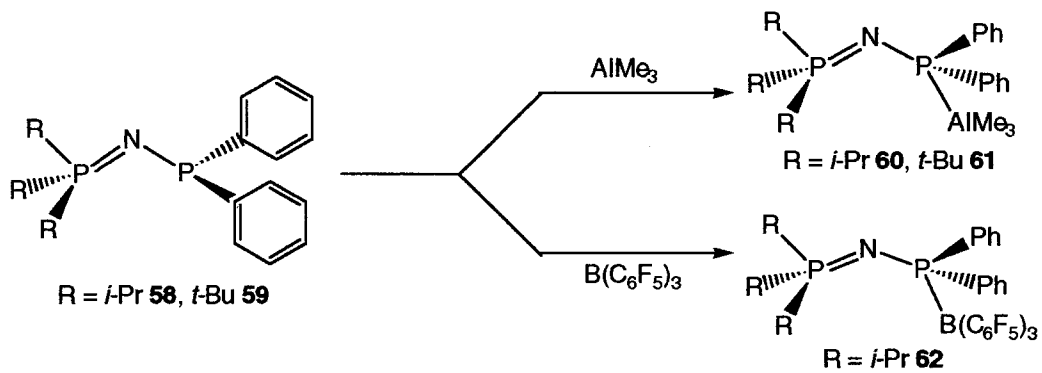

Scheme 3.2 Generation of compounds **60**, **61** and **62**.

P(III) atom was observed from the slight broadening of the upfield signal in the $^{31}P\{^1H\}$-NMR spectrum. The observation of a pair of doublets in the $^{31}P\{^1H\}$ NMR spectrum for compounds **60** and **61**, in addition to ^1H and $^{13}C\{^1H\}$ NMR spectra indicated the formation of one species. X-ray quality crystals of complex **60** were obtained in about 16 hours after the workup process. An X-ray crystallographic study of **60** confirmed the formulation and revealed the presence of two rotamers (Figure 3.3). It was found that the bond distances for P(1)-N(1) and P(3)-N(2) were 1.568(2) and 1.567(2) Å respectively, which were slightly shorter than that of compound **58** but still suggested of a P-N double bond. Similarly, the P(2)-N(1) and P(4)-N(2) bond lengths were 1.627(2) and 1.619(2) Å respectively, which were also slightly shorter than that seen in compound **58**. In contrast,

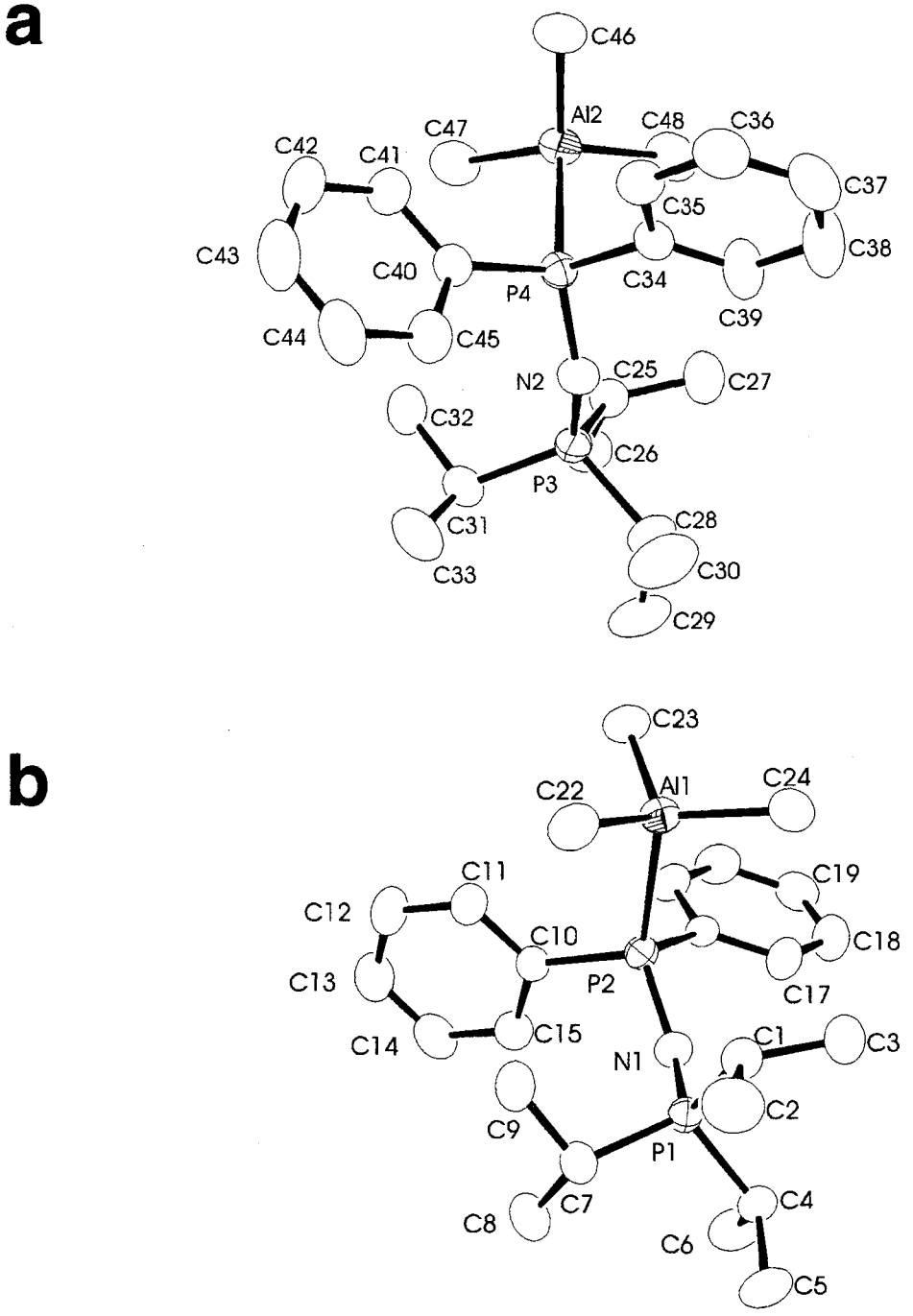

Figure 3.3 ORTEP drawings of the two molecules of **60** in the asymmetric unit; 30% ellipsoids are shown, hydrogen atoms have been omitted for clarity. Selected bond distances and angles: (a) Al(1)-P(2) 2.5190(11) Å; P(1)-N(1) 1.568(2) Å; P(2)-N(1) 1.627(2) Å; N(1)-P(2)-Al(1) 123.92(9) °; P(1)-N(1)-P(2) 141.52(16) °. (b) Al(2)-P(4) 2.5183(11) Å; P(3)-N(2) 1.567(2) Å; P(4)-N(2) 1.619(2) Å; N(2)-P(4)-Al(2) 124.72(10) °; P(3)-N(2)-P(4) 144.48(18) °.

the P(1)-N(1)-P(2) and P(3)- N(2)-P(4) angles of 124.72(10) and 144.48(18)° respectively, were found to be significantly larger than the P-N-P bond angle (126.55(19)°) of compound **58**. Unlike bis(phosphino)amide compounds, neither coordination of aluminum to nitrogen nor formation of dimeric species was observed.[91, 92]

Similarly, reaction of **58** with $B(C_6F_5)_3$ in hydrocarbon solvents at room temperature generated compound **62** in 87% yield (Scheme 3.2). A classically quadrupolar-broadened resonance in the $^{31}P\{^1H\}$-NMR spectrum, due to the presence of the ^{11}B nucleus (I = 3/2), was attributed to the P(III) atom was observed (Figure 3.4). This indicated the coordination of the boron atom occurs on the P(III) atom.

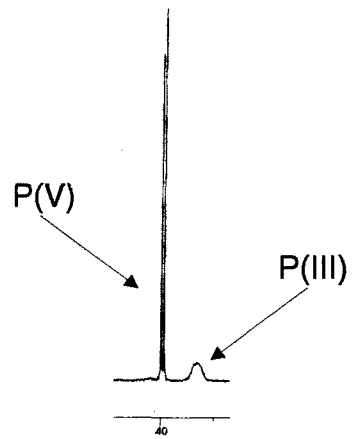

Figure 3.4 $^{31}P\{^1H\}$-NMR spectrum of **62**.

On the other hand, the resonance corresponded to P(V) maintained as a typical sharp doublet was observed. In addition, ^1H-, $^{13}C\{^1H\}$-, $^{11}B\{^1H\}$- and $^{19}F\{^1H\}$-NMR spectra agreed with the formation of a single species with the proposed structure depicted in Scheme 3.2. Single crystals of **62** were obtained and the X-ray structure was determined (Figure 3.5).

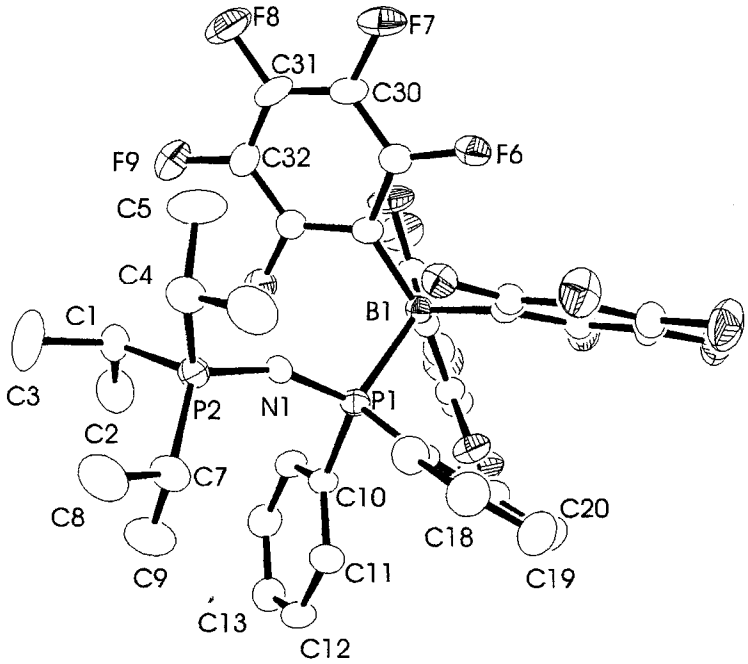

Figure 3.5 ORTEP drawing of **62**; 30% thermal ellipsoids are shown, hydrogen atoms have been omitted for clarity. Selected bond distances and angles: P(1)-N(1) 1.590(4) Å; P(1)-B(1) 2.135(5) Å; P(2)-N(1) 1.577(4) Å; N(1)-P(1)-B(1) 110.9(2)°; P(2)-N(1)-P(1) 157.1(3)°.

X-ray crystallographic study further confirmed the formation of compound **62**. The bond lengths P(1)-N(1) and P(2)-N(2) were 1.590(4) and 1.577(4) Å, both adopted partial double bond character. This suggests delocalization of the double bond may result from the interaction with the Lewis acidic of $B(C_6F_5)_3$. In addition, the P(2)-N(1)-P(1) bond angle of 157.1(3)° was found to be larger than that observed for both compounds **59** and **60**. The trend in increasing bond angles was presumably a result of an increase in steric congestion.

Oxidation of compounds **58** and **59** via Staudinger reaction with 1 equivalent of azidotrimethylsilane in the absence of solvent was investigated. Elimination of nitrogen gas gave the desired silylated phosphinimine-phosphinimine ligands **63** and **64** respectively in quantitative yield (Scheme 3.3). The proposed structures indicated in

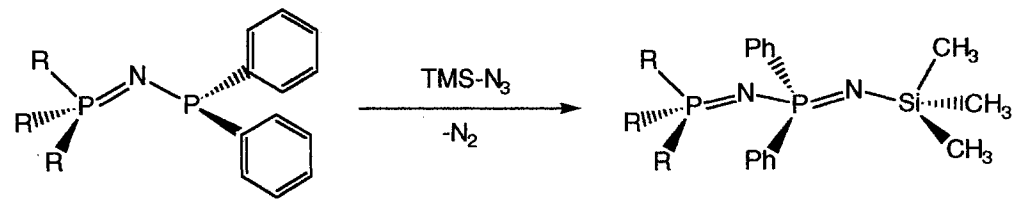

R = *i*-Pr **58**, *t*-Bu **59**

R = *i*-Pr **63**, *t*-Bu **64**

Scheme 3.3 Generation of P(V)-P(V) ligands **63** and **64** via Staudinger reaction.

Scheme 3.3 were formulated by $^{31}P\{^1H\}$-, ^1H, and $^{13}C\{^1H\}$-NMR spectra. A large shielding effect on the original P(III) resonance was observed from the $^{31}P\{^1H\}$-NMR spectrum. The chemical shifts were found to dramatically shifted from 38.90 ppm with a coupling constant of 80 Hz to –6.08 ppm and a coupling constant of 9 Hz.

Synthesis and methylation of 65 and 66

Reaction of the new phosphinimide-phosphinimine ligands **63** and **64** with $CpTiCl_3$ in non-polar hydrocarbon solvent afforded the titanium(IV) phosphinimine-phosphinimide complexes **65** and **66** respectively by metathetical elimination of Me_3SiCl, both in quantitative yield. Alternatively, complexes **65** and **66** were also prepared via a one pot synthesis of 1 equivalent of $TiCl_4$ with exactly 1.6 equivalent of $TMSN_3$, followed by the addition of 1 equivalent of either **58** or **59** in non-polar solvents (Scheme 3.4). The ^{31}P-NMR spectra of **65** and **66** consist of the typical AX spin pattern similar to that seen for compounds **63** and **64**. The formulation of **65** and **66** were confirmed with the corresponding ^1H- and $^{13}C\{^1H\}$-NMR spectra as well as X-ray crystallographic study of complex **64** (Figure 3.6).

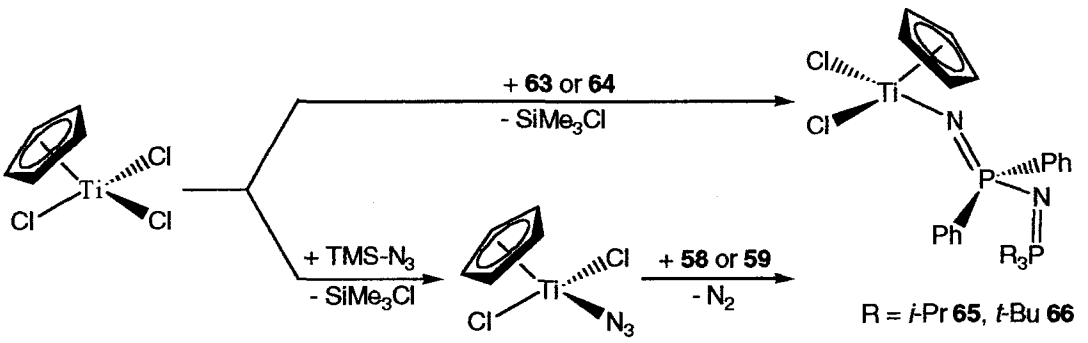

Scheme 3.4 Two synthetic strategies in generating **65** and **66**.

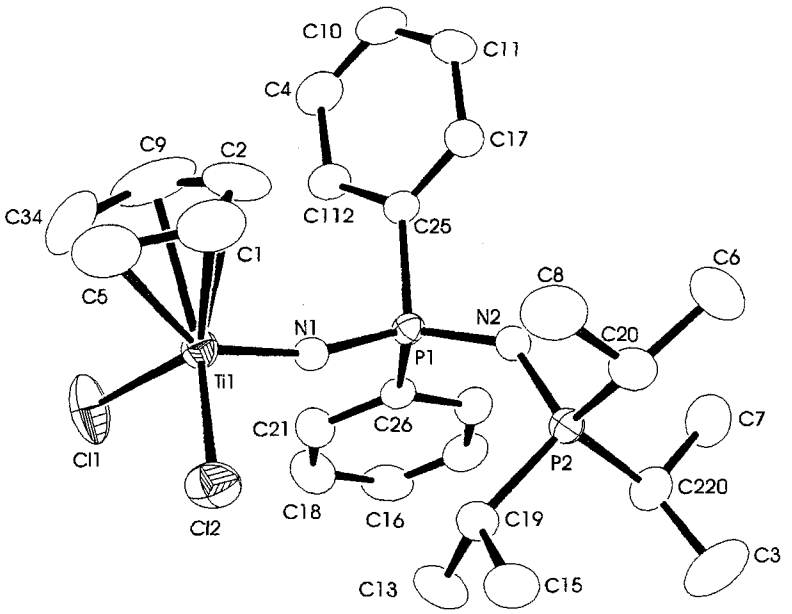

Figure 3.6 ORTEP drawing of **65**; 30% thermal ellipsoids are shown, hydrogen toms have been omitted fro clarity. Selected bond distances and angles: Ti(1)-N(1) 1.775(3) Å; P(1)-N(2) 1.598(4) Å; P(1)-N(1) 1.612(3) Å; P(2)-N(2) 1.593(4) Å; N(2)-P(1)-N(1) 118.16(18)°; P(1)-N(1)-Ti(1) 164.7(2)°; P(2)-N(2)-P(1) 134.9(2)°.

The bond distances Ti(1)-N(1) of 1.775(3) Å in complex **65** was found to be within the range of M-N double bond of 1.716(3) – 1.869(4) Å.[58b] It was interesting to note that the bond distance P(1)-N(1) of 1.612(3) Å was found to be slightly longer than

the P(1)-N(2) distance of 1.598(4) Å and P(2)-N(2) 1.593(4) Å. The bending moiety was also confirmed from the significant deviations of the bond angle P(1)-N(1)-Ti(1) of 164.7(2)°. This suggests the presence of some degree of the bonding mode **35B** for bent phosphinimide complexes mentioned in Chapter 1.

The analogous dimethyl derivatives of **65** and **66** were also prepared with 2 equivalents of methyl Grignard reagent in hydrocarbon solvents to give complexes **67** and **68** respectively under mild conditions, both in quantitative yields (Scheme 3.5). The

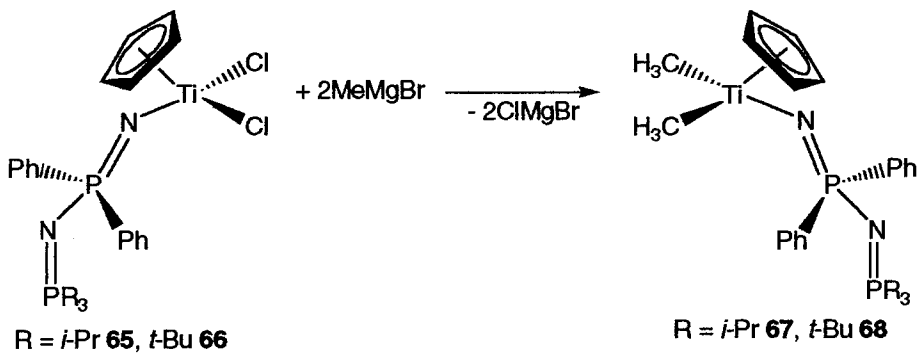

Scheme 3.5 Generation of **67** and **68** via alkylation.

proposed structures were formulated by the corresponding $^{31}P\{^1H\}$-, ^1H- and $^{13}C\{^1H\}$-NMR spectra.

Ethylene Polymerization of 65, 66, 67 and 68

Cyclopentadienyl phosphinimine-phosphinimide titanium dichloride complexes (**65**, **66**) and its analogous dimethyl derivatives (**67**, **68**) were tested for activity in ethylene polymerization. A large excess of MAO was used as the co-catalyst for complexes **65** and **66**, while exactly one equivalent of trityl

tetrakis(pentafluorophenyl)borate were employed for complexes **67** and **68**. The results are tabulated in Table 3.3.

Table 3.3 Ethylene Polymerization Data for 65, 66, 67 and 68

Catalyst Presursor	mmole of catalyst precursor	Cocatalyst[a]	Time (min)	Productivity (g mmol^{-1} h^{-1})	M_w[d]	M_w/M_n
65[c]	0.0179	MAO	3.00	299	118 700	1.74
66[b]	0.0163	MAO	60.00	109	1 083 000	2.24
67[c]	0.0194	TB	3.00	0	0	0
68[c]	0.0174	TB	3.00	0	0	0
Cp_2ZrCl_2[b]	0.0246	MAO	2.00	895	11,6353	2.8

[a]MAO: methylaluminoxane (500 equiv); TB: trityl tetrakis(pentafluorophenyl)borate (1 equiv). [b]Polymerizations were run at 33 psi pressure of ethylene and 60 - 65 °C. [c]Polymerizations were run at 1 atm pressure of ethylene and 25 °C. [d]Molecular weight data were recorded against polyethylene standards.

It was found that complexes **65** and **66** when activated by MAO achieved high activities of 299 and 109 g mmol^{-1} h^{-1}, while complexes **67** and **68** when activated by trityl tetrakis(pentafluorophenyl)borate showed no activity. Steric crowding as a result of the presence of the phosphinimide-phosphinimide ligand may inhibit coordination of ethylene to the titanium center. Additionally, preliminary studies on the deactivation pathway suggests dimerization of the cationic active species.[89] When comparing the activity of the catalysts derived from the dichloride complexes, the catalyst derived from complex **65** was found to have a higher activity than that of **66**. This was presumably a result from the fact that the tri-*t*-butylphosphinimine-diphenylphosphinimide ligand is bulkier than the tri-*i*-propylphosphinimine-dipenylphosphinimide ligand. This sterically more hindered ligand lowered the degree of access for olefin to coordinate to the titanium center. In addition, GPC data revealed that the polyethylene generated by the catalysts derived from complexes **65** and **66** have M_w(PDI) 118, 700 (1.74) and 1, 083, 000 (2.24) respectively. These data suggested these systems are in fact "single site" catalysts. The

discovery of these high active catalysts system suggests our designing strategy is promising.

3.4 Summary

The novel phosphinimide-phosphine ligands **58** and **59** were readily prepared. Crystallographic data revealed the nitrogen is in psuedo-tetrahedral geometry. Independent reactions with TMA and $B(C_6F_5)_3$ generated compounds **60**, **61** and **62**. This implied the strong Lewis basic nature for such ligands. Oxidation of ligands **58** and **59** with $TMSN_3$ led to the formation of compounds **63** and **64** respectively. These were then used to generate the corresponding titanium complexes **65** and **66** respectively. Methylation of complexes **65** and **66** generated the corresponding methyl derivatives **67** and **68**. As a consequence, complexes **65**, **66**, **67** and **68** were tested for activity in ethylene polymerization. Catalysts derived from complexes **65** and **66** achieved high activities while catalysts derived from complexes **67** and **68** achieved no activity. The results were presumably contributed from the steric crowding between the phosphinimine-phosphinimide ligands and the methyl groups. Also, a decrease in activity was observed from the catalyst precursors **65** to **66**. This was attributed to the more sterically hindered nature of the *tri*-t-butylphosphinimine-diphenylphosphinimide ligand. As a result, the degree of access for ethylene to coordinate was reduced. In addition, information obtained from the generated polyethylene suggests these catalysts are indeed "single site" catalysts. In conclusion, the strategy applied here results in new catalyst systems with high activity in ethylene polymerization indicating the potential of our ligand design.

Chapter Four
Summary

This thesis has described extensive studies on group(IV) phosphinimide complexes. The results provided vital information about designing group(IV) homogeneous catalyst precursors based on phosphinimide ligand systems.

The very first monomeric pentamethylcyclopentadienyl zirconium phosphinimide complexes **41** and **53** were prepared and fully characterized. Reactivity studies of complexes **41** and **53** proved to be quite fruitful. A variety of derivatives (**42-48**) were readily prepared via salt metathesis reactions under mild conditions. These complexes were tested for ethylene polymerization and showed minimal to low activities. This is presumably due to the fact that Cp* is highly electron donating and sterically hindered. In addition, the highly active substituted butadiene analogues **49** and **50** were generated via a modified one-pot synthetic strategy. A substantial increase in ethylene polymerization activity was observed for the catalyst derived from complex **49**. In contrast, no activity in ethylene polymerization was observed for complex **50**. This is presumably due to the steric crowding of the bulky tri-*tert*-butyl phosphinimide and Cp* ligands. Important information was also obtained from the polyethylene produced by various zirconium phosphinimide catalyst precursors. The bimodal molecular weight distribution is indicative of degradation of these precursors and the formation of more than one active species under the employed polymerization conditions.

The extension of phosphinimide ligands led to the development of the novel phosphinimide-phosphine ligands **58** and **59**. Reactivity studies of compounds **58** and **59** indicated that these ligands behave as Lewis bases. The corresponding cyclopentadienyl

phosphinimine-phosphinimide titanium complexes **65** and **66** were also prepared. The methyl analogues **67** and **68** were generated subsequently. All four complexes were tested for activity in ethylene polymerization. High activity was observed for complexes **65** and **66** while no activity was observed for the methyl analogues. This is presumably due to steric congestion. The obtained narrow molecular weight distributions of the generated polyethylene suggest complexes **67** and **68** are "single site" catalyst precursors.

In conclusion, this research has established a systematic study of the chemistry of group(IV) phosphinimide complexes. Although various zirconium phosphinimide complexes function as catalyst precursors in ethylene polymerization, possible degradation and the presence of multiple active species were observed. In contrast, titanium phosphinimide-phosphinimide complexes are in fact promising new homogeneous "single site" catalyst precursors.

References

1. (a) Ziegler, K.; Holzkamp, E.; Martin, H.; Breil, H. *Angew. Chem.* **1955**, *67*, 541. (b) Ziegler, K. *Angew. Chem.* **1964**, *76*, 545.
2. (a) Natta, G. *J. Am. Chem. Soc.* **1955**, *77*, 1708. (b) Natta, G. *Angew. Chem.* **1956**, *68*, 393. (c) *ibid* **1964**, *76*, 553.
3. Wesslau, H. *Makromol. Chem.* **1956**, *20*, 111.
4. Wilkinson, G.; Pauson, P. L.; Birminghan, M. J.; Cotton, F. A. *J. Am. Chem. Soc.* **1953**, *75*, 1011.
5. (a) Natta, G.; Pino, P.; Mazzanti, G.; Giannini, U. *J. Am. Chem. Soc.* **1957**, *79*, 2975. (b) Natta, G.; Pino, P.; Mazzanti, G.; Giannini, U.; Mantica, E. *J. Polym. Sci.* **1957**, *26*, 120.
6. Breslow, D. S.; Kewburg, N. R. *J. Am. Chem. Soc.* **1957**, *79*, 5072.
7. Reichert, K. H.; Meyer, K. R. *Makromol. Chem.* **1973**, *169*, 163.
8. Long, W. P.; Breslow, D. S. *Liebigs Ann. Chem.* **1975**, 463.
9. Andersen, A.; Cordes, H. G.; Herwig, H.; Kaminsky, W.; Merk, A.; Mottweiler, R.; Pein, J.; Sinn, H.; Vollmer, H. J. *Angew. Chem., Int. Ed. Engl.* **1976**, *15*, 630.
10. Sinn, H.; Kaminsky, W. *Adv. Organomet. Chem.* **1980**, *18*, 99.
11. Sinn, H.; Kaminsky, W.; Vollmer, H. J.; Woldt, R. *Angew. Chem., Int. Ed. Engl.* **1980**, *19*, 390.
12. Manson, M. R.; Smith, J. M. Bott, S. G.; Barron, A. R. *J. Am. Chem. Soc.* **1993**, *115*, 4971.

13. Stephan, D. W.; Stewart, J. C.; Guérin, F.; Spence, R. E.; Xu, W.; Harrison, D. G. *Organometallics* **1999**, *18*, 1116.

14. Stephan, D. W.; Guérin, F.; Spence, R. E.; Koch, L.; Gao, X.; Brown, S. J.; Swabey, J. W.; Wang, Q.; Xu, W.; Zoricak, P.; Harrison, D. G. *Organometallics* **1999**, *18*, 2046.

15. (a) Britovsek, G. J. P.; Gibson, V. C.; Wass, D. F. *Angew. Chem., Int. Ed. Eng.* **1999**, *38*, 428. (b) Alt, H. G.; Köppl, A. *Chem. Rev.* **2000**, *100*, 1205.

16. McKnight, A. L.; Waymouth, R. M. *Chem. Rev.* **1998**, *98*, 2587.

17. Bochmann, M. J. Chem. Soc., *Dalton Trans.* **1996**, 255.

18. Kaminsky, W. *J. Chem. Soc., Dalton Trans.* **1998**, 1413.

19. Eisch, J. J.; Bombrick, S. I.; Zheng, G. X. *Organometallics* **1993**, *12*, 3856.

20. (a) Jordan, R. F.; Dasher, W. E.; Echols, S. F. *J. Am. Chem. Soc.* **1986**, *108*, 1718. (b) Sishta, C.; Hathorn, R. M.; Marks, T. J. *J. Am. Chem. Soc.* **1992**, *114*, 1112.

21. Piers, W. E.; Chivers, T. *Chem. Soc. Rev.* **1997**, *26*, 345.

22. Chen, E. Y. –X.; Marks, T. J. *Chem. Rev.* **2000**, *100*, 1391.

23. Yang, X.; Stern, C. L.; Marks, T. J. *J. Am. Chem. Soc.* **1991**, *113*, 3623.

24. Yang, X.; Stern, C. L.; Marks, T. J. *J. Am. Chem. Soc.* **1994**, *116*, 10015.

25. Piers, W. E. *Chem. Eur. J.* **1998**, *4*, 13.

26. Hlatky, G. G.; Turner, H. W.; Eckman, R. R. *J. Am. Chem. Soc.* **1989**, *111*, 2728.

27. (a) Temme, B.; Erker, G.; Karl, J.; Luftmann, H.; Fröhlich, R.; Kotila, S. *Angew. Chem., Int. Ed. Engl.* **1995**, *34*, 1755. (b) Temme, B.; Karl, J.; Erker,

G. *Chem. Eur. J.* **1996**, *2*, 919. (c) Karl, J.; Erker, G.; Fröhlich, R. *J. Am. Chem. Soc.* **1997**, *119*, 11165.

28. Chen, Y. –X.; Marks, T. J. *Organometallics* **1997**, *16*, 3649.

29. Sun, Y.; Piers, W. E.; Rettig, S. J. *Chem. Commun.* **1998**, 127.

30. (a) Temme, B.; Erker, G.; Fröhlich, R.; Grehl, M. *Angew. Chem., Int. Ed. Engl.* **1994**, *33*, 1480. (b) Ahlers, W.; Temme, B.; Erker, G.; Fröhlich, R.; Fox, T. *J. Organomet. Chem.* **1997**, *527*, 191.

31. Spence, R. E. von H.; Piers, W. E. *Organometallics* **1995**, *14*, 4617.

32. Spence, R. E. von H.; Parks, D. J.; Piers, W. E.; MacDonald, M.; Zaworotko, M. J.; Rettig, S. J. *Angew. Chem., Int. Ed. Engl.* **1995**, *34*, 1230.

33. Ruwwe, J.; Erker, G.; Fröhlich, R. *Angew. Chem., Int. Ed. Engl.* **1996**, *35*, 80.

34. Larkin, S. A.; Golden, J. T.; Shapiro, P. J.; Yap, G. P. A.; Foo, D. M. J.; Rheingold, A. L. *Organometallics* **1996**, *15*, 2393.

35. Bochmann, M.; Lancaster, S. J.; Robinson, O. B. *J. Chem. Soc., Chem. Commun.* **1995**, 2081.

36. (a) Raufanov, K. A.; Kotov, V. V.; Kazennova, N. B.; Lemenovskii, D. A.; Avtomonov, E. V.; Lorberth, J. *J. Organomet. Chem.* **1996**, *525*, 287. (b) Stelck, D. S.; Shapiro, P. J.; Basickes, N.; Rheingold, A. L. *Organometallics* **1997**, *16*, 4546.

37. Burns, C. T.; Stelck, D. S.; Shapiro, P. J.; Vij, A.; Kunz, K.; Kehr, G.; Concolino, T.; Rheingold, A. L. *Organometallics* **1999**, *18*, 5432.

38. Quyoum, R.; Wang, Q.; Tudoret, M. –J.; Baird, M. C. *J. Am. Chem. Soc.* **1994**, *116*, 6435.

39. Wang, Q.; Quyoum, R.; Gillis, D. J.; Tudoret, M. –J.; Jeremic, D.; Hunter, B. K.; Baird, M. C. *Organometallics* **1996**, *15*, 693.

40. Ewart, S. W.; Sarsfield, M. J.; Jeremic, D.; Tremblay, T. L.; Williams, E. F.; Baird, M. C. *Organometallics* **1998**, *17*, 1502.

41. Pellecchia, C.; Proto, A.; Zambelli, A. *Macromol. Chem. Rapid Commun.* **1992**, *13*, 277.

42. Pellecchia, C.; Immirzi, A.; Grassi, A.; Zambelli, A. *Organometallics* **1993**, *12*, 4473.

43. Janiak, C.; Lange, K. C. H.; Versteeg, U.; Lentz, D.; Budzelaar, P. H. M. *Chem. Ber.* **1996**, *129*, 1517.

44. Van der Linden, A.; Schaverien, C. J.; Meijboom, N.; Ganter, C.; Orpen, A. G. *J. Am. Chem. Soc.* **1995**, *117*, 3008.

45. Repo, T.; Klinga, M.; Pietikäinen, P.; Leskelä, M.; Uusitalo, A. –M.; Pakkanen, T.; Hakala, K.; Aaltonen, P.; Löfgren, B. *Macromol.* **1997**, *30*, 171.

46. Chen, Y. –X.; Fu, P. –F.; Stern, C. L.; Marks, T. J. *Organometallics* **1997**, *16*, 5958.

47. Jäger, F.; Roesky, H. W.; Dorn, H.; Shah, S.; Noltemeyer, M.; Schmidt, H. –G. *Chem. Ber.* **1997**, *130*, 399. (b) Bürger, H.; Beiersdorf, D. *Z. Anorg. Allg. Chem.* **1979**, *459*, 111.

48. Mack, H.; Eisen, M. S. *J. Organomet. Chem.* **1996**, *525*, 81.

49. Horton, A. D.; de With, J. *Chem. Commun.* **1996**, 1375.

50. Sinnema, P. J.; van der Veen, L.; Spek, A. L.; Veldman, N.; Teuben, J. H. *Organometallics* **1997**, *16*, 4245.

51. Gomes, P. T.; Green, M. L. H.; Martins, A. M.; Mountford, J. *Organomet. Chem.* **1997**, *541*, 121.

52. Sernetz, F. G.; Muelhaupt, R.; Waymouth, R. M. *Macromol. Chem. Phys.* **1996**, *197*, 1071.

53. Guérin, F.; McConville, D. H.; Vittal, J. J. *Organometallics* **1996**, *15*, 5586.

54. Guérin, F.; McConville, D. H.; Payne, N. C. *Organometallics* **1996** *15*, 5085.

55. Gónezm, R.; Green, M. L. H.; Haggitt, J. *J. Chem. Soc., Chem. Commun.* **1994**, 2607.

56. Oberthür, M.; Arndt, P.; Kempe, R. *Chem. Ber.* **1996**, *129*, 1087.

57. Phillips, F. L.; Skapski, A. C. *J. C. S. Dalton*, **1976**, 1448.

58. (a) Dehnicke, K.; Strähle, J. *Polyhedron* **1989**, *8*, 707. (b) Dehnicke, K.; Krieger, M.; Massa, W. *Coord. Chem. Rev.* **1999**, *182*, 19.

59. Anfang, S.; Harms, K.; Weller, F.; Borgmeier, O.; Lueken, H.; Schilder, H.; Dehnicke, K. *Z. Anorg. Allg. Chem.* **1998**, *624*, 159.

60. Rubenstahl, T.; Weller, F.; Wacadlo, S.; Massa, W.; Dehnicke, K. *Z. Anorg. Allg. Chem.* **1995**, *621*, 953.

61. Lubben, T. V.; Wolczanski, P. T.; Van Duyne, G. D. *Organometallics* **1984**, *3*, 997.

62. Dehnicke, K.; Strähle, J. *Z. Anorg. Allg. Chem.* **1965**, *339*, 171.

63. Strähle, J. *Z. Anorg. Allg. Chem.* **1974**, *405*, 139.

64. (a) Staudinger, H.; Meyer, J. *Helv. Chim. Acta.* **1919**, *2*, 635. (b) Leffler, J. E.; Temple, R. D. *J. Am. Chem. Soc.* **1967**, *89*, 5235. (c) Gololobov, Y. G.; Zhmurova, I. N.; Kasukhin, L. F. *Tetrahedron* **1981**, *37*, 437. (d) Gololobov, Y. G.; Kasukhin, L. F. *Tetrahedron* **1992**, *48*, 1353.

65. Guérin, F.; Stephan, D. W. *Angew. Chem., Int. Ed. Engl.* **2000**, *39*, 1298.

66. Guérin, F.; Stewart, J. C.; Beddie, C.; Stephan, D. W. *Organometallics* **2000**, *19*, 2994.

67. (a) Dehnicke, K.; Weller, F. *Coord. Chem. Rev.* **1997**, *158*, 103. (b) Schmidbaur, H.; Jonas, G. *Chem. Ber.* **1967**, *100*, 1120.

68. Cromer, D. T.; Waber, J. T. *International Tables for X-ray Crystallography*; Knoch Press: Birmingham England, **1974**.

69. Guérin, F.; Stephan, D. W. Unpublished results.

70. Wolczanski, P. T.; Bercaw, J. E. *Organometallics* **1982**, *1*, 793.

71. Stahl, M. M.; Faza, N.; Massa. W.; Dehnicke, K. *Z. Anorg. Allg. Chem.* **1997**, *623*, 1855.

72. Grün, M.; Weller, F.; Dehnicke, K. *Z. Anorg. Allg. Chem.* **1997**, *623*, 224.

73. Erker, G.; Berg, K.; Angermund, K.; Krüger, C. *Organometallics* **1987**, *6*, 2620.

74. Walther, D.; Fischer, R.; Friedrich, M.; Gebhardt, P.; Görls, H. *Chem. Ber.* **1996**, *129*, 1389.

75. (a) Buchwald, S.; Watson, B. T. *J. Am. Chem. Soc.* **1986**, *108*, 7411. (b) Buchwald, S.; Nielsen, R. B. *Chem. Rev.* **1988**, *88*, 1047.

76. Erker, G. *J. Organomet. Chem.* **1977**, *134*, 189.

77. Stewart, J. C.; Stephan, D. W. Unpublished results.

78. Erker, G.; Wicher, J.; Engel, K.; Rosenfeldt, F.; Dietrich, W. *J. Am. Chem. Soc.* **1980**, *102*, 6348.

79. Wreford, S. S.; Whitney, J. F. *Inorg. Chem.* **1981**, *20*, 3918.

80. Yasuda, H.; Kajhara, Y.; Mashima, K.; Nagasuna, K.; Lee, K.; Nakamura, A. *Organometallics* **1982**, *1*, 388.

81. Dorf, U.; Engel, K.; Erker, G. *Organometallics* **1983**, *2*, 462.

82. Yasuda, H.; Nakamura, A. *Angew. Chem., Int. Ed. Engl.* **1987**, *26*, 723.

83. Fujita, K.; Ohuima, Y.; Yasuda, H.; Tani, H. *J. Organomet. Chem.* **1976**, *113*, 201.

84. (a) Yang, M.; Yamamoto, K.; Otake, N.; Ando, M.; Takase, K. *Tetrahedron Lett.* **1970**, 3843. (b) Yang, M.; Ando, M.; Takase, K. *ibid.* **1971**, 3529. (c) Nakano, Y.; Natsukawa, K.; Yasuda, H.; Tani, H. *ibid.* **1972**, 2833. (d) Baker, R.; Cookson, R. C.; Saunders, A. D. *J. Chem. Soc., Perkin Trans.* **1976**, *1*, 1809. (e) Akutagawa, S.; Otsuka, S. *J. Am. Chem. Soc.* **1976**, *98*, 7420. (f) Fujita, K.; Ohnuma, Y.; Yasuda, H.; Tani, H. *J. Organomet. Chem.* **1976**, *113*, 201. (g) Yasuda, H.; Nakano, Y.; Natsukawa, K.; Tani, H. *Macromolecules* **1978**, *11*, 586.

85. Yasuda, H.; Kazuyuki, T.; Nakamura, A. *Acc. Chem. Res.* **1985**, *18*, 120.

86. Krüger, C.; Müller, G.; Erker, G.; Dorf, U.; Engel, K. *Organometallics* **1985**, *4*, 215.

87. Kai, Y.; Kanehisa, N.; Miki, K.; Kasai, N.; Akita, M.; Yasuda, H.; Nakamura, A. *Bull. Chem. Soc. Jpn.* **1983**, *56*, 3735.

88. Hey-Hawkins, E.; Kurz, S. *J. Organomet. Chem.* **1994**, *479*. 125.

89. Yue, L. -S. N.; Stephan, D. W. Unpublished results.

90. Karl, J.; Erker, G.; Fröhlich, R. *J. Organomet. Chem.* **1997**, *535*, 59.

91. Braunstein, P.; Hasselbring, R.; Stalke, D. *New. J. Chem.* **1996**, *20*, 337.

92. Hasselbring, R.; Braunstein, P. *Phosphorus, Sulfur, and Silicon* **1994**, *93-94*, 423.

Appendix One
Supplementary Crystallographic Parameters for 41, 44, 46, 47, 49 and 50

Table A1.1: Positional Parameters and U(eq) for 41

Atom	x	y	z	B(eq)	Atom	x	y	z	B(eq)
Zr(1)	9600(1)	5206(1)	1070(1)	62(1)	C(8)	8190(30)	5600(30)	-644(9)	410(30)
Cl(1)	7545(2)	4034(2)	1450(1)	79(1)	C(9)	10900(30)	6684(10)	-213(13)	320(20)
Cl(2)	7572(4)	6470(2)	1100(1)	110(1)	C(10)	13583(17)	5140(20)	528(8)	390(30)
P(1)	11895(3)	5585(2)	2529(1)	78(1)	C(11)	12401(19)	4560(9)	2989(5)	130(5)
N(1)	10937(8)	5401(5)	1856(3)	70(2)	C(12)	10760(20)	4051(10)	3160(7)	157(6)
C(1)	11110(30)	4277(12)	220(7)	137(8)	C(13)	13620(30)	4049(13)	2598(9)	235(13)
C(2)	9720(30)	4391(11)	-34(9)	133(7)	C(14)	10660(20)	6199(10)	3121(5)	140(5)
C(3)	9470(15)	5134(16)	-235(5)	123(5)	C(15)	9570(20)	6816(14)	2888(8)	206(10)
C(4)	10660(20)	5661(7)	-69(6)	111(5)	C(16)	11234(17)	6267(9)	3869(5)	142(5)
C(5)	11871(13)	5124(14)	250(5)	113(5)	C(17)	13719(15)	6180(15)	2347(6)	168(8)
C(6)	11200(40)	3288(11)	361(12)	390(30)	C(18)	14853(18)	6339(17)	2972(8)	243(13)
C(7)	8200(30)	3802(16)	-265(10)	270(16)	C(19)	13380(20)	7098(10)	1975(7)	173(7)

Table A1.1: Positional Parameters and U(eq) for 44

Atom	x	y	z	B(eq)	Atom	x	y	z	B(eq)
Zr(1)	-2742(1)	-1646(1)	-2797(1)	40(1)	C(14)	-1589(10)	2104(6)	-3520(3)	127(3)
P(1)	-2245(1)	1521(1)	-1892(1)	38(1)	C(15)	-4295(5)	1726(4)	-1757(3)	68(1)
N(1)	-2525(3)	114(2)	-2348(2)	40(1)	C(16)	-4255(6)	2929(5)	-1180(4)	101(2)
C(1)	-4395(4)	-3878(3)	-3768(2)	50(1)	C(17)	-5521(6)	562(5)	-1556(5)	114(2)
C(2)	-3135(4)	-3293(4)	-4264(2)	56(1)	C(18)	-5001(7)	1788(6)	-2685(4)	111(2)
C(3)	-3381(5)	-2206(4)	-4439(2)	56(1)	C(19)	-1106(6)	1917(4)	-781(2)	65(1)
C(4)	-4821(4)	-2153(3)	-4066(2)	50(1)	C(20)	194(8)	1352(6)	-818(4)	116(2)
C(5)	-5430(4)	-3172(3)	-3638(2)	50(1)	C(21)	-437(7)	3314(4)	-339(3)	89(2)
C(6)	-4647(6)	-5105(4)	-3484(3)	76(1)	C(22)	-2343(10)	1205(6)	-165(3)	131(3)
C(7)	-1906(6)	-3841(5)	-4656(3)	95(2)	C(23)	169(5)	-1089(5)	-3140(5)	98(2)
C(8)	-2440(7)	-1370(5)	-5027(3)	94(2)	C(24)	-24(11)	-1802(14)	-2533(8)	202(6)
C(9)	-5694(6)	-1279(4)	-4206(3)	77(1)	C(25)	-827(10)	-2503(7)	-2133(7)	150(4)
C(10)	-7056(5)	-3536(5)	-3237(4)	87(1)	C(26)	-4029(8)	-2304(4)	-1563(3)	88(2)
C(11)	-981(5)	2636(3)	-2578(3)	64(1)	C(27)	-4505(11)	-3500(5)	-1312(4)	131(3)
C(12)	-838(7)	4017(4)	-2324(4)	89(2)	C(28)	-5654(12)	-4232(6)	-1102(5)	156(4)
C(13)	827(7)	2663(6)	-2521(5)	114(2)					

Table A1.2: Positional Parameters and U(eq) for 46

Atom	x	y	z	B(eq)	Atom	x	y	z	B(eq)
Zr(1)	1551(1)	5462(1)	1401(1)	37(1)	C(17)	503(4)	8169(8)	530(2)	103(3)
P(1)	2004(1)	8161(1)	1047(1)	46(1)	C(18)	1437(5)	9655(9)	364(3)	137(4)
N(1)	1718(2)	7018(3)	1220(1)	43(1)	C(19)	3096(3)	7996(6)	1031(2)	70(2)
C(1)	417(3)	4069(5)	1495(2)	70(2)	C(20)	3226(4)	6766(7)	892(2)	92(2)
C(2)	73(3)	5166(5)	1386(2)	60(1)	C(21)	3623(4)	8095(7)	1457(2)	96(2)
C(3)	379(3)	5934(4)	1699(2)	55(1)	C(22)	3379(4)	8873(7)	754(3)	106(3)
C(4)	909(3)	5323(5)	2002(2)	58(1)	C(23)	1552(3)	4380(4)	837(2)	54(1)
C(5)	938(3)	4180(5)	1877(2)	65(2)	C(24)	931(5)	4448(9)	512(2)	124(4)
C(6)	186(6)	2955(7)	1271(3)	133(3)	C(25)	920(5)	3931(9)	148(2)	133(4)
C(7)	-599(4)	5436(7)	1034(2)	97(2)	C(26)	1531(5)	3284(6)	105(2)	92(2)
C(8)	91(4)	7151(5)	1731(2)	78(2)	C(27)	2159(5)	3181(7)	412(2)	101(3)
C(9)	1319(4)	5813(7)	2402(2)	95(2)	C(28)	2166(4)	3723(7)	769(2)	86(2)
C(10)	1389(5)	3217(7)	2131(3)	113(3)	C(29)	2730(3)	5021(5)	1837(1)	53(1)
C(11)	1885(4)	9402(5)	1384(2)	77(2)	C(30)	3196(3)	5731(5)	2122(2)	63(1)
C(12)	2128(4)	8997(7)	1817(2)	95(2)	C(31)	3933(4)	5406(6)	2349(2)	78(2)
C(13)	2369(5)	10512(6)	1334(3)	124(3)	C(32)	4245(4)	4360(7)	2294(2)	82(2)
C(14)	999(4)	9760(6)	1318(3)	106(3)	C(33)	3819(4)	3627(6)	2020(2)	82(2)
C(15)	1381(4)	8406(7)	525(2)	84(2)	C(34)	3073(4)	3948(5)	1799(2)	69(2)
C(16)	1619(5)	7526(9)	233(2)	121(3)					

Table A1.3: Positional Parameters and U(eq) for 47

Atom	x	y	z	U(eq)	Atom	x	y	z	U(eq)
Zr(1)	3933(1)	5977(1)	1746(1)	34(1)	C(11)	3493(4)	6737(2)	2846(1)	43(1)
Cl(1)	1037(1)	5556(1)	1802(1)	57(1)	C(12)	4486(4)	7299(2)	2536(1)	38(1)
P(1)	2853(1)	7413(1)	417(1)	39(1)	C(13)	5985(4)	6872(2)	2513(1)	42(1)
N(1)	3528(3)	6913(2)	1072(1)	39(1)	C(14)	5945(4)	6063(2)	2845(1)	47(1)
C(1)	4413(4)	8067(2)	80(2)	57(1)	C(15)	3796(6)	5207(2)	3401(2)	77(1)
C(2)	5093(5)	8811(3)	534(2)	82(1)	C(16)	1847(4)	6965(3)	3027(2)	70(1)
C(3)	5795(5)	7481(3)	-68(2)	79(1)	C(17)	4075(5)	8220(2)	2314(2)	59(1)
C(4)	1285(4)	8205(2)	575(2)	50(1)	C(18)	7432(4)	7268(3)	2255(2)	68(1)
C(5)	425(5)	8687(3)	-37(2)	77(1)	C(19)	7406(5)	5497(3)	3071(2)	80(1)
C(6)	83(4)	7818(2)	992(2)	66(1)	C(20)	3860(5)	4827(2)	822(2)	62(1)
C(7)	2061(4)	6676(2)	-273(1)	55(1)	C(21)	5373(5)	5231(2)	880(2)	63(1)
C(8)	1848(5)	7035(3)	-981(2)	78(1)	C(22)	6262(5)	5026(3)	1498(2)	68(1)
C(9)	521(5)	6193(3)	-141(2)	76(1)	C(23)	5263(5)	4455(2)	1818(2)	68(1)
C(10)	4389(4)	5963(2)	3033(1)	47(1)	C(24)	3821(5)	4349(2)	1398(2)	65(1)

Table A1.4: Positional Parameters and U(eq) for 49

Atom	x	y	z	U(eq)	Atom	x	y	z	U(eq)
Zr(1)	2092(1)	996(1)	7057(1)	41(1)	C(12)	-301(3)	282(2)	6745(2)	57(1)
P(1)	536(1)	2767(1)	6461(1)	45(1)	C(13)	-118(3)	513(2)	7559(2)	53(1)
N(1)	1272(3)	1987(1)	6677(2)	50(1)	C(14)	1287(4)	469(2)	8139(2)	58(1)
C(1)	4556(4)	322(2)	7665(3)	70(1)	C(15)	-1710(4)	432(3)	6126(3)	80(1)
C(2)	4712(4)	1117(3)	7858(2)	74(1)	C(16)	-1349(4)	906(2)	7853(3)	74(1)
C(3)	4657(3)	1485(2)	7107(3)	65(1)	C(17)	-1380(4)	2656(2)	5903(2)	56(1)
C(4)	4402(4)	973(2)	6479(3)	66(1)	C(18)	-2366(4)	3343(3)	5826(3)	89(1)
C(5)	4356(4)	261(2)	6817(3)	67(1)	C(19)	-1503(5)	2272(3)	5069(2)	84(1)
C(6)	4736(5)	-2900(4)	8292(4)	155(3)	C(20)	452(4)	3324(2)	7384(2)	55(1)
C(7)	5100(6)	1460(5)	8705(4)	164(4)	C(21)	1987(5)	3485(3)	7891(3)	92(1)
C(8)	4950(5)	2310(3)	7002(4)	124(2)	C(22)	-460(5)	2939(2)	7913(2)	78(1)
C(9)	4318(6)	1122(4)	5575(3)	114(2)	C(23)	1536(4)	3361(2)	5855(2)	60(1)
C(10)	4270(5)	-470(3)	6347(4)	121(2)	C(24)	1880(5)	2956(3)	5106(3)	91(1)
C(11)	893(4)	-22(2)	6410(2)	61(1)	C(25)	891(6)	4143(2)	5620(3)	94(2)

Table A1.5: Positional Parameters and U(eq) for 50

Atom	x	y	z	U(eq)	Atom	x	y	z	U(eq)
Zr(1)	4241(1)	8724(1)	1895(1)	36(1)	C(14)	-83(6)	9035(5)	2115(4)	88(2)
P(1)	1959(1)	8811(1)	3235(1)	41(1)	C(15)	2499(6)	9238(4)	4224(3)	58(2)
N(1)	3079(4)	8801(3)	2710(2)	42(1)	C(16)	1575(6)	9085(5)	4827(3)	80(2)
C(1)	6617(4)	8727(4)	1550(3)	41(1)	C(17)	2688(7)	10215(4)	4169(4)	86(2)
C(2)	6408(5)	9493(3)	1914(3)	43(1)	C(18)	3814(6)	8893(5)	4512(4)	83(2)
C(3)	6197(5)	9324(3)	2671(3)	46(1)	C(19)	1357(7)	7699(4)	3353(4)	70(2)
C(4)	6568(5)	8429(4)	2763(3)	44(1)	C(20)	1276(8)	7251(4)	2575(4)	92(3)
C(5)	6515(5)	8075(3)	2067(3)	46(1)	C(21)	37(8)	7635(4)	3668(5)	98(3)
C(6)	7008(6)	8631(4)	757(3)	62(2)	C(22)	2396(9)	7205(4)	3876(5)	106(3)
C(7)	6547(6)	10358(3)	1574(4)	65(2)	C(23)	3863(6)	7696(4)	1022(3)	63(2)
C(8)	6066(6)	9970(4)	3277(3)	74(2)	C(24)	2671(6)	8131(4)	759(3)	63(2)
C(9)	6271(6)	7960(5)	3507(3)	78(2)	C(25)	2637(6)	8998(4)	667(3)	56(2)
C(10)	6770(6)	7153(4)	1932(4)	69(2)	C(26)	3791(6)	9853(4)	841(3)	57(2)
C(11)	616(6)	9516(4)	2791(4)	62(2)	C(27)	1452(7)	7606(5)	611(4)	92(3)
C(12)	1206(7)	10302(4)	2466(4)	81(2)	C(28)	1410(6)	9471(5)	409(4)	88(2)
C(13)	-409(6)	9780(5)	3310(4)	84(2)					

Appendix Two
Supplementary Crystallographic Parameters for 58, 60, 62 and 65

Table A2.1: Positional Parameters and U(eq) for 58

Atom	x	y	z	U(eq)
P(1)	8199(1)	8343(1)	508(1)	41(1)
P(2)	8141(1)	9076(1)	2223(1)	48(1)
N(1)	8582(3)	9096(2)	1239(2)	46(1)
C(1)	8156(6)	8918(3)	-531(2)	57(1)
C(2)	6969(6)	9653(3)	-697(3)	75(1)
C(3)	8155(6)	8316(3)	-1327(3)	81(2)
C(4)	6508(4)	7721(3)	559(3)	54(1)
C(5)	6130(6)	6955(3)	-102(3)	82(2)
C(6)	5203(5)	8345(3)	568(3)	75(1)
C(7)	9592(4)	7457(3)	570(2)	54(1)
C(8)	9715(5)	6922(3)	1424(3)	75(1)
C(9)	11097(5)	7872(3)	481(3)	77(1)
C(10)	9911(5)	9283(2)	2929(2)	47(1)
C(11)	10028(6)	9283(3)	3818(3)	64(1)
C(12)	11350(8)	9410(3)	4365(3)	83(2)
C(13)	12590(7)	9541(3)	4026(4)	82(2)
C(14)	12502(6)	9542(3)	3138(4)	83(2)
C(15)	11186(5)	9408(3)	2608(3)	64(1)
C(16)	7373(4)	10221(3)	2303(2)	48(1)
C(17)	6481(5)	10391(4)	2902(3)	71(1)
C(18)	5876(6)	11251(5)	2972(4)	90(2)
C(19)	6174(6)	11943(4)	2454(4)	91(2)
C(20)	7043(6)	11798(3)	1848(3)	79(2)
C(21)	7642(5)	10940(3)	1775(3)	59(1)

Table A2.2: Positional Parameters and U(eq) for 60

Atom	x	y	z	U(eq)	Atom	x	y	z	U(eq)
Al(1)	2551(1)	2646(1)	1267(1)	55(1)	C(21)	1540(2)	3046(2)	2640(1)	64(1)
Al(2)	5944(1)	2411(1)	1995(1)	61(1)	C(22)	2592(2)	1722(2)	639(2)	79(1)
P(1)	-136(1)	2776(1)	-130(1)	48(1)	C(23)	3301(2)	2439(2)	2223(2)	75(1)
P(2)	1139(1)	2520(1)	1293(1)	45(1)	C(24)	2617(2)	3884(2)	1017(2)	79(1)
P(3)	5058(1)	2709(1)	-272(1)	57(1)	C(25)	4298(2)	3164(2)	34(2)	65(1)
P(4)	6483(1)	2357(1)	1077(1)	49(1)	C(26)	3385(2)	3061(3)	-440(2)	98(1)
N(1)	281(1)	2783(2)	663(1)	57(1)	C(27)	4477(2)	4117(2)	252(2)	99(1)
N(2)	5953(2)	2627(2)	296(1)	63(1)	C(28)	5121(2)	3482(3)	-898(2)	84(1)
C(1)	553(2)	3213(2)	-507(1)	59(1)	C(29)	4374(2)	3502(3)	-1573(2)	120(2)
C(2)	350(2)	2985(3)	-1246(2)	98(1)	C(30)	5919(3)	3469(4)	-983(2)	126(2)
C(3)	671(2)	4204(2)	-396(2)	82(1)	C(31)	4611(2)	1668(2)	-662(2)	69(1)
C(4)	-1041(2)	3496(2)	-364(1)	57(1)	C(32)	4484(2)	1082(2)	-130(2)	89(1)
C(5)	-1628(2)	3462(3)	-1110(2)	86(1)	C(33)	5139(3)	1196(3)	-973(2)	108(1)
C(6)	-1509(2)	4308(3)	93(2)	93(1)	C(34)	7364(2)	3119(2)	1353(1)	55(1)
C(7)	-455(2)	1696(2)	-507(2)	64(1)	C(35)	8159(2)	2869(2)	1755(2)	72(1)
C(8)	-1104(2)	1265(2)	-296(2)	90(1)	C(36)	8795(2)	3491(3)	1990(2)	90(1)
C(9)	298(2)	1098(2)	-330(2)	86(1)	C(37)	8627(3)	4353(3)	1836(2)	96(1)
C(10)	968(2)	1471(2)	1622(1)	49(1)	C(38)	7845(3)	4606(3)	1429(2)	109(1)
C(11)	1573(2)	833(2)	1826(2)	68(1)	C(39)	7222(2)	3990(2)	1192(2)	86(1)
C(12)	1458(3)	44(2)	2096(2)	89(1)	C(40)	6982(2)	1301(2)	1079(2)	55(1)
C(13)	724(3)	-117(3)	2158(2)	88(1)	C(41)	7075(2)	674(2)	1568(2)	76(1)
C(14)	106(2)	500(3)	1948(2)	79(1)	C(42)	7450(2)	-122(2)	1574(2)	94(1)
C(15)	223(2)	1295(2)	1681(2)	66(1)	C(43)	7733(2)	-310(3)	1085(3)	101(1)
C(16)	1171(2)	3277(2)	1964(1)	46(1)	C(44)	7637(2)	291(3)	590(2)	97(1)
C(17)	881(2)	4118(2)	1807(2)	66(1)	C(45)	7267(2)	1094(2)	584(2)	78(1)
C(18)	954(2)	4726(2)	2306(2)	79(1)	C(46)	6980(2)	2258(3)	2821(2)	86(1)
C(19)	1319(2)	4494(2)	2971(2)	74(1)	C(47)	5149(2)	1428(3)	1813(2)	87(1)
C(20)	1612(2)	3652(3)	3140(2)	76(1)	C(48)	5494(2)	3598(3)	1977(2)	103(1)

Table 2.3: Positional Parameters and U(eq) for 62

Atom	x	y	z	U(eq)	Atom	x	y	z	U(eq)
P(1)	3370(1)	9652(1)	782(1)	38(1)	C(26)	5773(4)	8562(4)	2181(3)	53(1)
P(2)	1537(1)	7052(1)	1314(1)	47(1)	C(27)	4980(4)	8498(3)	1648(3)	45(1)
N(1)	2465(2)	7337(3)	1057(2)	43(1)	C(28)	3167(3)	9039(3)	375(2)	39(1)
B(1)	3917(4)	8176(4)	357(3)	38(1)	C(29)	3380(4)	9940(3)	679(2)	45(1)
C(1)	494(3)	7214(4)	579(3)	57(1)	C(30)	2715(4)	10654(3)	649(3)	53(1)
C(2)	481(4)	6605(5)	-80(3)	83(2)	C(31)	1818(4)	10516(4)	299(3)	62(1)
C(3)	-450(4)	7104(6)	799(3)	108(3)	C(32)	1563(4)	9658(4)	-41(3)	53(1)
C(4)	1405(4)	7953(4)	1971(3)	64(2)	C(33)	2237(4)	8963(3)	5(3)	43(1)
C(5)	1329(5)	8970(4)	1667(4)	101(2)	C(34)	3998(3)	8003(3)	-469(2)	38(1)
C(6)	2224(5)	7915(5)	2645(3)	90(2)	C(35)	4419(3)	7196(3)	-675(2)	42(1)
C(7)	1511(4)	5884(4)	1743(3)	65(2)	C(36)	4520(4)	7017(4)	-1356(3)	51(1)
C(8)	870(5)	5778(5)	2260(3)	97(2)	C(37)	4166(4)	7657(4)	-1883(3)	54(1)
C(9)	1327(5)	5053(4)	1218(4)	100(2)	C(38)	3767(4)	8473(4)	-1722(3)	52(1)
C(10)	3110(3)	5898(3)	192(2)	39(1)	C(39)	3695(3)	8631(3)	-1031(3)	43(1)
C(11)	3315(4)	4987(3)	471(3)	54(1)	F(1)	5936(2)	8212(2)	120(2)	61(1)
C(12)	3062(4)	4186(4)	36(3)	65(2)	F(2)	7498(2)	8348(3)	1135(2)	83(1)
C(13)	2613(4)	4283(4)	-665(3)	61(2)	F(3)	7444(2)	8587(3)	2525(2)	99(1)
C(14)	2397(4)	5175(4)	-942(3)	60(2)	F(4)	5737(2)	8694(3)	2866(2)	82(1)
C(15)	2645(3)	5984(3)	-525(3)	47(1)	F(5)	4153(2)	8572(2)	1851(1)	53(1)
C(16)	4284(3)	6487(3)	1529(2)	43(1)	F(6)	4278(2)	10179(2)	1022(2)	60(1)
C(17)	4150(4)	6536(4)	2226(3)	57(1)	F(7)	2993(2)	11513(2)	971(2)	76(1)
C(18)	4863(5)	6240(4)	2805(3)	74(2)	F(8)	1169(3)	11210(2)	270(2)	96(1)
C(19)	5693(5)	5900(5)	2707(3)	79(2)	F(9)	673(2)	9515(2)	-425(2)	80(1)
C(20)	5834(4)	5842(4)	2026(3)	68(2)	F(10)	1950(2)	8159(2)	-384(1)	56(1)
C(21)	5141(4)	6130(4)	1449(3)	54(1)	F(11)	4806(2)	6540(2)	-174(2)	59(1)
C(22)	4940(3)	8337(3)	930(2)	39(1)	F(12)	4948(2)	6217(2)	-1498(2)	82(1)
C(23)	5830(3)	8305(3)	799(3)	43(1)	F(13)	4228(2)	7483(3)	-2559(2)	81(1)
C(24)	6656(4)	8382(4)	1313(3)	57(1)	F(14)	3431(2)	9131(2)	-2236(2)	82(1)
C(25)	6627(4)	8505(4)	2017(3)	63(2)	F(15)	3306(2)	9493(2)	-937(2)	70(2)

Table 2.4: Positional Parameters and U(eq) for 65

Atom	x	y	z	U(eq)	Atom	x	y	z	U(eq)
Ti(1)	6791(1)	635(1)	6731(1)	43(1)	C(11)	8232(6)	1105(2)	11958(4)	68(2)
P(1)	8405(1)	1568(1)	8396(1)	35(1)	C(13)	9724(6)	1811(3)	5382(5)	78(2)
P(2)	10997(1)	1499(1)	7605(1)	44(1)	C(15)	11289(5)	1062(2)	5236(5)	71(2)
Cl(1)	4984(2)	1056(1)	5874(2)	98(1)	C(16)	7050(6)	3258(2)	7390(5)	69(2)
Cl(2)	7851(2)	438(1)	5025(1)	71(1)	C(17)	8685(5)	1223(2)	10840(4)	54(1)
N(1)	7662(3)	1171(1)	7433(3)	38(1)	C(18)	6337(6)	2831(2)	6984(5)	70(2)
N(2)	9920(3)	1547(1)	8533(3)	44(1)	C(19)	10368(5)	1338(2)	6039(4)	55(1)
C(1)	7451(9)	-179(3)	7614(9)	101(2)	C(20)	12070(5)	968(2)	8111(5)	65(1)
C(2)	7126(13)	143(3)	8522(7)	120(4)	C(21)	6730(5)	2320(2)	7271(4)	53(1)
C(3)	12954(7)	2156(3)	6808(8)	110(3)	C(22)	8562(5)	2674(2)	8421(4)	53(1)
C(4)	6172(6)	1418(3)	11245(6)	81(2)	C(23)	8162(6)	3183(2)	8097(5)	64(1)
C(5)	6383(13)	-299(3)	6897(7)	113(3)	C(25)	7880(4)	1443(2)	9907(4)	42(1)
C(6)	12763(6)	1080(3)	9387(6)	98(2)	C(26)	7850(4)	2236(2)	8000(4)	39(1)
C(7)	12161(6)	2389(3)	8837(6)	92(2)	C(34)	5389(9)	-49(5)	7345(12)	133(4)
C(8)	11341(7)	449(2)	8111(7)	94(2)	C(112)	6622(5)	1541(2)	10128(5)	63(1)
C(9)	5872(14)	238(4)	8361(11)	134(4)	C(220)	11825(5)	2150(2)	7577(5)	65(1)
C(10)	6983(7)	1200(2)	12163(5)	78(2)					

Vita Auctoris
Nancy L. S. Yue

Education

January 1999 - Present: M.Sc. (Candidate), School of Physical Sciences, Chemistry and Biochemistry, University of Windsor

June, 1998: Honours Bachelor of Science (Chemistry Specialist Program), University of Toronto

Experience

May - August 1998: Research Assistant, Department of Chemistry, University of Toronto

Publications

1. Phosphinimine – Phosphinimide Ligands: A New Class of Ancillary Ligands for Olefin Polymerization. Douglas W. Stephan, Nancy L. S. Yue. (Manuscript in preparation)

2. Zirconium Phosphinimide Complexes: Synthesis and Chemistry. Douglas W. Stephan, Nancy L. S. Yue. (Manuscript in preparation)

3. Group(IV) Phosphinimide Butadiene Complexes. Douglas W. Stephan, Nancy L. S. Yue. (Manuscript in preparation)

4. Cationic Dimerization: A New Pathway for Olefin Polymerization Catalyst Deactivation. Douglas W. Stephan, Nancy L. S. Yue. (Manuscript in preparation)

5. Oxidation of Aminals. M. K. Denk, S. Gupta, J. Brownie, R. Soong, N. L. S. Yue, J. Rodezno, L. Studnicki, A. Lough. (Manuscript in preparation)